Impact of sphingosine-1-phosphate receptor 3 deficiency and serum sphingosine-1-phosphate level alteration in the development of intimal hyperplasia

Dissertation

zur Erlangung des akademischen Grades eines
Doktors der Medizin (Dr. med.)

an der

Medizinischen Fakultät der Universität Hamburg

vorgelegt von

Yi Qin

aus

Jiangsu, China

2024

Angenommen von der Medizinischen Fakultät am: 26.05.2025

Veröffentlicht mit Genehmigung der Medizinischen Fakultät der Universität Hamburg

Prüfungsausschuss, der/die Vorsitzende: Prof. Dr. Viacheslav Nikolaev

Prüfungsausschuss, 2. Gutachter/in: Prof. Dr. Edzard Schwedhelm

Betreuer:in / Gutachter:in der Dissertation: Prof. Dr. Edzard Schwedhelm

Gutachter:in der Dissertation: Prof. Dr. Viacheslav Nikolaev

Vorsitz der Prüfungskommission: Prof. Dr. Viacheslav Nikolaev

Mitglied der Prüfungskommission: Prof. Dr. Maike Frye

Mitglied der Prüfungskommission: Prof. Dr. Ewa Klara Stürmer

Datum der mündlichen Prüfung: 26.05.2025

Table of contents

1. Introduction

1.1 Restenosis

Cardiovascular disease is the leading cause of mortality, resulting in over 30% of deaths worldwide. Also, more than 230 million adults are affected by lower extremity peripheral artery disease, and patients suffer from functional decline, pain, ulceration, and a higher risk of amputation (Song et al. 2019, Aday and Matsushita 2021). Arterial stenosis and occlusion contribute to the primary pathological basis of cardiovascular diseases. In the last decades, open surgeries and interventional techniques including arterial bypass, endarterectomy, angioplasty, and stent implantation have been developed, as the mainstay of treatment for hemodynamic recovery.

Restenosis, a serious complication of all procedures to restore arterial blood flow, refers to the re-occurrence of vessels narrowing (over 50% of the lumen area) (Singh et al. 2004). For peripheral artery disease, interventional procedures have been the more common choice due to the shorter convalescence, with postinterventional restenosis rates within one year ranging from 20 to 60%. The restenosis risk increases within long-segment lesions or extremely narrow lumen (Chalmers et al. 2013, Laird et al. 2014). Although bypass graft surgery is favored in some patients due to high durability, anastomotic or intrinsic graft lesions still lead to arterial ischemic symptoms in 20-30% of all cases (Beckman et al. 2021). For coronary artery disease, percutaneous coronary intervention procedures and the availability of bare-metal stents since the year 1987 contributed to a remarkable reduction in restenosis rates from 32-55% to 16-41% (Sigwart et al. 1987, Buccheri et al. 2016, Omeh and Shlofmitz 2023). Drug-coating balloons and drug-eluting stents prompt further improvement after angioplasties. However, restenosis is still a continued challenge with high prevalence in the clinic, where target lesion revascularization treatment occurred in up to 35% of the cases in one-year follow-up (Yerasi et al. 2020).

The pathophysiological processes that eventually lead to restenosis mainly include early elastic recoil (ER), vascular remodeling, intimal hyperplasia (IH), and neo-atherosclerosis in the long term (Jukema et al. 2012, Buccheri et al.

2016). After balloon dilatation treatment, the enrichment of elastin fibers in the elastic lamina causes ER after hyperextension, generating a dramatic lumen area reduction up to 60% in a few minutes (Yang et al. 2021). Constrictive remodeling is another prominent factor in narrowing the lumen after an acute arterial injury. Though the precise mechanisms have not been completely understood, endothelial dysfunction and shear stress alteration both contribute to arterial remodeling (Stone et al. 2003). Also, collagen accumulation and its cross-linking to elastin have been described to have a positive correlation with the degree of constrictive remodeling. The inhibition of oxidative stress has been demonstrated to prevent constrictive remolding, while transforming growth factor beta (TGF-β) may play a role in expansive remodeling (Pasterkamp et al. 2000, Brasselet et al. 2005). The application of stent implantation effectively eliminates ER after the dilatation procedure and circumvents the remodeling influences by providing long-term physical support to the vessel wall. Nevertheless, IH remains a challenging problem after stent implantation.

1.2 Intimal hyperplasia

Arterial injury induces inflammation, cell proliferation, and migration of vascular smooth muscle cells (VSMCs), and extracellular matrix (ECM) remodeling (Melnik et al. 2022), in all layers of the arterial wall: intima, media, and adventitia (see Figure 1). The intima includes the endothelium which has direct contact with the blood on one side and subendothelial-connected tissues on the other side. The media, composed mainly of VSMCs, elastin, and collagen, is separated from the intima and adventitia by the inner and external elastic lamina (IEL and EEL), respectively. The adventitia, the outer layer of the artery wall, consists of fibroblasts, resident progenitor cells, immune cells, adrenergic nerves, and vasa vasorum (Stenmark et al. 2013). Medial VSMCs exhibit a differentiated, contractile phenotype, which is characterized by the expression of α-actin and myosin and a low proliferation rate. In response to arterial injury, VSMCs change to a non-contractile phenotype, which is characterized by an increase in cell organelles, rough endoplasmic reticulum, reduced expression of α-actin and induced expression of pro-inflammatory cytokines along with a higher proliferation rate (Allahverdian et al. 2018, Chang et al. 2014). To allow

for vasodilation, an intact and healthy endothelium secretes nitric oxide (NO), prostacyclin (prostaglandin I2, PGI2), and heparin sulfates. All these mediators are also endogenous VSMC proliferation inhibitors and ensure the maintenance of the contractile phenotype (Marx et al. 2011, Déglise et al. 2023).

During vascular repair procedures, endothelial cells become damaged and VSMC and ECM are exposed to circulating blood components. Impaired endothelial function includes reduced NO and PGI2 generation, promoting VSMC proliferation and attenuating endothelial anti-platelet activity (Cornelissen and Vogt 2019). This can lead to platelet aggregation and fibrinogen deposition at the denudation site, which foreshadows the onset of thrombosis formation and inflammation process (Inoue et al. 2011). Under the stimulation of various pro-inflammatory cytokines such as interleukin-1 beta (IL1β), interleukin-6 (IL6) and tumor necrosis factor-alpha (TNFα) secreted by circulating monocytes or underlying VSMCs, ECs are induced to up-regulate the expression of cellular adhesion molecules, facilitating monocyte rolling, adhesion and trans-endothelial migration into subintima (Ostermann et al. 2002, Becker et al. 2018, Peng et al. 2019). Monocytes differentiate into macrophages and release more pro-inflammatory cytokines, increasing endothelial permeability. The released TNFα activates the transcription factor nuclear factor-kappa beta (NF-κB) through the canonical pathway, and NF-κB is a central regulator of inflammation-related genes (Liu et al. 2017a, Mussbacher et al. 2019). NF-κB signaling also promotes the phenotypic modulation of VSMC from a quiescent and contractile phenotype to a synthetic phenotype (Tang et al. 2008). Additionally, adherent and activated platelets and immune cells at the injury site release various growth factors including platelet-derived growth factor (PDGF), insulin-like growth factor 1 (IGF-1), TGF-β, vascular endothelial growth factor (VEGF), and basic fibroblast growth factor (bFGF). They contribute to diverse biological activities in the progression of neointima formation, inducing VSMCs proliferation, migration, and phenotypic switch, recruiting immune cells, stimulating ECM re-synthesis, and re-endothelization (Melnik et al. 2022). Increased expression of proteases is a significant driver of matrix remodeling. For example, matrix metalloproteinases (MMPs) degrade ECM, and facilitate

the migration of dedifferentiated VSMCs across the inner elastic lamina to the subintimal space (Rotmans et al. 2004), contributing to the neointima formation (Myit et al. 2003). Although VSMCs are commonly acknowledged to be the foremost contributor to IH, more recent studies have revealed that the adventitia also responds to vascular injury by expressing chemokines, adhesion molecules, and pro-inflammatory factors, thereby exacerbating the inflammatory reaction (Moos et al. 2005, Csányi et al. 2009, Ji et al. 2010). Adventitial fibroblasts, the most abundant cells in the vascular adventitia, can function as a robust source of paracrine factors (Tieu et al. 2009). Growth factors such as TGF-β1 stimulate fibroblast proliferation and differentiation toward a myofibroblast phenotype. These cells are also induced to express α-smooth muscle actin (SMA) to acquire VSMC characteristics, migrate toward the lumen, and promote ECM formation by enhancing protein synthesis (Majesky et al. 1991, Shi et al. 1996a, Shi et al. 1996b). Similarly, perivascular resident progenitor cells migrate to the intima and differentiate into mesenchymal cells (Tigges et al. 2013). The adventitia is also an active area for inflammatory cell accumulation, contributing to vascular remodeling. Neutrophils have been found to gather in the adventitia two to three days after angioplasty. Adventitial fibroblasts secreting VEGF also induce the migration and accumulation of macrophages to the adventitia

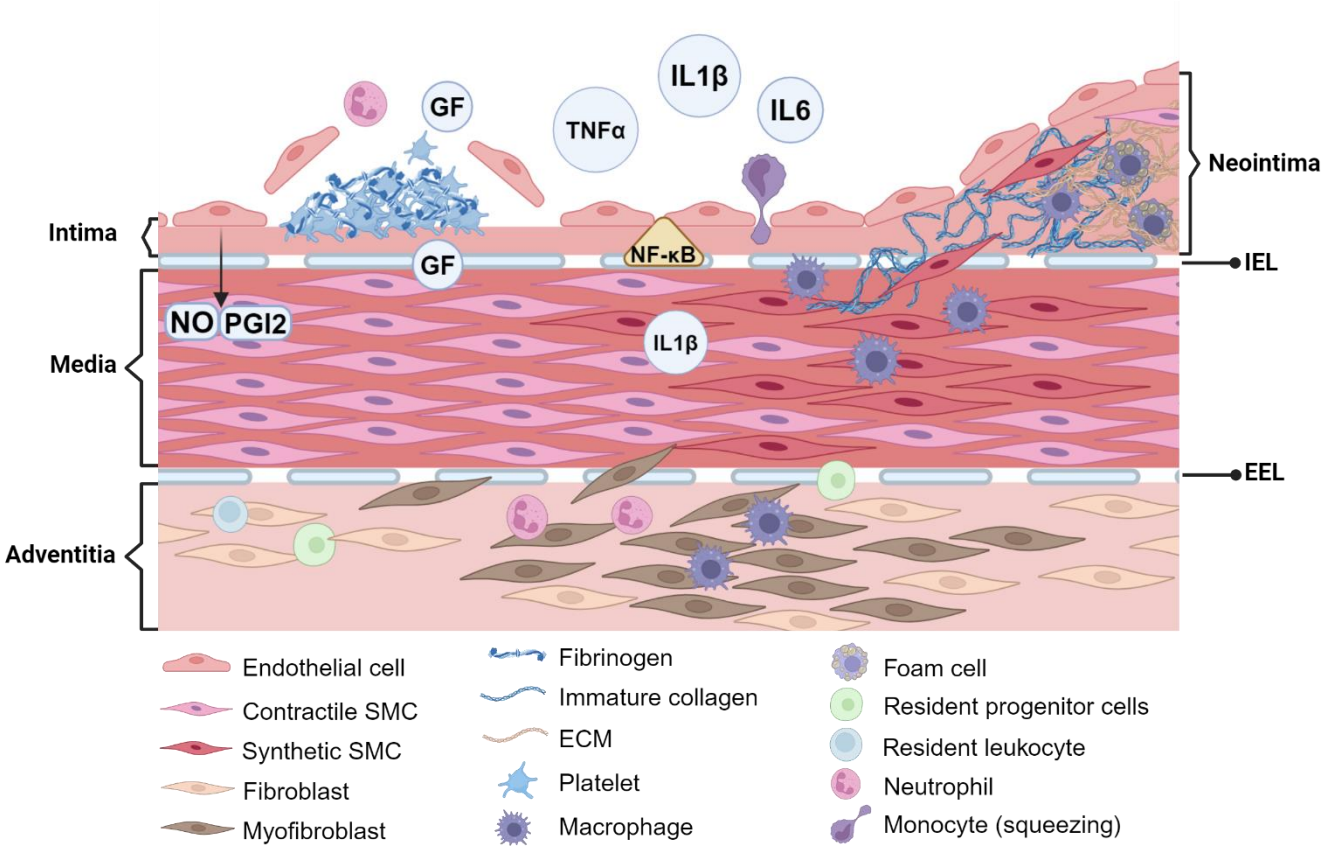

Figure 1 Pathology of intimal hyperplasia. Intimal hyperplasia is a pathological process after artery injury involving thrombotic and inflammatory pathways. The damage of the endothelial barrier induces various pro-inflammatory factors and stimulates the participation of immune cells, promoting phenotype conversion in smooth muscle cells. Synthetic smooth muscle cells proliferate and migrate into the intima, contributing to neointima formation. In this process, multiple components in adventitia also played a synergistic role. GF: growth factor, TNFα: tumor necrosis factor-alpha, IL1β: interleukin-1 beta, IL6: interleukin-6, NO: nitric oxide, PGI2: prostaglandin I2, IEL: inner elastic lamina, EEL: external elastic lamina, SMC: smooth muscle cell, ECM: extracellular matrix. (Author's own presentation)

1.3 Sphingosine-1-phosphate

1.3.1 Metabolism of sphingosine-1-phosphate

Sphingosine-1-phosphate (S1P) is a bioactive lipid second messenger (Spiegel and Milstien 2011, Prager et al. 2015) derived from sphingolipids, which are present in all eukaryotic bilayer cell membranes. Sphingolipid metabolism with ceramide as the core component (see Figure 2), generates important bioactive signaling molecules mediating various biological functions such as inflammation, apoptosis, and cell cycle (Ogretmen 2018, Iessi et al. 2020). The *de novo* pathway of sphingolipids commences with the condensation of serine and palmitoyl coenzyme A (palmitoyl-CoA) in the endoplasmic reticulum to 3-keto-

dihydrosphingosine, catalyzed by serine palmitoyltransferase (SPT). N-acyl sphingosine (dihydrosphingosine) is then formed via N-acylation, followed by desaturation to yield ceramide (Batheja et al. 2003, Merrill 2011). Catabolism of sphingolipids can also produce ceramides, by the reversible hydrolysis of sphingomyelin via sphingomyelin synthase and sphingomyelinase (Kitatani et al. 2008). S1P is the active terminal derivative of sphingolipid metabolism (Tani et al. 2007, Snider et al. 2010). In the salvage pathway, S1P is converted into sphingosine, which forms ceramide through the action of ceramide synthase. In turn, ceramide can be deacylated to sphingosine via ceramidase, and then sphingosine is phosphorylated to S1P by sphingosine kinase 1 (SPHK1) or sphingosine kinase 2 (SPHK2). Subsequently, S1P lyase (SPL) can irreversibly cleave S1P to phosphoethanolamine and hexadecenal intracellularly, while S1P phosphatase or broad-specificity lipid phosphate phosphatase dephosphorylates S1P reversibly (Fyrst and Saba 2010, Książek et al. 2015).

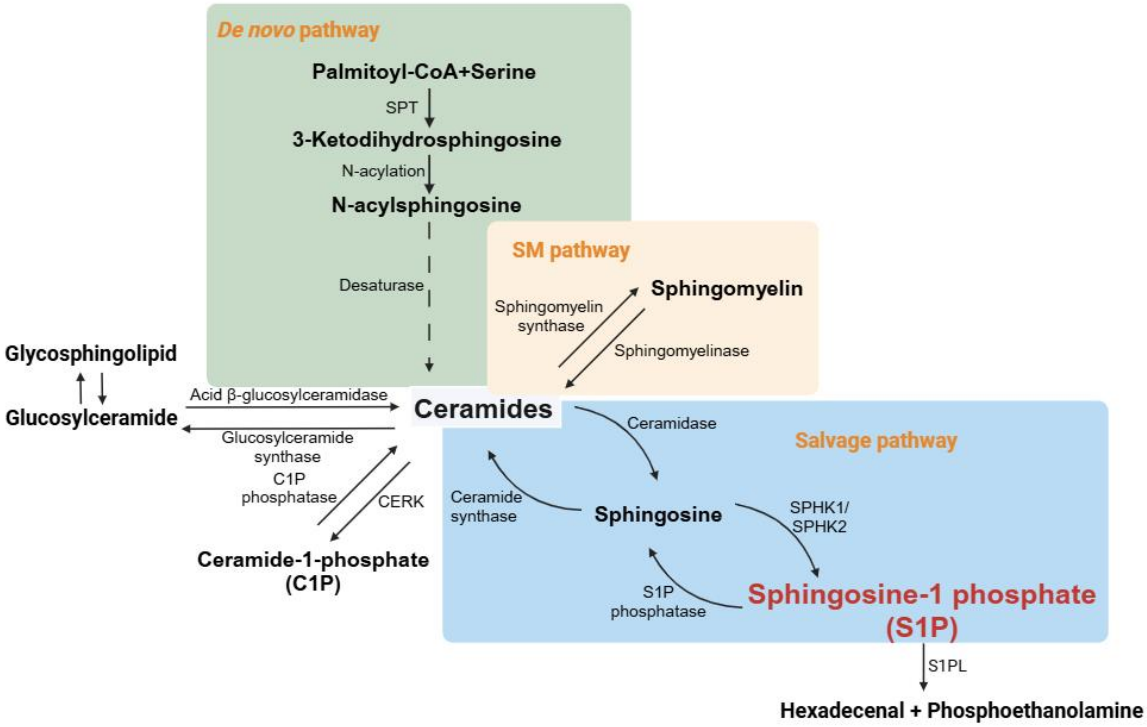

Figure 2 The metabolism of sphingosine-1-phosphate. Sphingosine-1-phosphate (S1P) originates from sphingosine phosphorylation. Sphingosine is a sphingolipid constituent of ceramides and sphingomyelin (SM). Three different pathways are known for sphingosine formation: *de novo*, SM, and salvage pathway. SPT: serine palmitoyltransferase, CERK: ceramide kinase, C1P: ceramide-1-phosphate, SM: sphingomyelin, SPHK: sphingosine kinase, S1P: sphingosine-1-phosphate, S1PL: sphingosine-1-phosphate lyase. (Modified from Mei et al. 2023)

In physiological conditions, a steep gradient of S1P exists between high concentrations in blood and low concentrations in tissue. Erythrocytes and ECs are the predominant sources of circulating S1P. Once activated, also platelets can produce a vast amount of S1P (Pappu et al. 2007, Pyne and Pyne 2017). It has been reported that leukocytes can incorporate extracellular sphingosine and produce S1P. However, the degradation rate of extracellular S1P by leukocytes exceeds its release rate (Książek et al.2015, Tolksdorf et al. 2022). Both erythrocytes and platelets lack the S1P degrading enzyme SPL, allowing them to accumulate large amounts of S1P. The generated S1P is transported to the extracellular space via the specific transporter major facilitator superfamily transporter 2b (Mfst2b) in erythrocytes and platelets and spinster homolog 2 (Spns2) in ECs, and then it is bound to albumin or the high-density lipoprotein (HDL)-associated specific S1P chaperone protein apolipoprotein M (ApoM) (Obinata and Hla 2019). Erythrocytes and ECs release S1P spontaneously without specific stimulation (Hänel et al. 2007, Książek et al.2015). Although platelets are characterized by higher SPHK activity (Yatomi et al. 2004), they contribute less to circulating S1P concentrations and only release S1P under conditions of platelet activation (Jonnalagadda et al. 2014).

The S1P gradient between high intravascular S1P concentrations (0.1-1.2 μmol/L in human plasma) and low tissue S1P concentrations (0.5-75 pmol/mg) is mainly due to rapid degradation of S1P in tissues (Venkataraman et al. 2008, Xiong and Hla 2014, Nagahashi et al. 2016). Several cell types, e.g. lymphocytes or VSMC are attracted by S1P and thus migrate towards higher S1P concentrations (Baeyens and Schwab 2020). Mature lymphocytes require S1P to migrate from lymphoid organs into the circulation via a sphingosine-1-phosphate receptor-1 (S1PR1)-dependent chemotaxis. Partial injury and inflammatory response may disrupt the equilibrium of local S1P gradients and subsequently alter the activity and migration of immune cells. Thus, the concentration of S1P and the apparent S1P gradient between blood/lymph circulation and the interstitial fluid are critical for maintaining physiological homeostasis (Li et al. 2023).

1.3.2 The roles of sphingosine-1-phosphate in arterial blood vessels

The SPHK/S1P axis is a fundamental signaling pathway in vasculogenesis (Jozefczuk et al. 2020). Clear evidence came from *Sphk1/Sphk2*-/- mouse embryos which die prematurely due to inefficient vascularization and disrupted neurogenesis (Mizugishi et al. 2005), and the research on cell-type-specific *Sphk1/Sphk2* null mice identified erythrocytes as the main source of embryonic S1P (Xiong et al. 2014). Likewise, S1P is also essential for homeostasis in mature vascular systems (Wang et al. 2023a).

Vascular homeostasis: The endothelial barrier is a dynamic structure that maintains vascular integrity and controls fluid and solute exchange. Global or endothelial-specific deficiency of S1PR1 leads to embryonic lethality in mice due to hemorrhage (Liu et al. 2000, Allende et al. 2003). Camerer et al. (Camerer et al. 2009) also reported that mutant mice selectively lacking S1P in plasma suffered from increased vascular leakage after exposure to inflammation challenges, while erythrocyte transfusion restored EC barrier function via supplementing S1P generation. Endothelial glycocalyx (EG), as a part of the barrier, is a protective layer covering the surface of the endothelium (Zeng et al. 2014). S1P participates in EG synthesis through the phosphoinositide 3-kinases (PI3K) signaling pathway and stabilizes its structure by affecting the activity of metalloproteinases (Zeng et al. 2015, Zhang et al. 2016, Mensah et al. 2017). S1P was reported to prevent EG degradation in the mesenteric microcirculation of rats induced by hemorrhagic shock and resuscitation (Alves et al. 2019). It was further speculated from *in vitro data*, that plasma blood product administration in hemorrhagic shock or trauma patients could improve impaired vessel leakage by maintaining or restoring S1P blood pools (Diebel et al. 2019).

Blood pressure and vascular tone: Previous studies have shown a significant increase of S1P levels in the angiotensin II (AngII)-mediated hypertension animal model. Notably, the knockout of *Sphk* in mice could prevent the blood pressure-raising effect of AngII (Cantalupo et al. 2015, Siedlinski et al. 2017, Meissner et al. 2017). Circulating S1P activates S1PR1 in the renal medulla, and then the signal acts on epithelial sodium channels, affecting blood volume via natriuretic effects to regulate blood pressure (Zhu et al. 2011). Moreover,

S1P signaling promotes vasodilation through S1PR1/3 signaling in ECs and promotes vasoconstriction through S1PR2/3 signaling in VSMCs to achieve balanced vascular tension regulation (Wilson et al. 2015). These functions involve the increase of intracellular Ca^{2+}, the induction of endothelial NO synthase (NOS3), and the production of NO (Igarashi and Michel 2009).

Angiogenesis: In addition to participating in plenty of physiological processes, angiogenesis is the cornerstone of tissue regeneration and functional recovery in arterial diseases (Liman and Endres 2012, Cochain et al. 2013). *Sphk1-/-* mice exhibited delayed wound healing due to impaired angiogenesis and inflammatory cell recruitment, which suggested the potential role of S1P in the healing process (Aoki et al. 2019). As the master regulator of angiogenesis, VEGF increases vascular permeability and induces EC activity (Krock et al. 2011). Early studies show that S1P/S1PR1 counteracts the function of VEGF and seals the endothelial barrier thereby preventing excessive vascular sprouting (Gaengel et al. 2012). Mascall et al. (Mascall et al. 2012) also reported that S1P inhibited angiogenesis via the release of tissue inhibitors of MMP2 in VSMCs. However, it is later reported that S1P also promotes neovascularization by inducing EC proliferation and migration (Jin et al. 2018, Wang et al. 2022). These contradictory effects can be explained by the involvement of different S1PRs.

Arterial stenosis: Many studies have identified the S1P level as a potential predictor for arterial obstructive disease (Egom et al. 2013, Soltau et al. 2016, Liu et al. 2020). Potì et al. (Potì et al. 2015) found that SPHK1 inhibitors aggravated atherosclerotic lesions in LDL receptor knockout mice, while the atherosclerotic response was attenuated in mice engineered to be SPL deficient (Bot et al. 2013). Coronary artery disease patients appeared to have reduced HDL-S1P levels (Sattler et al. 2010), while S1P loading could restore defective signaling and HDL functions (Sattler et al. 2015). As a protective factor, S1P can activate S1PR1 in ECs and thereby improve the endothelial barrier as well as induce vasodilation (Warboys and Weinberg 2021). S1P signaling also regulates VSMC proliferation and migration, which are essential for arterial stenosis pathological processes. S1PR1 signaling has been demonstrated to

promote VSMC proliferation and phenotype modulation while S1PR2 appears to antagonize this function (Wamhoff et al. 2008, Wang et al. 2023a). On the other hand, growing evidence shows that S1P can promote inflammatory reactions. As a typical example, an S1P gradient and the surface residence of S1P receptors on immune cells are significant inducers for mediating lymphocyte egress from the lymphoid organs into the systemic circulation (Cyster and Schwab 2012) and recruiting lymphocytes to the inflammatory sites (Goetzl and Graler 2004, Swan et al. 2010). S1P facilitates intracellular calcium signaling, activation of NF-κB, and the production of TNFα in macrophages and monocytes (Keul et al. 2011, Lewis et al. 2013). In some cases, S1P was found to enhance the expression of adhesion molecules (Alewijnse and Peters 2008), promoting the local accumulation of monocyte recruitment and triggering a series of inflammatory reactions (Galkina and Ley 2007, Wolf and Ley 2019). Overall, the role of S1P in arterial ischemic diseases is yet ambiguous (see Figure 3).

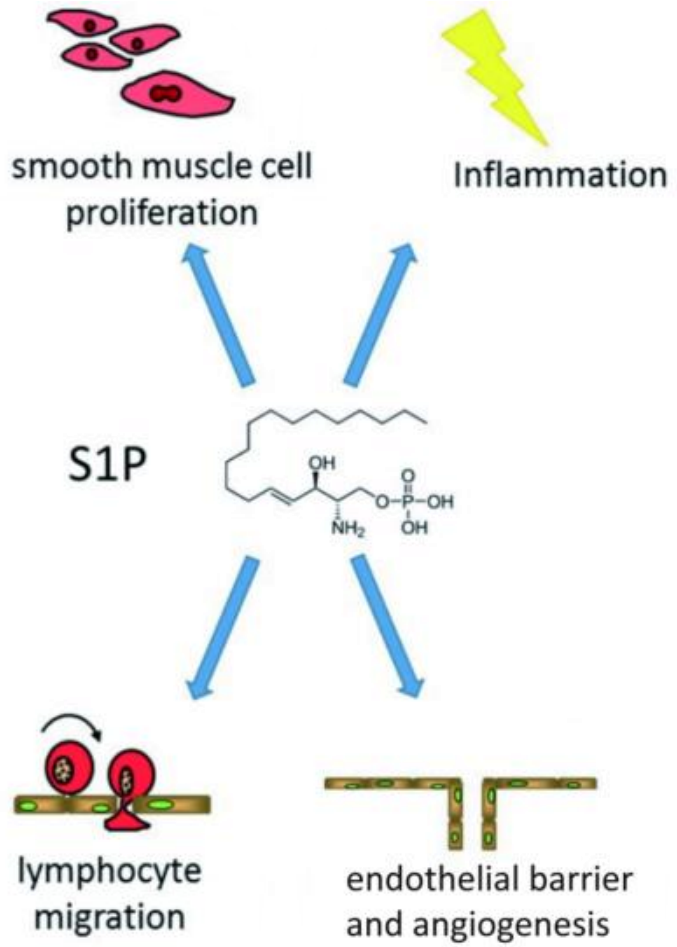

Figure 3 The roles of sphingosine-1-phosphate in arterial stenosis. S1P signaling impacts arterial stenosis development in several aspects. It regulates VSMC proliferation and promotes inflammation response via mediating immune cell migration and invasion. It is also essential for endothelial barrier maintenance, angiogenesis, and re-endothelization after injury. S1P: sphingosine-1-phosphate. (Modified from Schwedhelm et al. 2021)

1.3.3 Sphingosine-1-phosphate lyase inhibitor

4-Deoxypyridoxine (DOP) is an inhibitor of SPL and its administration causes an accumulation of S1P in lymphoid organs and plasma (Schwab et al. 2005). Many approaches have been taken to study the effects of increased S1P levels on cardiovascular disease. In early trials on animals that underwent the left anterior descending coronary artery ligation, intravenous injection with S1P in advance of reperfusion effectively reduced the infarct size (Brulhart-Meynet et al. 2015). Similarly, the S1P supplementation upon reperfusion after ischemia injury improved the recovery of cardiac function in rats (Vessey et al. 2008). However, these experiments only evaluated the impact of a transient S1P elevation. In the mouse myocardial infarction model via left anterior descending coronary artery ligation, impaired post-ischemic cardiac remodeling, and diminished scar size were observed depending on the incremental increase of S1P in blood by continuous oral application of DOP (Polzin et al. 2023). In contrast, Zhang et al. (Zhang et al. 2016) found that oral application of the SPL inhibitor tetrahydroxybutylimidazole induced adverse cardiac structural transformations and up-regulated expression of remodeling genes, disclosing its possible harmful role in the same myocardial infarction mouse model. Conflicting results have also been published for the role of increasing S1P concentrations in atherosclerosis development. In one case, disruption of the S1P gradient by transplantation of *Spl1-/-* bone marrow into LDL receptor-deficient mice led to lymphopenia and eventually prevented atherosclerotic lesion progression (Bot et al. 2013). In another case, oral DOP administration, which led to a comparable S1P gradient disruption and a remarkable reduction in circulating lymphocytes, resulted in the accelerated development of atherosclerosis (Keul et al. 2022).

1.3.4 Heparin and sphingosine-1-phosphate

Heparin, a sulfated glycosaminoglycan, is clinically used for the prevention and treatment of thrombotic diseases based on its anticoagulant effects. At the site of endothelial injury, contact of factor XII with exposed phospholipids (known as the endogenous pathway) or the integral membrane protein tissue factor (TF) with factor VII-containing plasma (known as the exogenous pathway) elicits the coagulation cascade, which subsequently promotes factor Xa (FXa) and thrombin formation. The latter can activate various components to amplify the coagulation cascade. Thrombin converts fibrinogen to fibrin to ultimately form a clot. The anticoagulant activity of heparin manifests via a complex with antithrombin, facilitating the interaction between antithrombin and thrombin or FXa (Onishi et al. 2016). Our previous study revealed that in cardiac surgery patients, serum S1P levels significantly decreased at the time point of preoperative heparinization (Greiwe et al. 2021). From this observation, we speculated on the possibility of heparin reducing the circulating S1P concentration by interacting with blood cells.

Platelets can store large amounts of S1P due to the lack of SPL activity and secrete S1P abundantly following stimulation (Ulrych et al. 2011, Ono et al. 2013, Rauch 2014). Studies have demonstrated that the coagulation process or direct activation with protein kinase C (PKC) signaling agonists like thrombin triggers the release of S1P in platelets (Yatomi et al. 2000, English et al. 2000). In addition, Böhm et al. (Böhm et al. 2013) found that FXa induced higher *Sphk1* mRNA expression in human VSMC, causing enhanced synthesis and release of intracellular S1P, subsequently fostering cell mitogenesis and migration. Thus, heparin-mediated inhibition of the coagulation cascade might indirectly lead to an attenuation of S1P generation and release. *In vitro*, heparin was proven to inhibit the mitogenic effect of FXa (Rauch et al. 2004) and can also promote the change of VSMC morphology to a contractile phenotype (de Mel et al. 2008). We hypothesize that heparin could affect IH development by modulating S1P concentrations in blood.

1.4 Sphingosine-1-phosphate receptors

Five high-affinity receptors for S1P have been discovered, described as S1PRs (S1PR1, S1PR2, S1PR3, S1PR4, S1PR5), a group of G-protein-coupled

receptors (GPCRs) exerting partial synergistic and antagonistic functions on cell proliferation, migration, and apoptosis. S1PR1-3 are ubiquitously expressed while S1PR4 and S1PR5 are expressed specifically in the immune system and nervous system. (Bryan and Del Poeta 2018). ApoM is the main circulating chaperone of S1P transport and it appears to amplify the affinity of S1P to S1PR1/3 (Kurano and Yatomi 2018). The remaining amount of S1P is primarily bound and transported by albumin (30-40%) and a small amount via LDL and very low-density lipoprotein (VLDL) (Christoffersen et al. 2011, Książek et al.2015).

Among the five known S1PRs, S1PR1, S1PR2, and S1PR3 were found to be predominantly expressed in cardiovascular tissues (Peters and Alewijnse 2007). S1P signaling is mainly mediated by S1PR1 in cardiomyocytes (Zhang et al. 2007), while S1PR3 takes the ruling role in cardiac fibroblasts (Landeen et al. 2008). Concerning ECs, S1PR1 is the dominant receptor type expressed, followed by S1PR3 and, less frequently, S1PR2 (Panetti 2002). Previous studies validated the expression of these three receptors in both the aortic media and adventitia of mice (Jiang 2021, dissertation, von Lucadou 2023, dissertation). Depending on which S1PR is involved, S1P/S1PR activates different isoforms of G proteins, including $G\alpha_{i/o}$, $G\alpha_{q,}$ and $G\alpha_{12/13}$, subsequently followed by the initiation of various cell signal transduction pathways (Chun et al. 2021) (see Figure 4). S1PR1 couples to $G\alpha_{i/o}$ and is critical for vascular integrity (Shao et al. 2015). The binding to $G\alpha_{i/o}$ advances the activation of small guanosine triphosphatases (GTPases). Ras, at the helm of a signaling pathway including extracellular signal-regulated kinase (ERK), promotes cell proliferation. Activation of Rac and PI3K/protein kinase B (PKB) stimulates cell migration and in EC, strengthens the vascular barrier and induces vasodilation. Phospholipase C (PLC) is also stimulated, which causes an increase in intracellular free Ca^{2+}, while adenylyl cyclase (AC) activity is inhibited and the generation of cyclic adenosine monophosphate (cAMP) is reduced. Besides $G\alpha_{i/o}$, S1PR2/3 couples mainly with $G\alpha_{12/13}$ and additionally with $G\alpha_{q}$. The small GTPase Rho and Rho-associated protein kinase (ROCK) can be activated through $G\alpha_{12/13}$, and signaling through $G\alpha_{q}$ primarily activates PLC pathways to inhibit cell migration,

reduce endothelial barrier function, and induce vasoconstriction (Chun et al. 2021, Wang et al. 2023a).

As the various S1P/S1PR axes function synergistically or antagonistically, the role of S1P signaling in arterial diseases depends on the expression levels of the individual S1PR. For example, VSMCs derived from FVB and C57BL/6 mice migrate similarly strongly toward PDGF alone but differently when S1P is present. FVB-VSMCs that express higher levels of S1PR1 migrate faster, while C57BL/6 VSMCs that express higher levels of S1PR2 migrate slower (Inoue et al. 2007). Clear evidence is provided that S1PR1 signaling induces VSMC proliferation and phenotypic modulation (Kitano et al. 2019) while S1PR2 antagonizes these effects and promotes the contractile phenotype in VSMC via its stronger affinity to $G\alpha_{12/13}$ (Medlin et al. 2010, Ishii et al. 2002).

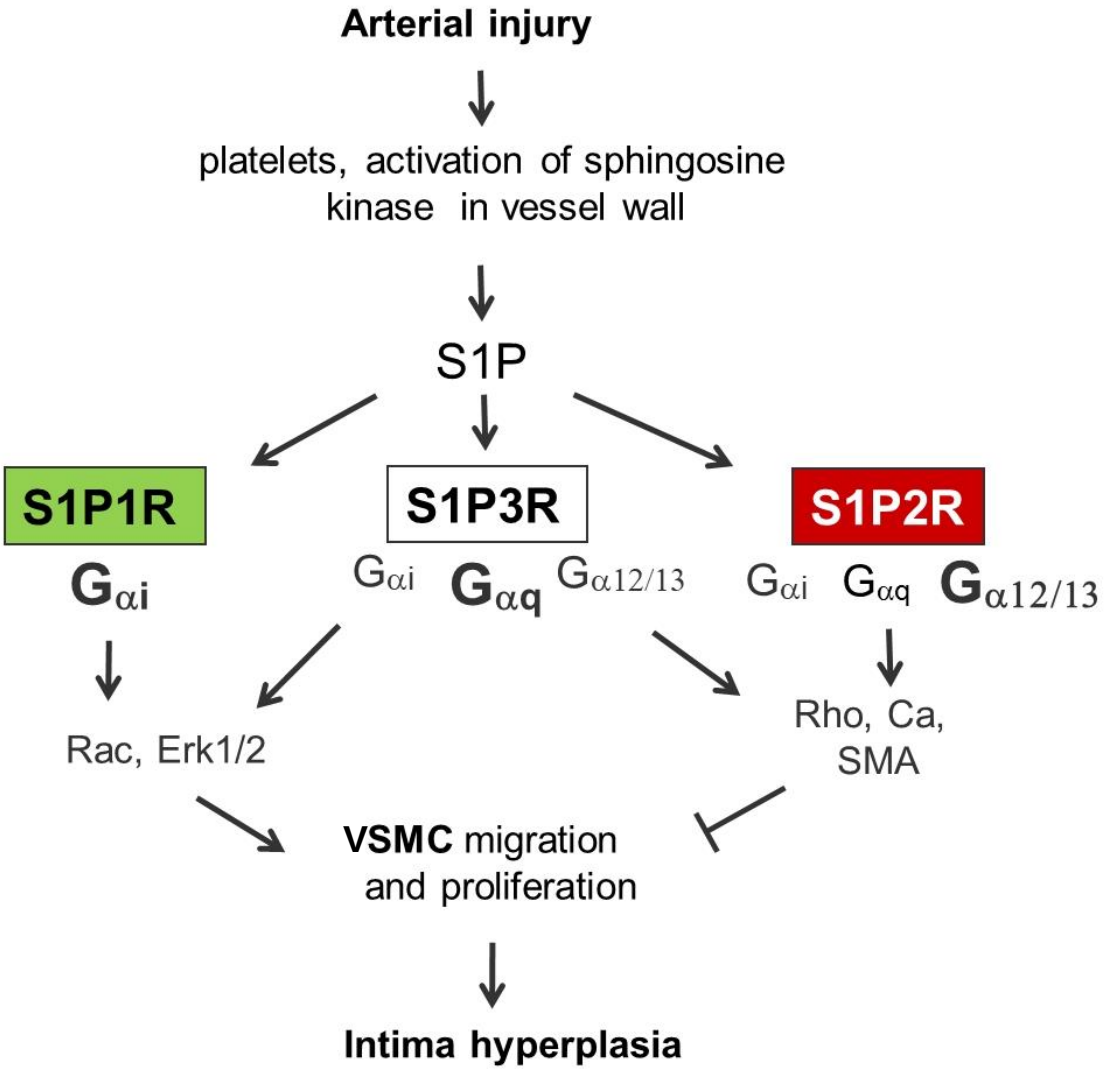

Figure 4 Sphingosine-1-phosphate receptors 1/2/3 signaling in arterial injury. The complicated influence of S1P on intimal hyperplasia depends on the diversity of S1P/S1PR signaling via distinct G protein subtypes. S1P: sphingosine-1-phosphate, S1PR: sphingosine-1-phosphate receptors, Erk: extracellular signal-regulated kinase. SMA: α-smooth muscle actin, VSMC: vascular smooth muscle cell. (Provided by Günter Daum)

Sphingosine-1-phosphate receptors 1 and 2: S1PR1 is indispensable for vasculogenesis during embryogenesis in vertebrates. *S1pr1-/-* mice die in utero from severe hemorrhage associated with immaturity of the vascular system (Allende et al. 2003). S1PR1 signaling is mainly acknowledged to exert an anti-atherosclerotic effect (Potì. et al. 2013) based on its activity in EC barrier protection (Camerer et al. 2009), attenuating monocyte adhesion (Bolick et al. 2005) and reducing pro-inflammatory adhesion protein expression (Galvani et al. 2015). On the other hand, S1PR1 may promote IH after arterial injury by stimulating VSMC migration and proliferation. Its capacity for IH induction is supported via the enhanced S1PR1-$G\alpha_{i/o}$ protein signaling (Braetz et al. 2018). Additionally, S1PR1 expression is required for lymphocyte egress from lymph organs into blood circulation. A high level of S1P in the blood induces S1PR1 internalization and then the S1PR1 expression recovers under a low S1P level environment upon lymphocyte migration through high endothelial venules into lymph nodes to allow the sense and chemotaxis of lymphocytes to high S1P concentration environment again (Tsai and Han 2016). The participation of S1PR1 signaling in immune cell migration generates a robust correlation between its activity and inflammatory response in tissues (Kim et al. 2023).

S1PR2 mainly couples to $G\alpha_{12/13}$ (Ishii et al. 2002), which can counteract the anti-inflammatory actions of S1PR1-$G\alpha_{i/o}$ signaling in the endothelium (Zhou et al. 2022). S1PR2 deficiency has been discovered to reduce aortic atherosclerotic lesions in *ApoE-/-* mice, suggesting a promoting effect of S1PR2 on atherosclerosis (Ganbaatar et al. 2021). Previous research also claimed reduced macrophage-like foam cells in the atherosclerotic plaques as well as decreased inflammatory cytokines in the serum of *ApoE -/- S1pr2-/-* mice (Skoura et al. 2011). In converse, S1PR2 deficient mice exhibit larger neointimal lesions after arterial injuries (Shimizu et al. 2007, Grabski et al. 2009), possibly due to enhanced VSMC migration and phenotypic modulation as both processes are inhibited by S1PR2 (Inoue et al. 2007, Grabski et al. 2009). In

line, recent research reported that the local application of myeloid-derived growth factor protected rat carotid arteries against VSMCs dedifferentiation and neointima formation after balloon injury via its affinity to S1PR2. This inhibitory effect was circumvented by the S1PR2 antagonist or ROCK signaling inhibitor application (Yang et al. 2024).

Sphingosine-1-phosphate receptor 3: The functions of S1PR3 are complicated. S1PR3 has been shown to activate pro-inflammatory pathways in the endothelium by binding to $G\alpha_{12/13}$ and $G\alpha_{q}$ and increase vascular endothelial permeability in lipopolysaccharides (LPS) induced inflammation (Sammani et al. 2010). On the other hand, it has been shown that HDL induces endothelial proliferation and migration to enhance barrier integrity and promote vascular angiogenesis through S1PR3-dependent VEGFR2 activation (Jin et al. 2018). S1P can induce endothelial progenitor cell (EPC) proliferation via binding to S1PR3, indicating the protective role of S1PR3 in arterial stenosis (Wang et al. 2018). The intravenous infusion of EPCs pre-incubated with S1P has been proven to restore blood flow in mouse ischemic hind limbs and alleviate arterial ischemic symptoms. Whereas in *S1pr3 -/-* mice, the EPCs exhibit attenuated angiogenesis activity and migration under S1P stimulation, and blood flow recovery is dramatically reduced in the artery ligation model (Walter et al. 2007). Applying models of IH, one study in *S1pr3-/-* mice noticed more pronounced lesion formation after carotid artery ligation (Keul et al. 2011). In contrast, the study from Shimizu et al. (Shimizu et al. 2012) on the iliac artery denudation model reported a remarkable reduction in neointimal lesion size by 90% in the *S1pr3-/-* mice, indicating the IH promotion activity of S1PR3. Another study confirmed with siRNA-induced S1PR3 inhibition that PDGF-B-induced migration of VSMCs was mediated by S1PR3 (Mousseau et al. 2012). The acquisition of high S1PR3 expression in cultured mice VSMCs via retroviral gene transfer promoted S1P-mediated cell migration and proliferation. However, Shimizu et al found the S1P/S1PR2/Rho signaling was not inhibited by overexpression of *S1pr3* in these cells (Shimizu et al. 2012). In addition, S1PR3 signaling in EC mediates vasodilation via the $G\alpha_{i/o}$/PI3K/PKB/NOS3 coupling, while

vasoconstriction could prevail in VSMC via coupling of S1PR3 to $G\alpha_{12/13}$/Rho and $G\alpha_q/Ca^{2+}$ (Cantalupo et al. 2017, Katunaric et al. 2022).

S1PR3 participates in multiple biological activities of immune cells. P-selectin-dependent leukocyte rolling as a critical initial step in inflammatory cell recruitment can be induced by intra-arterial injection of S1P and is diminished by S1PR3 or $G\alpha_q$ deficiency (Nussbaum et al. 2015). In an earlier study by Keul et al. (Keul et al. 2011), although S1PR3 deficiency had no impact on lesion size in *ApoE-/-* mice, macrophage density was remarkably reduced, indicating the activity of S1PR3 in promoting macrophage recruitment. The necessity of *S1pr3* expression for cholesterol efflux from cultured macrophage has been proven as well (Vaidya et al. 2019). Keul et al. (Keul et al. 2022) found that *S1pr3* and *ApoE* double knockout mice fed with a high-cholesterol diet exhibited reduced cholesterol efflux from macrophage and manifested larger lesions compared to *ApoE-/-* mice expressing *S1pr3*. Moreover, the inhibition of macrophage apoptosis by HDL-associated S1P is mediated via S1PR3, indicating its plaque-stabilizing effect in advanced atherosclerosis (Feuerborn et al. 2017). S1PR2/3-dependent $G\alpha_{i/o}$/PI3K signaling has also been identified to mediate S1P-induced M1 polarization in bone marrow macrophages (Yang et al. 2018). Heo et al. (Heo and Im 2019) demonstrated that TY52156, as a selective S1PR3 antagonist, inhibited LPS-induced pro-inflammatory factor expression, such as cyclooxygenase-2 (COX2), NOS2, IL-1β, IL6, and TNFα in peritoneal macrophages.

Table 1 Functions of S1PR3 signaling at the cellular level

Cell Type	The function of S1PR3 signaling
ECs and EPCs	● increases vascular endothelial permeability ● promotes EC migration and proliferation ● promotes angiogenic activity and proliferation of EPC ● promotes endothelium-dependent vasorelaxation
VSMCs	● regulates VSMC proliferation and migration ● regulates VSMC-dependent vascular tone
Immune cells	● promotes leukocyte rolling by mobilizing endothelial P-selectin ● mediates macrophage recruitment

	• facilitates cholesterol efflux from macrophages • inhibits macrophage apoptosis • promotes M1 polarization • promotes expression of inflammatory cytokines

EC: endothelial cell, EPC: endothelial progenitor cell, VSMC: vascular smooth muscle cell.

Considering the multiple functions at the cellular level (see Table 1), S1PR3 could be a key regulator in IH. To study the importance of S1P and S1PR3 in IH, an abdominal aortic clamping injury model in C57BL/6 mice has been established in our lab (Jiang 2021, dissertation). Subsequently, it was shown in this model that *S1pr3-/-* mice exhibit decreased neointimal lesions after injury when compared to wild-type mice (von Lucadou 2023, dissertation). In my thesis, the abdominal aortic clamping model is used to determine the S1PR3-dependent gene alterations after arterial injury to explore the mechanism by which S1PR3 inhibits IH development. In addition, mice are applied to continuous DOP or heparin application to investigate the effect of SPL inhibitor or heparin on S1P serum concentration, and their subsequent impact on neointima formation after clamping surgery to evaluate the role of S1P level maintenance in IH development.

2. Aim of the study

This thesis addresses two main questions.

1. To explore S1PR3-dependent changes in the expression of specific genes of interest during the response to arterial injuries. For this purpose, the abdominal aorta will be removed from *S1pr3* +/+ or *S1pr3*-/- mice at 4, 7, 14, 21, and 28 days after the clamping surgeries and from *S1pr3* +/+ or *S1pr3*-/- control mice without surgery. To detect the expression of the target genes in the abdominal aorta, the adventitia will be separated from the media. The expression of the genes will be determined by real-time quantitative polymerase chain reaction (RT-qPCR).

2. To explore the impact of DOP and heparin on IH development. DOP is an inhibitor of SPL and has been shown to elevate S1P levels in blood. This may affect IH formation by stimulating VSMC proliferation and migration, or by inhibiting inflammation via preventing leucocyte egress. Heparin will be used to test the hypothesis that heparin may inhibit IH by lowering S1P levels in blood. Firstly, using oral application (DOP) or intraperitoneal injection (heparin), the effects of DOP and heparin on S1P levels in blood will be measured. Secondly, the effects of continuous DOP and heparin application on IH will be examined using the aortic clamping model.

3. Methods and materials

3.1 Animal procedures

All studies with laboratory animals were approved by the local animal care committee (Behörde für Lebensmittelsicherheit und Veterinärwesen, Freie und Hansestadt Hamburg), project number: N093/19. Operations on mice were performed under guidelines from the animal facility of the University Hospital Hamburg-Eppendorf (UKE). C57BL/6 mice, *S1pr3-/-* mice, and their wild-type littermates (*S1pr3+/+*) were used in the experiments.

3.1.1 Sphingosine-1-phosphate receptor 3 knock out mice

The *S1pr3+/+* and *S1pr3-/-* mice (Kono et al. 2004) were kindly provided by Dr. Günter Daum (Vascular Medicine, University Medical Center Hamburg-Eppendorf). The *S1pr3* mice were maintained on heterozygous breeding, and the *S1pr3+/+* and *S1pr3-/-* littermates were generated by homozygous breeding. Only male animals were used for the experiments.

3.1.2 Abdominal aorta clamping model

For preparation, the mouse was weighed and injected with a mixture of buprenorphine (0.1mg/kg body weight, Bayer Vital GmbH, Germany) and carprofen (0.006 mg/kg body weight, Pfizer GmbH, Germany) diluted in Ringer's solution (B. Braun Melsungen AG, Germany) subcutaneously 30 min before surgery. Anesthesia was induced with 4-5% isoflurane (Baxter Deutschland GmbH, Germany) in the anesthesia chamber and maintained at a concentration of 1.5% – 2% via a mask throughout the surgery. The operation was performed on a warming platform, and the mouse eyes were protected with eye ointment (Dr. Mann Pharma GmbH, Germany). After fixing the mouse, the surgical area was shaved and disinfected with betaisodona (0.1 g/ml ACA Müller/ADAG Pharma AG, Germany) and 70% ethanol. A 2 cm - 2.5 cm skin incision was made along the midline of the abdomen with scissors (Fine Science Tools, USA). Then, the peritoneum was cut along the white line to avoid bleeding. For a more precise surgical field, the intestines were carefully placed on a piece of gauze near the incision by two cotton swabs and covered with another piece of gauze. The gauze and swabs were moistened with Ringer's to protect the

gastrointestinal tract from drying out. Three retractors (Fine Science Tools) were used to lateralize surrounding tissues to expose the abdominal aorta. The infrarenal abdominal aorta was separated from the inferior vena cava with two forceps (Fine Science Tools), and if present, the arterial branch above the vena cava was cut after ligation with a 10-0 ETHILON suture (Johnson & Johnson Medical Ltd, USA). After preparation, a strong pressure clamp (Fine Science Tools) was applied to the infrarenal abdominal aorta in 4 continuous locations for 2 minutes per clamping from the proximal part of aortic bifurcation (see Figure 5). This procedure was repeated three times. After the clamping procedure, the moistened intestines were moved back into the abdominal cavity. The peritoneum was closed with a continuous 6-0 absorbable suture (Healthium Medtech Limited, USA), and the skin wound was closed with a 6-0 silk mattress suture (Johnson & Johnson Medical Ltd), followed by disinfection. Metamizole (200 mg/kg body weight, Ratiopharm GmbH, Germany) and tramadol (12 mg/kg body weight, Grünenthal GmbH, Germany) were administered via drinking water for pain prophylaxis after anesthetic resuscitation for seven days. Daily assessments on the wound and status were conducted until sacrifice.

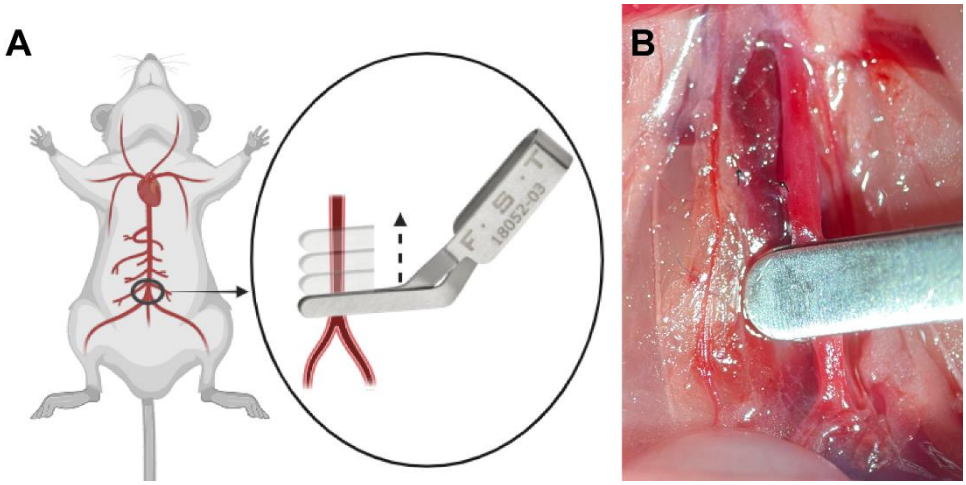

Figure 5 Abdominal artery clamping procedure. (A) A high-pressure vascular clamp was applied to the infrarenal abdominal aorta after laparotomy from the proximal part of the bifurcation for 2 min at four continuous sites. (B) The photo of the clamping procedure during the surgery.

3.1.3 Drug application

Application of heparin: Heparin was applied as a bolus or as a combination of a bolus and a continuous infusion via intraperitoneal implantation of osmotic pumps (Alzet pump Model 1007D, Durect Corporation, USA) with a release rate

of 0.5 µl/h efficacious for 7 days. Bolus heparin (1000 IU/kg body weight) was injected intraperitoneally for individual application. As a combination, the pump was filled with the heparin (500 IU/kg per 24 hours, body weight, B. Braun Melsungen AG) diluted in the Ringer's solution and then placed for 30 minutes in the Ringer's solution in advance. After clamping the abdominal artery, the pump was put inside the abdomen, followed by the closure of the peritoneum (see Figure 6). A dose of heparin (400 IU/kg body weight) was injected intraperitoneally right after the suture. Ten days after the clamping operation, the pump was removed through the original incision under inhalational anesthesia with isoflurane. The peritoneum and the skin were closed separately, and cotton swabs were used to stop bleeding if necessary.

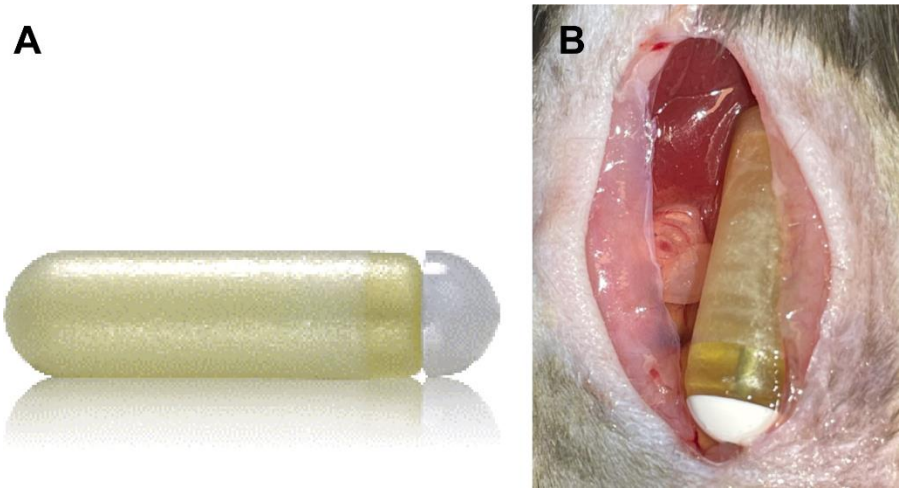

Figure 6 Application of heparin via osmotic pumps. (A) The pump used in the procedure with a volume of 100 µl can deliver drugs continuously at a controlled rate of 0.5 µl/h for 7 days. (B) The pump was implanted before the closure of the peritoneum.

Application of sphingosine-1-phosphate lyase inhibitor: DOP (4-deoxypyridoxine) was applied via drinking water (30 mg/l, Sigma-Aldrich Company, Germany). The application started seven days before the surgical procedure and continued until the third day after the operation. The drinking water with DOP was freshly prepared every day.

3.1.4 Sacrifice and aorta collection

An intraperitoneal injection of an overdose of pentobarbital (800 mg/kg body weight, Boehringer Ingelheim Vetmedica GmbH) was applied to sacrifice the mouse. The abdominal and thoracic cavities were fully opened along the original incision. The right ventricle was slightly incised to allow perfusate to

drain off. Ice-cold Ringer's solution was then injected into the left ventricle with a 22G infant scalp needle until the perfusate became clear. Depending on the further analysis, the following procedure was used.

For qPCR analysis, after perfusion of Ringer's solution, the different parts of the aorta were transferred into 500 µL enzyme mix (see Table 8), followed by incubation at 37°C for 15 min. The tissue samples were placed on a petri dish filled with cold Ringer's solution. The adventitia and media (including the endothelium or neointima) of the aorta artery were carefully separated under a microscope. The samples were stored in RNAlater (ThermoFischer Scientific, Germany) at room temperature for 24 hours and then frozen at -20°C for further procedures.

For histology, 20 ml of 4% formalin (Grimm med. Logistik GmbH, Germany) was then perfused and the aortic arch, thoracic aorta, and abdominal aorta were separated and stored in 4% formalin under room temperature individually.

3.2 Histology

3.2.1 Paraffin embedding and cutting

After fixation for 24 hours in formalin, dehydration was performed on the tissue sample according to the procedure below (see Table 2). The abdominal aorta sample was cut in half along the middle. The two halves were kept upright in melted paraffin (Sakura Finetek Germany GmbH, Germany) with the cutting side downwards in a metal cassette. The block was cooled down at -10°C for at least 30 minutes till the paraffin solidified. Then, the paraffin block was removed from the metal cassette and stored at -20°C for more than 24 hours before cutting. A slide microtome (Leica Mikrosysteme Vertrieb GmbH, Germany) was used to cut the frozen tissue block, and five serial 3 µm cuts were contained on one slide. After every ten slides, 20 µm of the tissue block was discarded. Five groups, 50 slides in total, were cut from one tissue block, and one slide was taken from each group for histology examination. As each cut included two samples of the abdominal aorta, one from the proximal part and one from the distal, ten data points were finally available for one abdominal aorta sample.

Table 2 Procedure of tissue fixation and dehydration

Procedure	Time
70% Isopropanol	20 min
70% Isopropanol	20 min
80% Isopropanol	20 min
85% Isopropanol	20 min
90% Isopropanol	20 min
90% Isopropanol	20 min
96% Isopropanol	20 min
96% Isopropanol	20 min
100% Isopropanol	20 min
100% Isopropanol	20 min
56°C Paraffin	45 min

3.2.2 Elastic van Gieson staining

The slides were first deparaffinized in xylene (Th. Geyer GmbH & Co. KG, Germany) three times (5min each), dehydrated in 99% ethanol (Walter CMP, Germany) two times, in 96% ethanol one time, and then in 70% ethanol one time (5 min each). The slides were stained in 1% resorcin fuchsin solution (Waldeck GmbH & Co KG, Germany) for 25 min, after which the excessive dye was rinsed off with tap water and again with distilled water. The tissues were differentiated with 70% ethanol incubation until elastic fibers turned dark purple under the microscope, and water washing terminated the differentiation. The next step was incubation in Weigert's ferric-hematoxylin (Waldeck GmbH & Co KG) for 15 min, and the slides were then washed in water for 10 min. The slides were transferred into distilled water before incubation with thiazine red picric acid solution (AppliChem GmbH, Waldeck GmbH & Co KG) for 5 min. The following wash steps (5 min each) were carried out first in distilled water, then in 70% ethanol and 96% ethanol. Finally, the tissue sections were dehydrated in 99% ethanol two times (5 min each) and washed in xylene three times (5 min

each). The slides were covered by coverslips with permanent mounting media (Sigma-Aldrich Co.) in between. Drying took place overnight at room temperature.

3.2.3 Histology analysis

For the morphometric analysis, one EvG-stained slide per level was randomly selected. As five levels, including ten sections, have been cut from the tissue block, ten measurements were performed for each abdominal aorta sample. The sections were scanned with the Zeiss Axio Scan Z1 (Carl Zeiss AG, Germany), and high-quality photos were taken with the NetScope program (Net-Base Software GmbH). The ImageJ program (National Institute of Health, USA) measured the figures, and the scale of the figure was set at the beginning of the measurement. For statistical analysis, at least 6 levels should be available for evaluation (3 from the distal part and 3 from the proximal part). Using the 'Polygon Selection' tool of the ImageJ program, the EEL (external elastic lamina) and the IEL (internal elastic lamina) were marked. If a neointima was visible, the border of the lumen was also determined manually. After selection, the software automatically measured the circumference and area of each component. Each figure was measured individually (see Figure 7). The size of the media and neointima were calculated as follows:

Area of Media = Area under EEL - Area under IEL

Area of Neointima = Area under IEL - Area under Lumen

Size of Lesion (I/M value) = Area of Neointima/ Area of Media

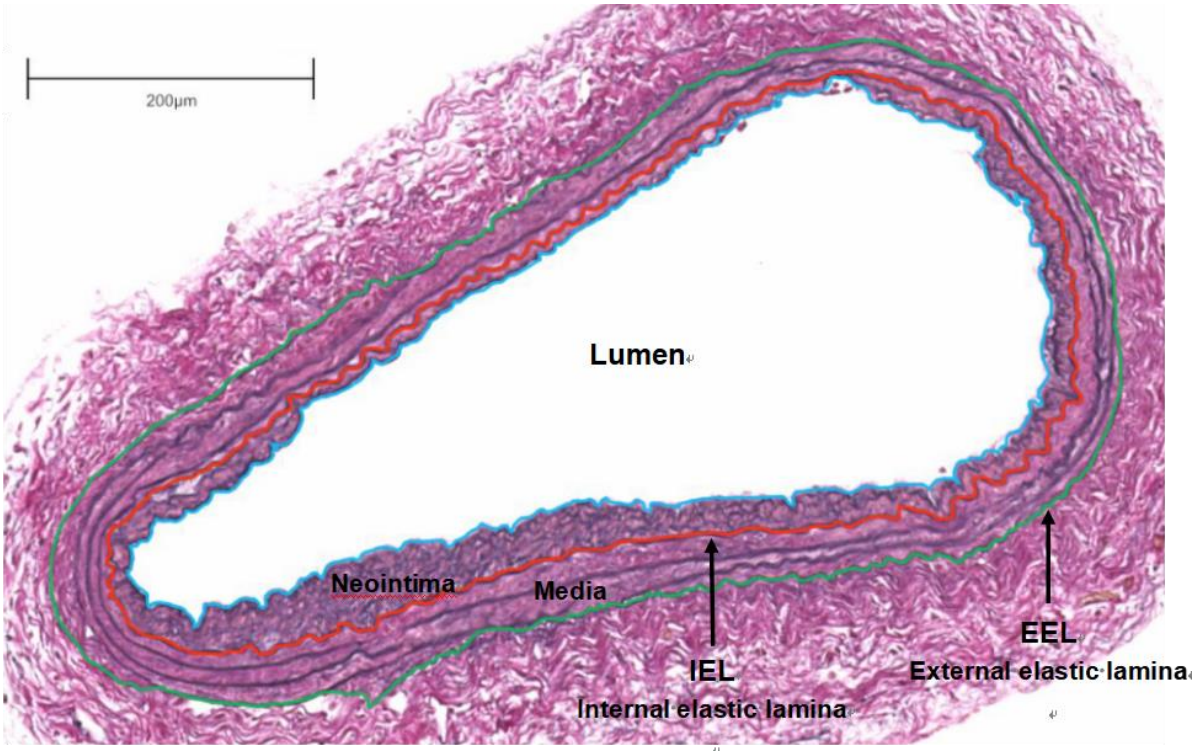

Figure 7 Illustration of morphological measurement. The samples of the abdominal aorta from mice underwent EvG staining. Lesions formed between the lumen and internal elastic lamina. IEL: internal elastic lamina; EEL: external elastic lamina; Blue line: outline of internal lumen; Red line: outline of internal elastic lamina; Green line: outline of external elastic lamina. Scale bars equal 200 μm.

The ratio of intima and media (I/M ratio) was calculated at each level from the abdominal aorta samples. The average of 10 levels in each group was calculated for the final analysis.

3.3 Measurements of gene expression by real-time quantitative polymerase chain reaction

3.3.1 RNA isolation and concentration measurement

RNA extraction from tissues was done with the RNeasy® Fibrous Tissue Mini Kit (Qiagen GmbH, Germany). Each sample in the RNA-later solution containing adventitia or media of infrarenal abdominal aorta from two mice was marked and kept on ice. The tissues from each sample were crushed by the scalpel on a slide and then transferred into a 2 ml reaction tube with two metal beads inside. 300 μl buffer RLT mixed with 3 μl β-mercaptoethanol (ThermoFischer Scientific) was added to the reaction tube. To homogenize the samples, they were placed in the TissueLyser® LT (Qiagen GmbH) for four

cycles, mixing at 500 Hz for 5 min each time. The samples were cooled on ice while the container was cooled on dry ice for 5 min after each cycle. The solution in each reaction tube was then transferred into a new 1.5 ml reaction tube, mixed with 590 µl of RNase-free water and 10 µl proteinase K, and incubated at 55°C for 30 min. The supernatant of each sample was collected into a 1.5 ml reaction tube after centrifugation at 10,000 x g for 3 min. 450 µl of 99% ethanol was added to the sample and pipetted several times. 700 µl of the mixed solution was transferred onto a RNeasy Mini column placed in a 2 ml collection tube, and the flow through the column was discarded following centrifugation at 10,000 x g for 1 min. This step was repeated with the remaining sample solution. Buffer RW1 (350 µl) was added to the column before centrifuging at 10,000 x g for 1 min. After discarding the flow through, the mixture of DNase stock solution (10 µl) and buffer RDD (70 µl) was pipetted onto the membrane at the bottom of the column. The column stood at room temperature for 30 min with the lid open. Afterward, a 3-step washing procedure was performed in order, while centrifugation at 10,000 x g for 1 min was carried out after each step. Buffer RW1 (350 µl) was first used, followed by the buffer RPE (500 µl) for two rounds. The column was placed into a new collection tube and centrifuged at 10,000 x g for 2 min to remove the remaining liquid. The RNA was extracted with 50 µl RNase-free water by centrifugation at 10,000 x g for 1 min. Before further experiments, the RNA samples were stored under -20°C or -80°C for the long term.

The concentration and purity of the RNA samples were measured by the Epoch™ Spectrophotometer (BioTek Instruments, Inc., USA). In one measurement, 2 µl of each RNA sample was applied to a microtitre plate while nuclease-free water was used as a blank. According to Lambert-Beer's law, the quantity of the RNA sample was determined by the absorbance at a wavelength of 260 nm. The purity of the RNA sample was measured by the optical density ratio at 260 nm (maximum absorbance of nucleic acids) or 280 nm (maximum absorbance of proteins), and a quotient between 1.8 and 2.0 indicated pure RNA isolation. The data was analyzed with Gen5™ 2.0 software.

$E_{260} = \varepsilon_{260} \times c \times d \rightarrow c = \frac{E260}{\varepsilon 260 \times d}$

E, absorbance at 260 nm

Ɛ, RNA specific extinction coefficient at 260 nm

c, RNA concentration (ng/µl)

d, length of the light through (1 cm)

3.3.2 cDNA synthesis

To synthesize the complementary DNA, the reaction mixtures were prepared with the cDNA reverse transcription kit (ThermoFischer Scientific). A total volume of 20µl components was mixed on ice, and the protocol is shown below (see Table 3).

Table 3 The protocol of reaction components for cDNA synthesis

Component	Volume
10 x RT Buffer	2 µl
25 x dNTP Mix (100mM)	0.8 µl
10 x RT Random Primers	2 µl
MultiScribe™ Reverse Transcriptase	1 µl
Template RNA	200 ng
Nuclease-free H_2O	to 20 µl

The reaction mixtures were vortexed and then briefly centrifuged. The samples were placed in the PCR machine (Bio-Rad Laboratories, Germany) for synthesis reaction. The thermal cycler was programmed (BioTek®) using the conditions below (see Table 4). After synthesis, the cDNA samples were stored in the fridge at -20°C until further steps.

Table 4 The incubation conditions for cDNA synthesis

Settings	Temperature	Time
Step 1	25°C	10 min
Step 2	37°C	120 min
Step 3	85°C	5 min
Step 4	4°C	Hold

3.3.3 RT-qPCR and result analysis

The target gene expression in the obtained cDNA samples was quantified by real-time quantitative polymerase chain reaction with the Rotor-Gene® SYBR® Green PCR Kit (Qiagen GmbH). The SYBR Green stain preferentially binds to double-stranded DNA so that the fluorescence intensity would increase in proportion to the amount of amplicon. The Rotor-Gene Q real-time PCR cycler (Qiagen GmbH) carried out all the measurements and analyzed them with the manufacturer's software (Rotor-Gene Q Series, Version 2.3.1, Qiagen GmbH). For each sample, three independent aliquots were tested, while the expression of the housekeeping gene glyceraldehyde-3-phosphate dehydrogenase (*Gapdh*) was used as the reference gene. The number of elapsed cycles was depicted on the X-axis, and the fluorescence intensity was depicted on the Y-axis. In order to evaluate the relative concentration of the target genes, the curves of the target gene were compared to the reference gene. A threshold value was set in the linear increasing section of the exponential curve to determine the CT value (cycle threshold), describing the specific cycle at which the preset threshold was exceeded. The lower CT value represented a higher concentration of cDNA. When the curve was below the defined threshold, the CT value was recorded as 40. Each sample was pipetted in triplicates, and the average of the three CT values was recorded when the standard deviation was smaller than 0.5. Otherwise, the measurement was repeated. The primers used for RT-qPCR in this study have been listed below in Table 5.

Table 5 The list of primers used for RT-qPCR

Gene	Forward Primer	Reverse Primer
Gapdh	5'-TCCTGCACCACCAACTGCTT-3'	5'-AGGGGCCATCCACAGTCTTC-3'
Adamts5	5'-CCCAGGATAAAACCAGGCAG-3'	5'-CGGCCAAGGGTTGTAAATGG-3'
Adamts15	5'-TCTACACCTGACGCCAGATG-3'	5'-TCACATACCCGGAATAGAAGCA-3'
Palld	5'-AGAAACTGAGGAGCCAAGAAGT-3'	5'-AGTGGATCTGAACGTCAGGAC-3'
Comp	5'-ACTGCCTGCGTTCTAGTGC-3'	5'-CGCCGCATTAGTCTCCTGAA-3'
Nos2	5'-GTTCTCAGCCCAACAATACAAGA-3'	5'-GTGGACGGGTCGATGTCAC-3'

Nlrp3	5’-ATCAACAGGCGAGACCTCTG-3’	5’-GTCCTCCTGGCATACCATAGA-3’
Csf2	5’-AGGGTCTACGGGGCAATTTC-3’	5’-GGCAGTATGTCTGGTAGTAGCTG-3’
Tbxa2r	5’-GTGGTCTTCGGGCTCATATTC-3’	5’-CCCACGAGCTGAACCATCAT-3’
Tf	5’-TCAAGCACGGGAAAGAAAAC-3’	5’-CTGCTTCCTGGGCTATTTTG-3’
Fr21	5’-CGCAGCGTTTTACGGGAAC-3’	5’-CTGGATCGGATACACCACCG-3’
Pai1	5’-CAAGCTCTTCCAGACTATGGTG-3’	5’-ACCTTTGGTATGCCTTTCCAC-3’
Cd19	5’-TTCCGGTGGAATGCTTCAGAC-3’	5’-GTTCCCCAGACCTTAGGATGG-3’

For each reaction, a mixture of 3 µl RNase-free water, 5 µl SYBR Green solution, and 1 µl target or housekeeping gene primer mix (forward and reverse) was added into a reaction tube. 1 µl of the cDNA sample was then pipetted into the reaction tube. The qPCR reaction was performed under the conditions in Table 6.

Table 6 The RT-qPCR conditions

Procedure	Temperature	Time	Cycle
1. Initial Denaturation	95°C	10 min	1
2. Denaturation	95°C	10 s	
3. Annealing	60°C	15 s	40
4. Elongation	72°C	20 s	
5. Melting curve	72°C – 95°C	90 s per 1°C	1

The raw data of the qPCR measurement was determined using the Roter Gene software and then analyzed with Microsoft Excel according to the following formula:

$$Target\ gene\ expression\ (\%Gapdh) = 2^{-(CT\ (Target\ gene) - CT(GAPDH))} \times 100$$

The average CT value of the three repeats for each sample was calculated. The expression of the target gene was normalized by *Gapdh* (housekeeping gene) and recorded as a percentage.

3.4 Flow cytometry

Flow cytometry analysis was performed by Dr. Björn Rissiek (Experimental Research Group in Stroke and Inflammation, Head and Neurology Centre, University Medical Center Hamburg-Eppendorf). The peripheral blood of untreated mice, mice with DOP application (30 mg/l) for 7 days, and mice accepted clamping surgeries with DOP application (7 days in advance and 3 days after) were taken via submandibular veins. 100-150 µl blood of each mouse was collected in the 1.5 ml Eppendorf tube, respectively. The determination was conducted with BD FACS Symphony after proper sample preparation. In the experiment, the number of CD4(+) T helper cells, CD4(+) T regs, CD8(+) T cells, B cells, monocytes, neutrophils, and natural killer (NK) cells were counted in each blood sample and analyzed with BD Flowjo software.

3.5 Determination of the sphingosine-1-phosphate concentration

The quantification of S1P concentrations in the serum and tissues was performed according to a protocol established previously in the lab (von Lucadou 2023, dissertation). In brief, peripheral blood was taken from mice by punctuating submandibular veins. Tissue samples (spleen and thymus) were taken from mice after sacrifice. Quantification was carried out by applying liquid chromatography-tandem mass spectrometry (LC-MS/MS).

3.5.1 Calibration and sample preparation

The blood sample was centrifuged at 2500 x g for 15 min and serum was aliquoted into 20 µl each in a low protein binding microcentrifuge tube (ThermoFischer Scientific) and stored at -20°C. For tissue samples, preparation steps were first applied, and the protein concentration was also determined for statistic standardization. Each tissue sample was cut into small pieces with a scalpel and collected into a 2ml tube with two metal beads. 300 µl RIPA buffer (150 mM NaCl, 1.0% NP-40, 0.5% Na-deoxycholate, 0.1% SDS, 50 mM Tris-HCl pH8) was added into each tube, followed by 4 cycles of mixing on Tissue Lyzer (Qiagen GmbH) at 500 Hz for 5 min each time. Subsequently, the supernatant was transferred into a new 1.5 ml tube for 5 min centrifugation at a speed of 14000 x g. 20 µl of the supernatant was pipetted into a low protein binding microcentrifuge tube for S1P concentration determination while the rest was frozen at -20°C.

All pipette tips and microtitre plates were siliconized in advance. Sigmacote (Sigma-Aldrich Co.) was pipetted into the microtiter plates and then poured out again. The siliconized materials were washed with distilled water and dried overnight at 60°C in a drying cabinet. Calibrator solutions were prepared for each microtitre plate. 20 µL of serum or tissue homogenate were added to 20 µL of 1 µmol/L stable isotope-labeled internal standard d7-S1P (Avanti Polar Lipids, Alabaster, AL, USA) solved in methanol and 350 µL of acetonitrile/water (80/20, vol/vol) in a 1.5 ml Eppendorf tube. The tube was then vortexed thoroughly and centrifuged for 15 min at 10,000 x g at 4°C. The supernatant (200 µl) was transferred to one well of the 96-well microtitre plate.

3.5.2 Liquid chromatography-tandem mass spectrometry

Supernatants were subjected to ultra-performance liquid chromatography on an AQUITY UPLC BEH C8 1.7 µm column (2.1x75 mm, Waters, Germany) using an elution gradient of the two mobile phases (A) 0.1 % formic acid in water and (B) 0.1 % formic acid in acetonitrile, at a flow rate of 0.4 mL/min over 4.2 minutes. Quantification was performed on a Xevo Triple Quadrupole Mass Spectrometer (Waters) with positive electrospray ionization in the multiple reaction mode. The analytes were ionized in the ion source (positive electrospray ionization, ESI+). The charged molecules are separated in the mass analyzer according to their mass-to-charge ratio (*m/z*) and finally fragmented by collision with the noble gas argon. S1P (*m/z* 380) was fragmented into its daughter ion with the mass-to-charge ratio 264, and S1P-d7 (*m/z* 387) was fragmented into the daughter ion *m/z* 271.

3.5.3 Quantification of sphingosine-1-phosphate

Peak area ratios of analyte and internal standard were calculated for calibration (four levels), quality control (QC-low and -high), and samples and used for quantification. The peak areas of the analytes were calculated using the MS Data Review software. First, the ratio of the peak areas of the calibrators to the internal standard was calculated, and a calibration line was created. The slope of the calibration line was used to determine the S1P concentration of the samples.

$$S1P\ concentration\ [\mu M] = \frac{\frac{AUC\ S1P}{AUC\ IS}}{Slope\ [\frac{1}{\mu M}]}$$

AUC S1P: Peak area of S1P

AUC IS: Peak area of the internal standard (S1P-d7)

The S1P level in the tissue sample was standardized by the protein quantity. If coefficients of variation for QCs were above 10 %, samples were re-analyzed. When the S1P concentration was below the minimum detection level, 0.01µM would be recorded as a result for final statistical analysis.

3.5.4 Determination of the protein concentration in the tissue sample

The protein levels of the tissue samples were evaluated with Advanced Protein Assay Reagent (Cytoskeleton Inc., USA). 1 ml of 1X Advanced Protein Reagent was added into a 1.5 ml tube. 10 µl of the sample solution was added into the same tube. After a slight vortex, 300 µl of the mixture was transferred into a 96-well plate.1X Advanced Protein Reagent was used as a blank control to read the absorbance of the sample at 590 nm by the spectrophotometer (BioTek Instruments, Inc.). The protein concentration was calculated based on the formula:

1.0 OD_{590nm} = 30µg protein per ml reagent per cm.

3.6 Statistical Analysis

The statistical analysis was carried out with GraphPad 8 software. The data were described as average ± standard error of mean (SEM). The comparison of the two groups was analyzed with the unpaired Student t-test and corrected according to the Holm-Šidák method. For comparisons of more groups, an analysis of variance (ANOVA) was performed and a Dunnett test was used as a post-hoc test. A P value < 0.05 was considered statistically significant.

4. Results

The first objective of this study was to determine which genes were differently expressed between *S1pr3*+/+ and S*1pr3-/-* mice in response to arterial injury. The tissues from non-operated mice were included as the baseline and the mice that underwent surgeries were sacrificed on days 4, 7, 14, 21, or 28. The expression levels of different genes were determined separately in media (including endothelium or neointima) and adventitial tissues by RT-qPCR and described as percentages to *Gapdh*. Each data point of the gene expression represents 5 repeats and tissue samples from 2 mice were pooled for one measurement. In total, 60 *S1pr3*+/+ mice and 60 *S1pr3-/-* mice were used.

4.1 Gene expression in the abdominal aorta after arterial injury

4.1.1 Gene expression of ADAMTS proteases

Adamts5 and *Adamts15* encode members of a disintegrin and metalloproteinase with thrombospondin motifs (ADAMTS) protein family. In untreated mice, the mRNA level of *Adamts5* is more than double as high in the adventitia (2.93% of *Gapdh*) than in the media (1.15% of *Gapdh*). After injury, the expression of *Adamts5* in both adventitia and media decreases at day 4, followed by a rapid recovery in the adventitia (see Figure 8A). In the media, gene *Adamts5* expression steadily recovers to reach baseline levels in the *S1pr3-/-* mice after 14 days. Apparently, in *S1pr3*+/+ mice, the recovery of *Adamts5* expression is less pronounced (see Figure 8B).

At baseline, *Adamts15* is expressed at similar levels in the media and adventitia (8.47% of *Gapdh* and 6.58% of *Gapdh,* respectively). In the two strains, decreased *Adamts15* expression is observed in both tissues on day 4 after injury. In the adventitia, the expression recovers to baseline levels within 14 days, while in the media, the expression remains below 50% of the baseline level (see Figure 8C, D). A statistically higher expression of *Adamts15* is observed in the media of *S1pr3-/-* mice (4.89% of *Gapdh*) compared to *S1pr3*+/+ mice (2.44% of *Gapdh*) 28 days after injury (see Figure 8D).

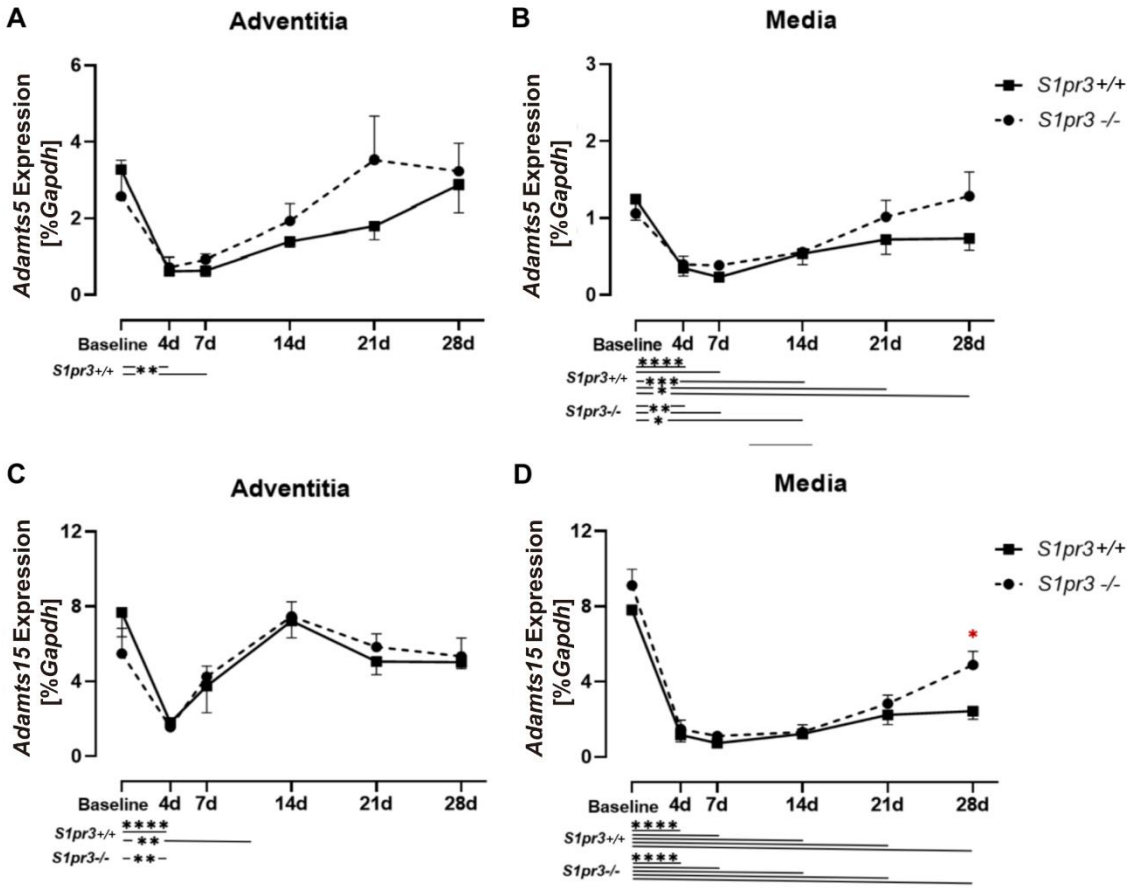

Figure 8 Time-dependent expression of *Adamts5* and *Adamts15* in the adventitia and media of the abdominal aorta after injury. For each data point, n=5 pools (2 aortas each pool). Non-operated mice are included as baseline. (A) Expression of *Adamts5* in the adventitia. (B) Expression of *Adamts5* in the media. (C) Expression of *Adamts15* in the adventitia. (D) Expression of *Adamts15* in the media. Data points are mean±SEM,* P<0.05, ** P<0.01, *** P<0.001, **** P<0.0001. two-sided t-test (*S1pr3*+/+ vs *S1pr3*-/-) and two-way ANOVA (Baseline vs. 4d or 7d or 14d or 21d or 28d).

4.1.2 Gene expression of a cytoskeletal protein

For Palladin (encoded by gene *Palld*), no difference in gene expression levels is observed in tissues between *S1pr3*+/+ and *S1pr3*-/- mice. At baseline, expression is higher in the adventitia (0.023% of *Gapdh*) compared to the media (0.0031% of *Gapdh*) and after injury, it slightly increased in adventitia (see Figure 9A, B).

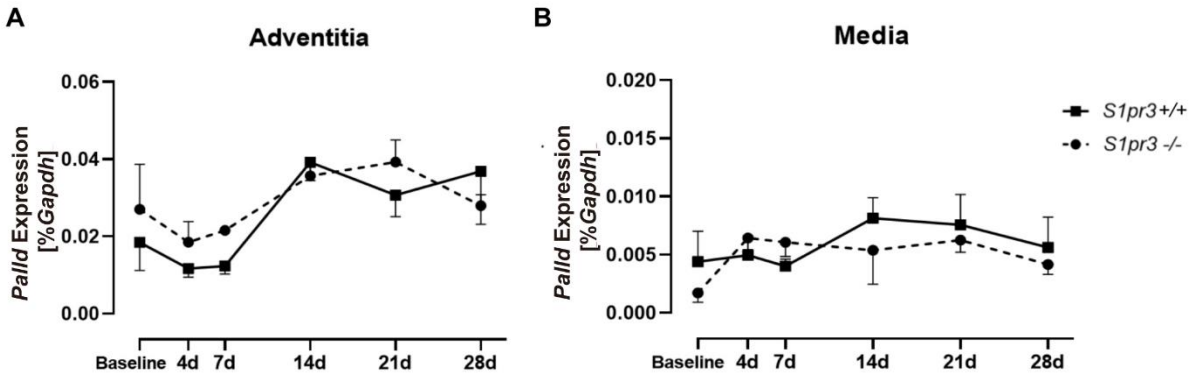

Figure 9 Time-dependent *Palld* expression in the adventitia and media of the abdominal aorta after injury. For each data point, n=5 pools (2 aortas each pool). Non-operated mice are included as baseline. (A) Expression of *Palld* in the adventitia. (B) Expression of *Palld* in the media. Data points are mean±SEM, two-sided t-test (*S1pr3*+/+ vs *S1pr3*-/-) and two-way ANOVA (Baseline vs. 4d or 7d or 14d or 21d or 28d).

4.1.3 Gene expression of a non-collagenous extracellular matrix

Regarding Cartilage Oligomeric Matrix Protein (COMP), also known as thrombospondin-5, no difference in expression is observed between the two genotypes (see Figure 10). *Comp* is expressed 10-fold higher in the adventitia (9.41% of *Gapdh*) compared to media (0.89% of *Gapdh*) in non-operated mice. At later time points after injury, increased *Comp* expression is observed in both media and adventitia. *Comp* expression is found to be over 5-fold increased in the adventitia compared to baseline on day 14 and maintained at a high level subsequently in both strains (see Figure 10A). In the media, an over 10-fold increase in expression compared to baseline is observed after day 21 (see Figure 10B).

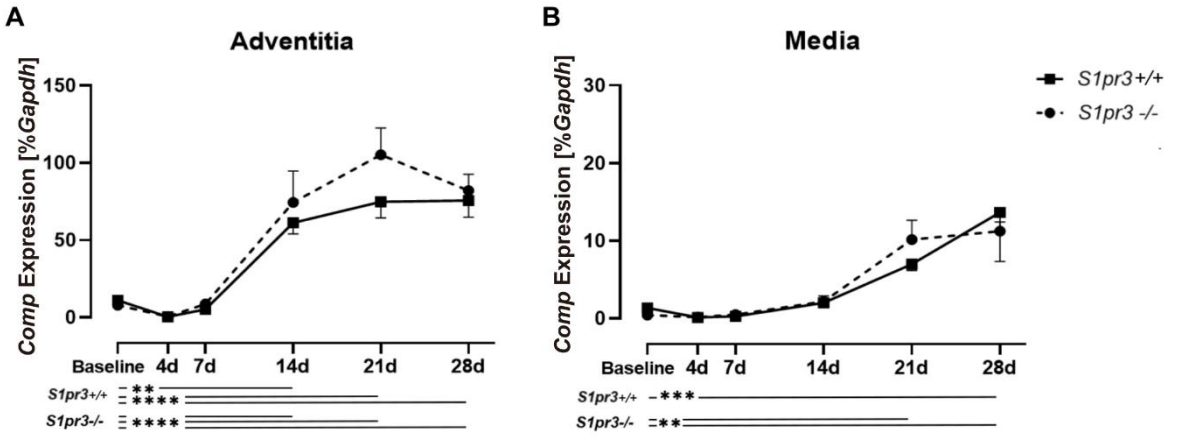

Figure 10 Time-dependent *Comp* expression in the adventitia and media of the abdominal aorta after injury. For each data point, n=5 pools (2 aortas each pool). Non-operated mice are

included as baseline. (A) Expression of *Comp* in the adventitia. (B) Expression of *Comp* in the media. Data points are mean±SEM, ** P<0.01, *** P<0.001, **** P<0.0001. two-sided, t-test (*S1pr3*+/+ vs *S1pr3*-/-) and two-way ANOVA (Baseline vs. 4d or 7d or 14d or 21d or 28d).

4.1.4 Expression of inflammation-related genes

Gene expression of nitric oxide synthase 2

A statistically significant difference in gene expression of *Nos2*, also known as inducible nitric oxide synthase, is observed between *S1pr3*+/+ and *S1pr3*-/- mice after arterial injury (see Figure 11). *Nos2* expression at baseline is very low in media as well as in adventitia and increases in both tissues after injury. In both strains, the highest adventitial expression levels are measured at day 14 whereby the *Nos2* expression in *S1pr3*+/+ mice (0.31% of *Gapdh*) is significantly higher than in *S1pr3*-/- animals (0.13% of *Gapdh*) (see Figure 11A). A rapid induction of expression is also observed in the media of *S1pr3*+/+ mice between day 4 and 7 after injury, while in *S1pr3*-/- mice, expression increases much slower resulting in lower expression levels at day 7 (*S1pr3*+/+ 0.50% of *Gapdh* vs *S1pr3*-/- 0.20% of *Gapdh*) and day 14 (*S1pr3*+/+ 0.68% of *Gapdh* vs *S1pr3*-/- 0.28% of *Gapdh*) compared to wild-type mice (see Figure 11B).

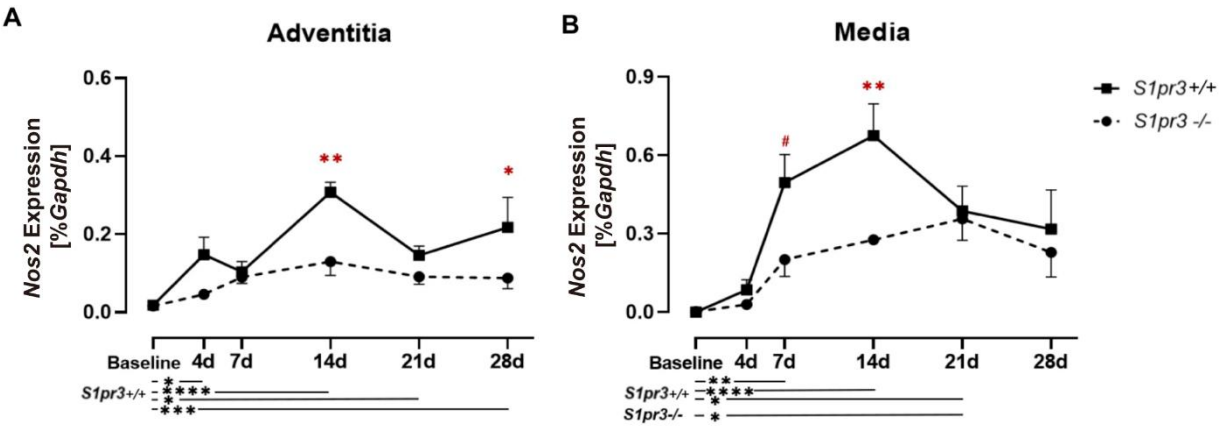

Figure 11 Time-dependent *Nos2* expression in the adventitia and media of the abdominal aorta after injury. For each data point, n=5 pools (2 aortas each pool). Non-operated mice are included as baseline. (A) Expression of *Nos2* in the adventitia. (B) Expression of *Nos2* in the media. Data points are mean±SEM, * P<0.05, ** P<0.01, *** P<0.001, **** P<0.0001. two-sided t-test (*S1pr3*+/+ vs *S1pr3*-/-) and two-way ANOVA (Baseline vs. 4d or 7d or 14d or 21d or 28d).

Gene expression of an inflammasome sensor

Gene *Nlrp3* (Nucleotide-binding oligomerization domain, leucine-rich repeat, and pyrin domain containing 3) encodes a sensor component of the NLRP3 inflammasome. In baseline tissues of both strains, *Nlrp3* expression is higher in

the adventitia (0.27% of *Gapdh*) than in the media (0.0075% of *Gapdh*). Early after injury, *Nlrp3* expression increases over 10-fold in both tissue samples and then stays elevated through all later time points investigated. No statistical difference in expression levels is observed between the two genotypes (see Figure 12A, B).

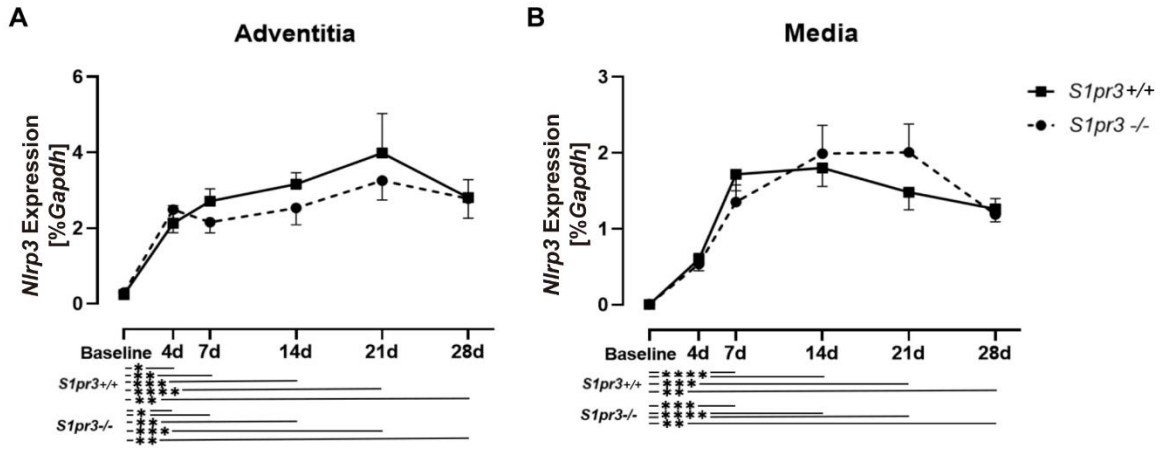

Figure 12 Time-dependent *Nlrp3* expression in the adventitia and media of the abdominal aorta after injury. For each data point, n=5 pools (2 aortas each pool). Non-operated mice are included as baseline. (A) Expression of *Nlrp3* in the adventitia. (B) Expression of *Nlrp3* in the media. Data points are mean±SEM, * P<0.05, ** P<0.01, *** P<0.001, **** P<0.0001. two-sided t-test (*S1pr3*+/+ vs *S1pr3*-/-), and two-way ANOVA (Baseline vs. 4d or 7d or 14d or 21d or 28d).

Gene expression of a proinflammatory cytokine

Gene *Csf2* (Colony Stimulating Factor 2) encodes a pro-inflammatory cytokine mainly derived from ECs, fibroblasts, and hematopoietic cells. *Csf2* expression does not differ statistically between the two genotypes. In the adventitia, injury causes CSF2 expression to decline on day 4 followed by a gradual rebound to baseline levels (see Figure 13A). In the media, *Csf2* expression is barely detectable at baseline, but gradually increases after injury, reaching a peak at day 14 in both genotypes. Then, it gradually falls back to baseline levels (see Figure 13B).

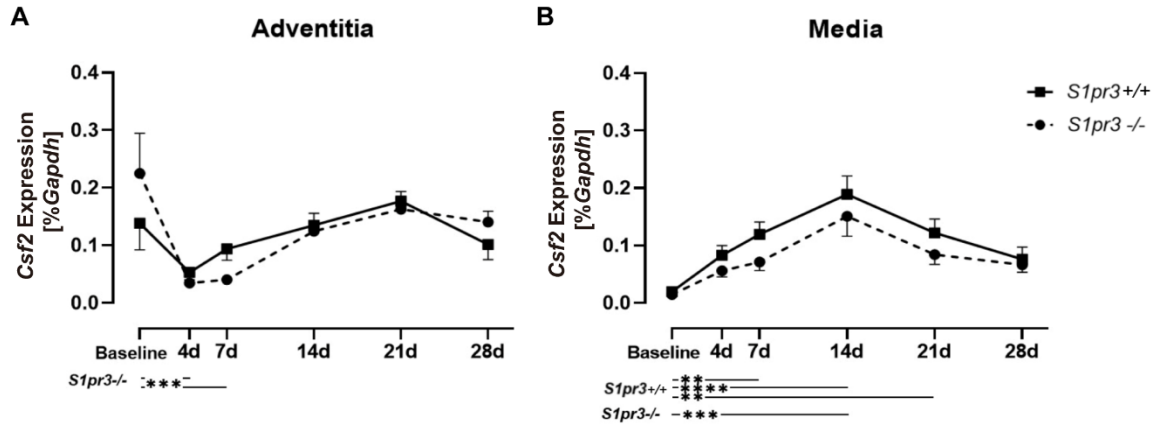

Figure 13 Time-dependent *Csf2* expression in the adventitia and media of the abdominal aorta after injury. For each data point, n=5 pools (2 aortas each pool). Non-operated mice are included as baseline. (A) Expression of *Csf2* in the adventitia. (B) Expression of *Csf2* in the media. Data points are mean±SEM, ** P<0.01, *** P<0.001, **** P<0.0001 two-sided t-test (*S1pr3*+/+ vs *S1pr3*-/-) and two-way ANOVA (Baseline vs. 4d or 7d or 14d or 21d or 28d).

4.1.5 Expression of coagulation-related genes

Gene expression of a thromboxane receptor

Tbxa2r (Thromboxane A2 Receptor) encodes a receptor for thromboxane A2 (TXA2). No statistically significant difference in *Tbxa2r* expression is observed between the two genotypes at any time point investigated. The expression of adventitial *Tbxa2r* declines significantly 4 days after injury, followed by a steady increase of expression to reach baseline levels again (see Figure 14A). In the media, a significant decrease in gene expression is also observed on day 4 after injury, and the expression remains at a lower level till the end of the time course (see Figure 14B).

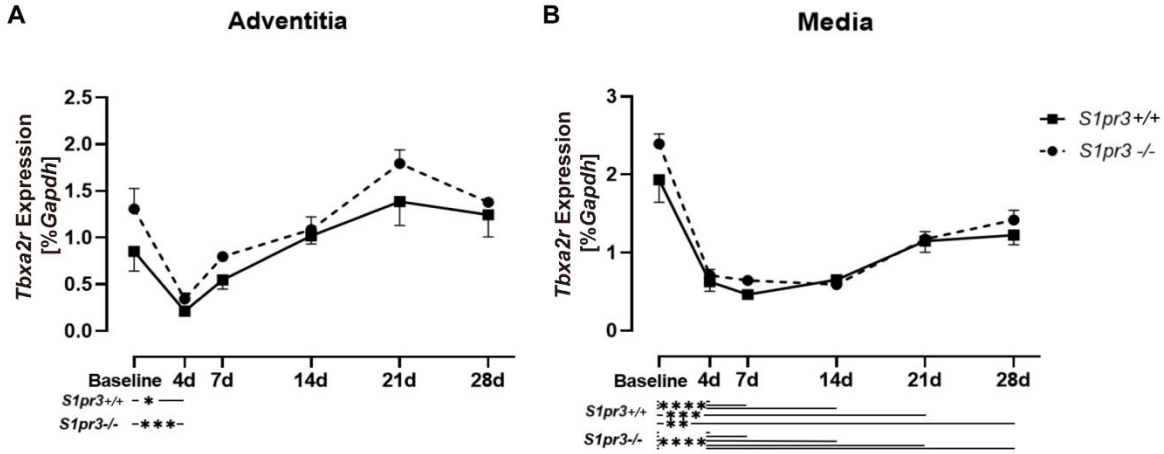

Figure 14 Time-dependent *Tbxa2r* expression in the adventitia and media of the abdominal aorta after injury. For each data point, n=5 pools (2 aortas each pool). Non-operated mice are included as baseline. (A) Expression of *Tbxa2r* in the adventitia. (B)

Expression of *Tbxa2r* in the media. Data points are mean±SEM, * P<0.05, ** P<0.01, *** P<0.001, **** P<0.0001. two-sided t-test (*S1pr3*+/+ vs *S1pr3*-/-) and two-way ANOVA (Baseline vs. 4d or 7d or 14d or 21d or 28d).

Gene expression of a coagulation factor

Tf (Tissue factor) encodes coagulation factor III, typically expressed in fibroblasts. At baseline of both groups of mice, *Tf* is about 40-fold higher expressed in the adventitia (20.51% of *Gapdh*) compared to media (0.45% of *Gapdh*). In both strains and tissues, *Tf* expression exhibits a similar time course, with a pronounced reduction to proximate 10% of baseline levels at day 4 after the operation followed by a slow increase. A significant difference in *Tf* expression between mouse strains is only observed in the media at baseline with a higher expression in *S1pr3*+/+ animals (*S1pr3*+/+ 0.59% of *Gapdh* vs *S1pr3*-/- 0.31% of *Gapdh*) (see Figure 15A, B).

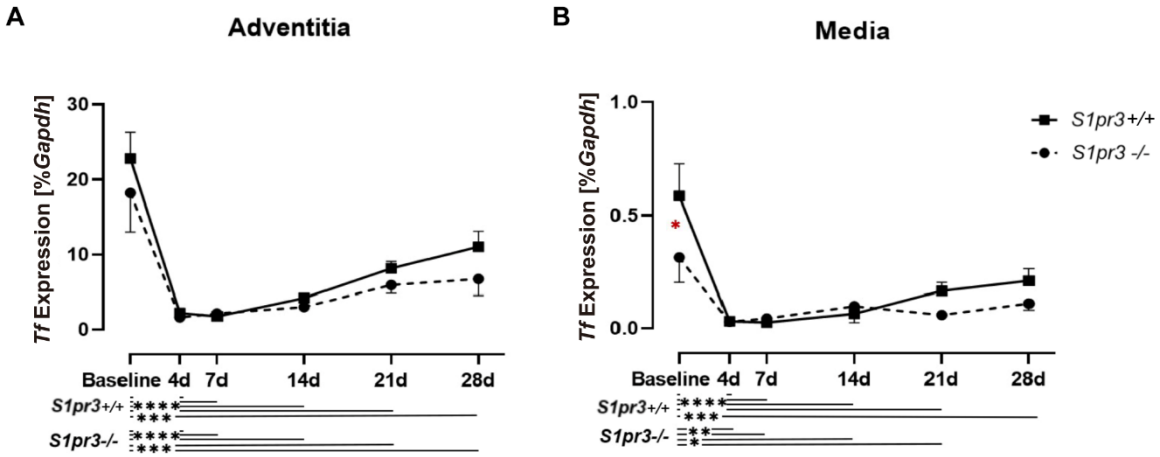

Figure 15 Time-dependent *Tf* expression in the adventitia and media of the abdominal aorta after injury. For each data point, n=5 pools (2 aortas each pool). Non-operated mice are included as baseline. (A) Expression of *Tf* in the adventitia. (B) Expression of *Tf* in the media; Data points are mean±SEM, * P<0.05, ** P<0.01, *** P<0.001, **** P<0.0001. two-sided t-test (*S1pr3*+/+ vs *S1pr3*-/-) and two-way ANOVA (Baseline vs. 4d or 7d or 14d or 21d or 28d).

Gene expression of a thrombin receptor

Expression of gene *F2r* (Coagulation Factor II (Thrombin) receptor), also known as gene *Par1* (Protease-activated receptor 1), is not statistically different between the two genotypes, and no significant injury-induced changes in the expression have been observed in the adventitia (see Figure 16A). In the media, however, a slight decrease in gene expression is observed on day 7 after injury, followed by a gradual increase until day 28, resulting in a doubling of expression compared to the baseline (see Figure 16B).

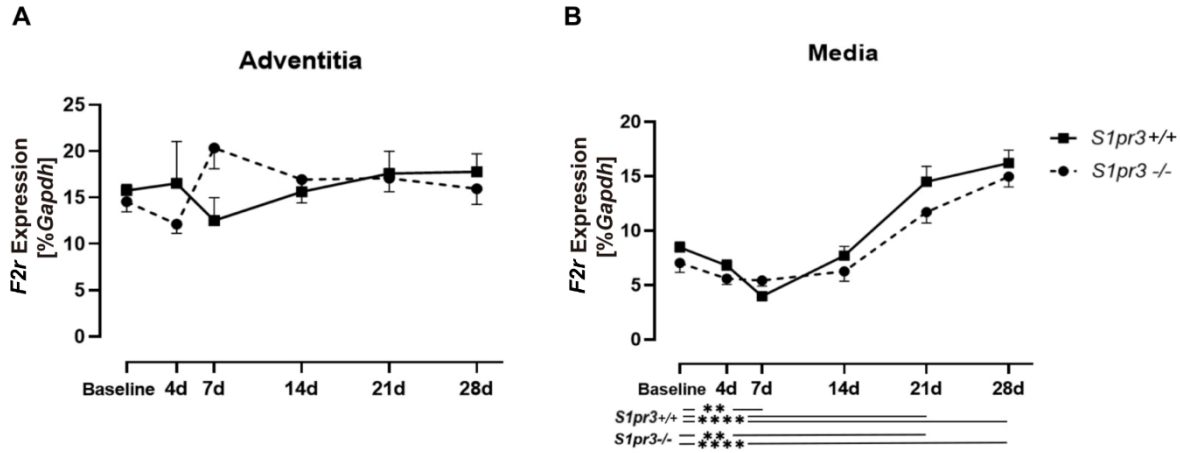

Figure 16 Time-dependent F2r expression in the adventitia and media of the abdominal aorta after injury. For each data point, n=5 pools (2 aortas each pool). Non-operated mice are included as baseline. (A) Expression of *F2r* in the adventitia. (B) Expression of *F2r* in the media. Data points are mean±SEM, ** P<0.01, **** P<0.0001. two-sided, t-test (*S1pr3*+/+ vs *S1pr3-/-*) and two-way ANOVA (Baseline vs. 4d or 7d or 14d or 21d or 28d).

Gene expression of a plasminogen activator inhibitor

Gene *Pai1* (Plasminogen activator inhibitor I) encodes a principal inhibitor of tissue plasminogen activator and urokinase. A significant decrease in *Pai1* expression is detected in the adventitia at day 4 after injury, followed by an increase to the baseline level (see Figure 17A). In the media, *Pai1* expression decreases at day 14 after injury and then increases to reach the baseline level (see Figure 17B). No difference in *Pai1* expression between the two genotypes is observed.

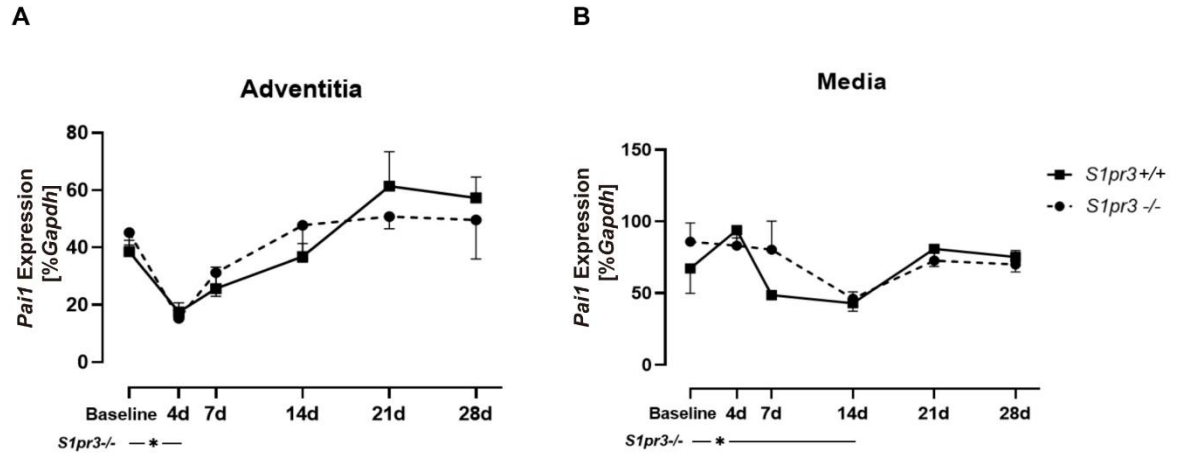

Figure 17 Time-dependent *Pai1* expression in the adventitia and media of the abdominal aorta after injury. For each data point, n=5 pools (2 aortas each pool). Non-operated mice are included as baseline. (A) Expressions of *Pai1* in the adventitia. (B) Expressions of *Pai1* in the media. Data points are mean±SEM, * P<0.01. two-sided t-test (*S1pr3*+/+ vs *S1pr3-/-*) and two-way ANOVA (Baseline vs. 4d or 7d or 14d or 21d or 28d).

4.1.6 Gene expression of a B cell marker

CD19 (Cluster of differentiation 19), known as B-lymphocyte surface antigen, is a reliable marker for B cells. *Cd19* mRNA levels are not statistically different between the two genotypes, and after injury, no significant changes in the expression over time have been observed in the media or adventitia. Notably, however, baseline expression of *Cd19* is higher in the adventitia than in the media (adventitia 0.12% of *Gapdh* vs media 0.019% of *Gapdh*) (see Figure 18A, B).

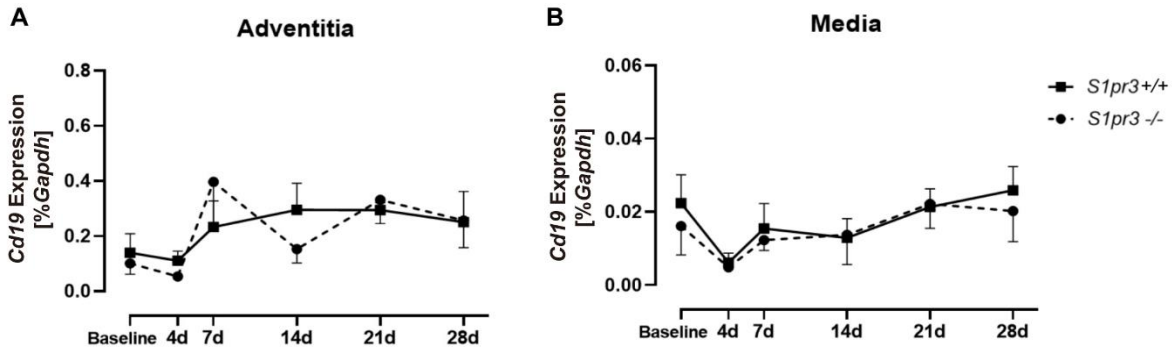

Figure 18 Time-dependent *Cd19* expression in the adventitia and media of the abdominal aorta after injury. For each data point, n=5 pools (2 aortas each pool). Non-operated mice are included as baseline. (A) Expression of *Cd19* in the adventitia. (B) Expression of *Cd19* in the media. Data points are mean±SEM, two-sided t-test (*S1pr3*+/+ vs *S1pr3-/-*) and two-way ANOVA (Baseline vs. 4d or 7d or 14d or 21d or 28d).

4.1.7 Summary of potential sphingosine-1phosphate receptor 3-dependent differences in gene expression

As described above, expression levels of 12 genes at different time points were measured in both *S1pr3*+/+ and *S1pr3-/-* mice, which had been subjected to clamping operations. Here, all genes are listed that show expression differences between the two genotypes (see Table 7)

Table 7 Genes differently expressed in the two genotypes

Gene	Time point	Location	Comparison (*S1pr3+/+ vs S1pr3-/-*)	P value
Adamts15	28 days	Media	2.44 vs 4.89 % of *Gapdh*	P=0.0029
Nos2	14 days	Adventitia	0.31 vs 0.13 % of *Gapdh*	P=0.0020
	28 days	Adventitia	0.22 vs 0.087 % of *Gapdh*	P=0.0330

	14 days	Media	0.68 vs 0.28 % of *Gapdh*	P=0.0067
Tf	Baseline	Media	0.59 vs 0.31 % of *Gapdh*	P=0.0161

After arterial injury operations, 3 genes listed in the table expressed significantly differently in abdominal tissue samples between the two strains of mice, which indicated that *Adamts15*, *Nos2,* and *Tf* expressed in artery tissues might *S1pr3*-dependently participate in the response to arterial injury.

4.2 Effect of the sphingosine-1-phosphate lyase inhibitor DOP or heparin on sphingosine-1-phosphate blood concentrations

The first objective of this part of the study was to determine the S1P concentration in blood serum of mice after applying heparin or DOP. Secondly, the effect of continuous heparin or DOP application on IH was investigated in mice that underwent abdominal artery clamping surgeries.

4.2.1 Sphingosine-1-phosphate lyase inhibitor (DOP) increases serum sphingosine-1-phosphate concentrations and induces lymphocytopenia

To investigate the extent of change in S1P concentrations induced by an oral application of DOP, 18 mice were treated with DOP (30 mg/L) via drinking water for 7 days. Before and after drug application, blood was taken to measure serum S1P concentrations. We find that the S1P concentration in the serum of the DOP-treated mice compared to controls is significantly increased (see Figure 19A).

The thymus glands and the spleens from 3 controls (no DOP) and 5 mice that had been fed with DOP (30 mg/L via drinking water) for 7 days were harvested. In both tissues, DOP feeding leads to an increase in S1P concentrations, over 10-fold in spleen and over 100-fold in thymus glands (see Figure 19B, C).

The blood of 4 mice was taken after 7 days of DOP application for flow cytometry analysis. Four non-DOP-fed mice were included as controls. An additional group of 6 mice was also treated with DOP for 7 days before aortic clamping injury was performed. DOP feeding was continued until these animals were sacrificed on day 3 after injury. As shown in Figure 19D, the number of blood CD4(+) T helper cells (Thelp), CD4(+) regulatory T cells (Treg), and CD8(+) T cells in the DOP group all are reduced to less than 10% of the control group. The NK cell counts of the DOP group are only 70% of controls. The

effect of DOP on leukocyte numbers is also seen in mice that have been subjected to aortic clamping.

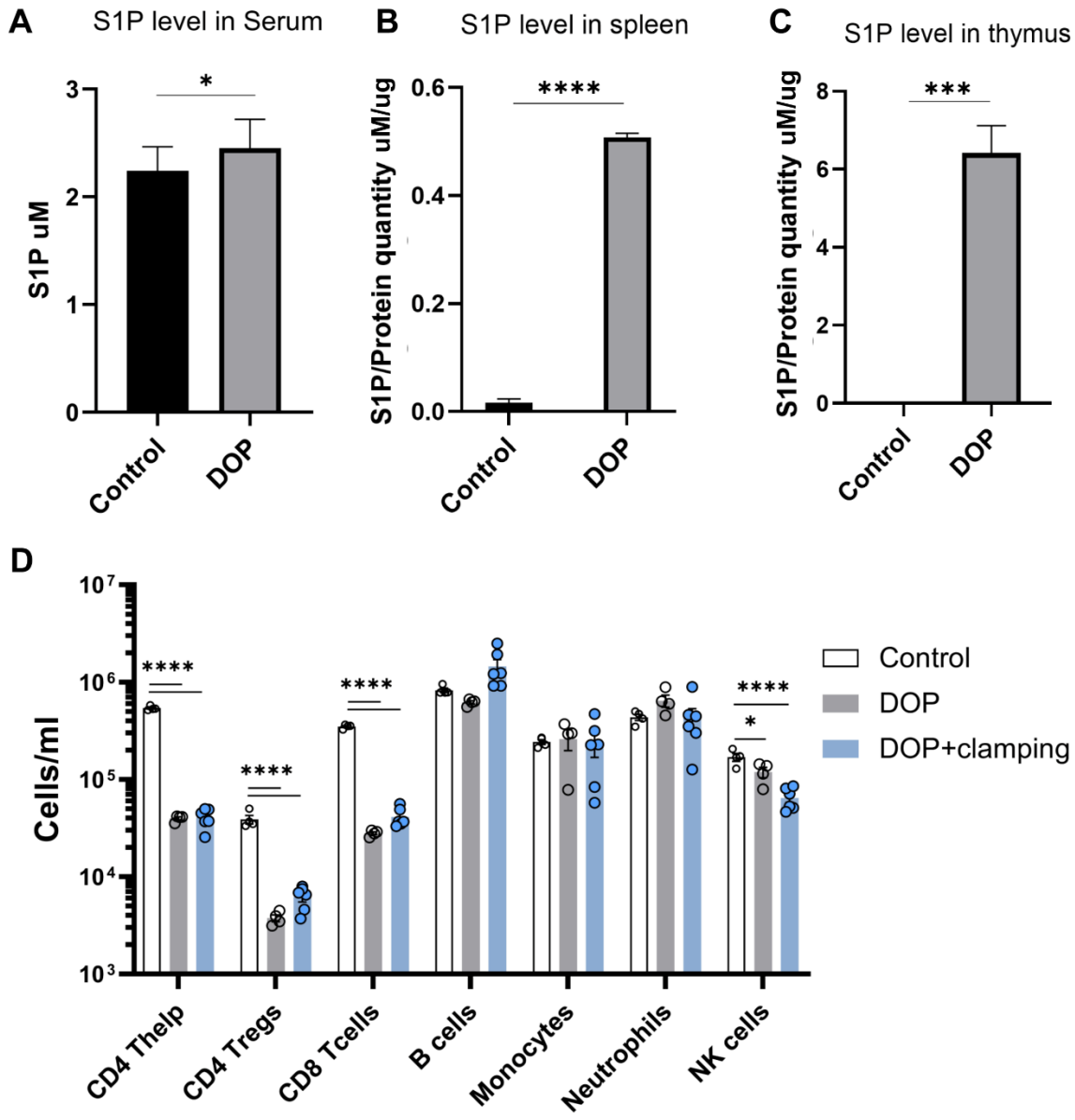

Figure 19 Effect of DOP on serum S1P levels and leukocyte counts. (A) S1P concentration in mice serum after DOP treatment compared with the baseline level before drug application (n=18). (B) Comparison of S1P level in spleen standardized with protein quantity (Control group: n=3, DOP group: n=5). (C) Comparison of S1P level in spleen standardized with protein quantity (Control group: n=3, DOP group: n=5). (D) The leukocyte counts in blood were determined via FACS. Mice without DOP application were taken as the control group (n=4), mice fed with DOP were taken as the DOP group (n=4), and mice underwent abdominal artery clamping surgery with continuous DOP application were taken as the DOP+clamping group (n=6). Data points are mean±SEM, * P<0.05, *** P<0.001, **** P<0.0001, two-sided t-test (S1P levels comparisons), and One-way ANOVA (Blood leukocyte counts).

4.2.2 Heparin decreases serum sphingosine-1-phosphate concentrations

We investigated the administration of heparin in 15 mice. Blood was taken from mice before (baseline) and at several time points after an intraperitoneal injection of heparin (1000 IU/kg body weight). The baseline blood from all the mice was taken as the control group, then five mice were grouped for blood taken at each time point (1 hour, 4 hours, or 12 hours after the injection). After 24 hours, all 15 mice were used for blood sample collection. Following heparin injections, the serum S1P concentration is significantly decreased at one 1 hour and 4 hours and then increases to reach baseline levels at 12 hours (see Figure 20).

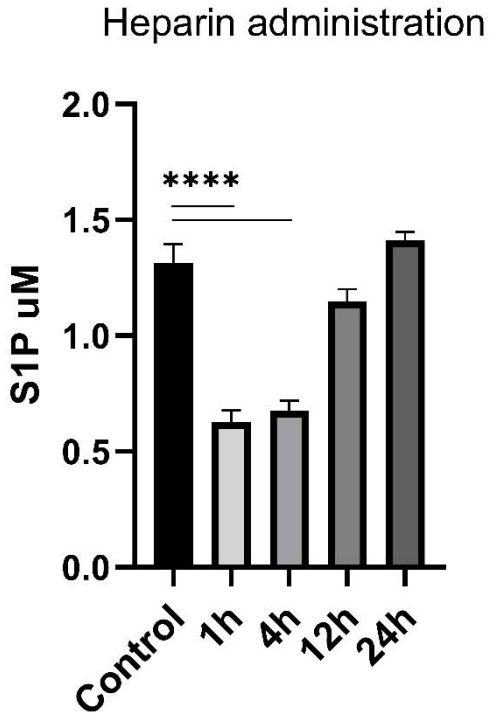

Figure 20 Effect of heparin application on serum S1P levels. Mice were injected with heparin intraperitoneally and then the S1P level in serum was determined at different time points. Baseline blood before heparin administration was taken as the control (Control group or 24h group: n=15 1h,4h or 12h group: n=5). Data points are mean±SEM, **** P<0.0001, two-sided, One-way ANOVA.

4.3 The impact of sphingosine-1-phosphate lyase inhibitor and heparin in an arterial injury model

To determine whether DOP or heparin application would affect IH development induced by aortic injury, 47 mice in total were subjected to infrarenal abdominal aorta clamping surgeries.

A group of 11 mice were given DOP (30 mg/L) via drinking water from 7 days before surgeries until 3 days after, while 23 mice served as non-DOP controls. The mice in the two groups were fed with regular food.

Pilot experiments showed that heparin-treated mice (an intraperitoneal injection pre-surgery of 1000 IU/kg body weight) died from intra-abdominal hemorrhage following abdominal aorta clamping surgeries. Thus, to lower the risk of bleeding, a slow-release osmotic pump filled with heparin solution (500 IU/kg body weight, per 24h, for 7 days) was implanted, and a lower dose of heparin (400 IU/kg body weight) was injected as replenishment in the abdomen instantly after suturing in 7 mice. In comparison, 6 mice were given intraabdominal osmotic pumps with Ringer's solution as a control group. The pumps were taken out 10 days after implantation. After 28 days, the mice were sacrificed, and the abdominal aortas were dissected and prepared for histological analysis, as described in sections 3.1.5 and 3.2.

Compared to controls, mice treated with DOP or heparin exhibit significantly smaller neointimal lesions as shown by significantly reduced I/M ratios (see Figure 21).

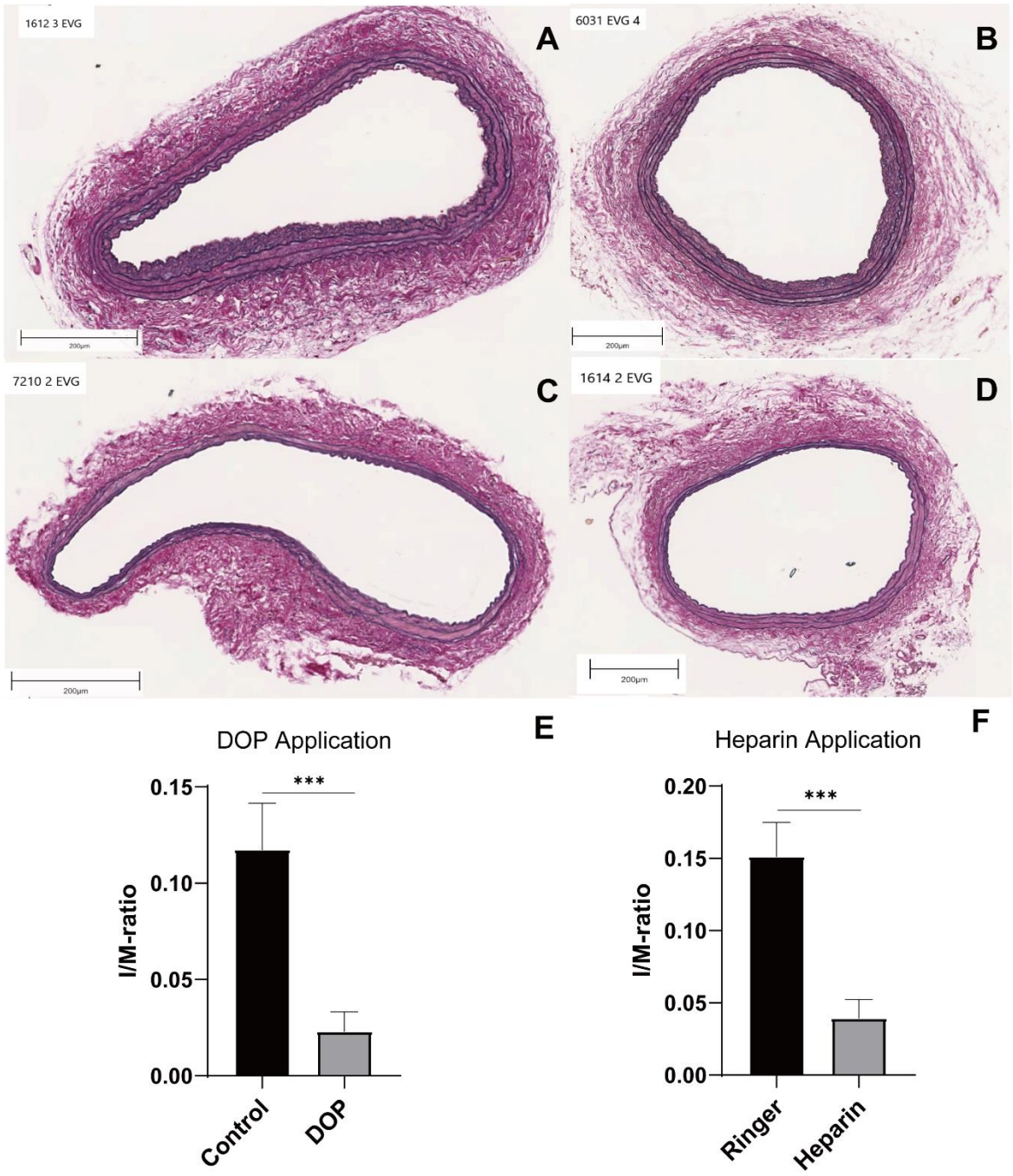

Figure 21 Both DOP as well as heparin inhibit intimal hyperplasia. (A-D) Vessel samples from mice in different groups were harvested 28 days after clamping surgeries and sections were subjected to EvG staining. Representative tissue sections are shown. Scale bars equal 200 µm. (A) One typical example of the mice of the control group accepted only operation. (B) One typical example of the mice applied with Ringer's solution via the pump. (C) One typical example of the mice with DOP treatment. (D) One typical example of the mice with heparin treatment. (E) The average I/M ratio in mice 28 days after arterial injury with continuous DOP application (n=11) compared to the control group (n=23). (F) The average I/M ratio in mice 28 days after arterial injury with heparin application (n=7) compared to Ringer's application (n=6). Data points are mean±SEM, *** P<0.001, two-sided, non-parametric test (DOP vs Control), t-test (Heparin vs Ringer's).

5. Discussion

IH development is a primary pathophysiological process underlying restenosis, and limiting the long-term patency rate after vascular treatment (Buccheri et al. 2016). Previous results from experimental models of intimal hyperplasia in mice (von Lucadou 2023, dissertation) suggested that the S1P receptor subtype 3 could be involved in sensing altered circulating S1P concentrations associated with IH. In this study, we aimed to investigate the potential mechanisms by which *S1pr3-/-* mice developed smaller lesions after arterial injury. A series of genes were selected to measure their expression levels at different time points after arterial injury in *S1pr3+/+* as well as *S1pr3-/-* mice.

Circulating S1P levels are crucial for maintaining vascular homeostasis and the concentration alterations are essential in the onset and progression of vascular diseases (Wang et al. 2023a, Liu et al. 2020). We further aimed to evaluate the impact of DOP or heparin on S1P concentrations and IH development.

5.1 Change of gene expression after abdominal artery injury

In C57BL/6 mice, we successfully established a mouse model of IH induced by abdominal aortic clamping injury (Shirali et al. 2016, Jiang 2021, dissertation). Compared to the most commonly used murine arterial injury models such as ligation or mechanically-induced denudation of carotid or femoral arteries (Hui 2008), the main advantage of this model is that the aorta is a larger vessel and thus more tissue can be obtained per animal which reduces the overall number of laboratory animals required. Recently, increasing attention has been paid to the essential role of the adventitia in maintaining vascular homeostasis and the development of vascular diseases (Milutinović et al. 2020, Majesky and Weiser-Evans 2022). Thus, we determined the target gene expression in both adventitia and media (including endothelium or neointima) to further investigate their potential roles in the vascular injury response. In our previous study, we applied this injury model to *S1pr3-/-* and *S1pr3+/+* mice and observed smaller IH lesions in *S1pr3-/-* mice (von Lucadou 2023, dissertation), but the mechanisms involved remained unclear. Therefore, in this study, we determined expression levels of specific genes in abdominal aortas from both genotypes at

different time points after arterial injuries to investigate the mechanisms by which S1PR3 signaling promotes IH.

***Adamts* expression was downregulated after arterial injury**

In humans and mice, 19 genes encode zinc metalloproteinases, constituting the ADAMTS protease family, known to be involved in a wide range of vascular physiological and pathological conditions (Mead and Apte 2018, Santamaria and de Groot 2020). The most noticeable function of ADAMTS family members is the cleavage of proteoglycans (PGs). The biophysical properties of the ECM are regulated by obtaining a balance between PGs and proteases (Azeloglu and Albro 2008, Brouillard et al. 2017). In this study, *Adamts5/15* expression was downregulated after vascular injury (see Figure 8).

***Adamts5*：** ADAMTS5 is known for a higher aggrecanase activity compared to ADAMTS1/4 (Santamaria et al. 2019). *Adamts5* is expressed in VSMCs and macrophages in adult mice (Santamaria and Groot 2020) and is co-expressed with versican in the aorta (Santamaria 2020). Lack of ADAMTS5 has been claimed to be a risk for acute aortic dissection (Zeng et al. 2020). Studies on mice have revealed that ADAMTS5 deficiency led to severe heart valve abnormalities (Dupuis et al. 2019) and increased aortic dilation under AngII stimulation (Suna et al. 2018). Another clear evidence for the role of ADAMTS5 in arterial diseases is that ADAMTS5 affects LDL binding. It releases LDL from the vascular matrix, preventing atherosclerosis development (Didangelos et al. 2012). *Adamts5* expression was detected in both media and adventitia of untreated mice in our experiments, with decreased expression 4 days after injury (see Figure 8A, B). This result was similar to the significant reduction of *Adamts5* in the early stage after coronary stent implantation in porcine observed by Suna et al. (Suna et al. 2018). Although there was no significant difference in expression between the two genotypes, the restoration of ADAMTS5 signaling was relatively slower in the media of *S1pr3*+/+ mice compared to S*1pr3-/-* mice and did not compensate for the decline within the observation period (see Figure 8B).

***Adamts15*：** ADAMTS15 can also cleave PGs, albeit with lower aggrecanase activity than ADAMTS5 (Santamaria and de Groot 2020). It is known to be

strongly expressed in the mouse heart during the early development of the cardiovascular system, but its role in vascular diseases has been poorly understood (Dancevic et al. 2013, Binder et al. 2020). Its expression decreased significantly after injury in both tissues investigated at day 4 (see Figure 8C, D). The expression in media remained at a low level in *S1pr3*+/+ mice during the following observation. A recovery trend was noticed in *S1pr3*-/- mice, leading to a significantly higher expression level than *S1pr3*+/+ animals at day 28 (see Figure 8D).

Expression of *Adamts5/15* after injury could be related to an accumulation of PGs including versican and aggrecan (Humphrey et al. 2014, Koch and Lee 2020). An increased versican content is a consistent feature of neointima after arterial injury, and its isoform V1 has been reported to promote VSMC proliferation and migration (Huang et al. 2006, Kenagy et al. 2006). An imbalance of PG levels due to the relatively slower recovery of *Adamts5/15* expression in media could contribute to severe IH development in *S1pr3*+/+ mice. Notably, in a rat cardiac ischemia-reperfusion model, *Adamts15* gene expression in the myocardium was found to correlate negatively with the protein level of IL-1β and positively correlated with the cardiac IL-10 protein content (Zuo et al. 2023). Interestingly, higher expression of *Il-1β* in *S1pr3*+/+ mice 7 days after injury has been discovered in our previous studies (von Lucadou 2023, dissertation). The differential expression of *Adamts15* lagged behind that of *IL-1β* in tissue, suggesting that amplified IL-1β signaling after injury might suppress *Adamts15* upregulation in tissue to enhance IH progression in *S1pr3*+/+ mice.

***Palld* expression remained statistically unchanged after arterial injury**

Palld is widely expressed in actin-based subcellular structures with multiple isoforms, and the expression of isoform 4 (90-92kDa) was determined in this study as this isoform has been demonstrated to be a prerequisite for the induction of VSMC marker genes like *Sma* and *Sm22* in cell culture (Jin et al. 2010). Transfection of PALLD by electroporation significantly promotes human iliac vein VSMC as well as fibroblast migration (Jin et al. 2007). Moreover, deficiency of PALLD in platelets has been reported to enhance the small

GTPase Rac signaling and accelerate hemostasis and thrombosis formation (Jin 2011, Chen et al. 2017). However, no significant difference in *Palld* expression was seen between the two genotypes. In addition, no significant changes in *Palld* expression were observed in either the media or the adventitia after injury (see Figure 9). Since PALLD occurs in several isoforms and the protein content was not examined in this study, we cannot exclude the possibility that PALLD is involved in the arterial injury response.

***Comp* expression increased after arterial injury**

Comp encodes the cartilage oligomeric matrix protein, a non-collagen ECM glycoprotein belonging to the thrombospondin family, contributing to collagen secretion and assembly and the stability of ECM (Koelling et al. 2006). COMP deficiency has been proven to exacerbate arteriosclerotic lesions in *ApoE-/-* mice (Fu et al. 2016). It has also been described as being involved in the maintenance of the contractile phenotype in VSMC (Fu and Kong 2017) and in counteracting the vascular damage induced by AngII (Fu et al. 2021). Lv et al. (Lv et al. 2021) reported that COMP or a COMP-derived peptide inhibited EC activation in inflammatory responses triggered by oscillatory shear stress. In our experiments, significant up-regulation of *Comp* was observed in both media and adventitia (see Figure 10), indicating a spontaneous anti-inflammation process encountered with injury stress.

***Nos2* expression differed in the two genotypes after arterial injury**

The vasodilator NO is crucial for the vascular system also by serving as a potent vascular protective agent by inhibiting platelet aggregation, modulating leukocyte chemotaxis, suppressing VSMC proliferation and migration, and promoting EC survival and growth. Under physiological conditions, NO is primarily generated by NOS3 in vascular ECs. When stimulated by inflammatory cytokines, NOS2 is responsible for a vast amount of NO production, which contributes to the subsequent blood pressure drop (Kibbe et al. 1999). IL-1β, together with TNFα, and LPS were reported to drastically induce *Nos2* expression in cultured VSMC (Wen and Han 2000). IL-1β secreted by macrophages is also a promoter for the increase in *Nos2* expression in adventitial fibroblasts after arterial injury (Zhang et al. 2016). In our study,

significantly higher *Nos2* expression was found in tissue from *S1pr3*+/+ mice, i.e. at 14 days after injury in both media and adventitia and at 28 days still in the adventitia when compared with *S1pr3*-/- mice (see Figure 11). Considering the temporary higher *Il-1β* expression in *S1pr3*+/+ mice at 7 days after arterial injury (von Lucadou 2023, dissertation), higher *Nos2* expression in *S1pr3*+/+ mice may be due to an amplified IL-1β signaling. Although physiological amounts of NO are expected to have a protective effect against IH (Kibbe et al. 2001, Wang et al. 2003), excessive amounts of NO can be harmful to the cardiovascular system (Bian et al. 2008). Overexpressed *Nos2* has been demonstrated to cause endothelial dysfunction and promote peroxynitrite accumulation, which is related to apoptosis in ECs (Roy et al. 2023). Moreover, dysregulated NO production leads to a functional deficiency in mitochondria (Haynes et al. 2003) and upregulation of COX in cells, thereby contributing to the pro-inflammatory cascade (Lind et al. 2017). Thus, a possible reason for a decreased IH in *S1pr3*-/- mice compared to wild-type animals is reduced IL-1β signaling followed by a smaller NO burst after injury.

***Nlrp3* expression increased after arterial injury**

There is growing evidence that IL-1β secretion is primarily regulated by the NLRP3 inflammasome. The NLRP3 inflammasome is expressed in innate immune cells (such as macrophages and neutrophils) as well as in non-immune cells (such as endothelial cells, cardiomyocytes, and fibroblasts), and these cells can recognize various stimuli via the expression of *Nlrp3*. Once activated, the NLRP3 inflammasome is assembled to recruit pro-caspase-1, followed by an autocatalytic activation of caspase-1. Subsequently, caspase-1 induces proteolytic activation of the pro-inflammatory cytokines IL-1β and IL-18 (de Nardo and Latz 2011, He et al. 2015, Ding et al. 2016). These processes would exacerbate IH development in response to vascular injury (Bruder-Nascimento et al. 2016, Takahashi 2022). IL-1β is able to induce its own expression, suggesting enhanced NLRP3 signaling promotes active IL-1β secretion for further stimulating *Il-1β* expression in cells which constitutes a positive signaling amplification loop (Libby 2017). In untreated mice, *Nlrp3* was expressed at a very low level in the adventitia and was nearly undetectable in the media.

Expression was rapidly up-regulated after operations, indicating the involvement of the NLRP3 inflammasome in the arterial injury process (see Figure 12). Recently, it was reported that S1PR3 inhibition via an antagonist application suppressed *Nlrp3* and *Il-1β* gene expression in mice bone marrow-derived macrophages under LPS stimulation and diminished ATP-induced NLRP3 inflammasome activation (Wang et al. 2023b). However, in our study, a differential expression of *Nlrp3* was not observed between the two genotypes. One explanation is that S1PR2 could compensate for the lack of S1PR3 in *S1pr3-/-* mice. Future investigations of inflammasome activity in this arterial injury model still might provide evidence of a role for S1PR3 in NLRP3 signaling.

***Csf2* Expression increased in media after arterial injury**

CSF2 is considered an important regulator of inflammatory reactions. In untreated mice, *Csf2* expression is higher in the adventitia, which was considered to originate from fibroblasts. The expression in the adventitia decreased along with the cell apoptosis after injury and recovered during the vascular remodeling (see Figure 13A). The endothelium denudation during the operation exposes the media to the blood, where TNFα secreted by circulating monocytes can stimulate *Csf2* expression in VSMC (Harris et al. 2009), potentially leading to gradually enhanced signaling in the media (see Figure 13B). The release of CSF2 may further recruit monocytes and activate the conversion of macrophages to a pro-inflammatory M1 phenotype (Peet et al. 2020, Duncan et al. 2020), contributing to damage exacerbation. These observations are in line with an earlier study which reported that CSF2-deficient mice exhibited less macrophage infiltration and milder IH (Harris et al. 2009). Another study by Shen et al. (Shen et al. 2024) found that in the myocardial ischemia-reperfusion model, macrophages recruited by an enhanced release of CSF2 activated the NLRP3/Caspase-1/IL-1β signaling pathway. Nevertheless, no significant expression difference was uncovered between the two genotypes in our study.

***Tbxa2r* expression decreased in media after arterial injury**

TBXA2R triggers a broad spectrum of effects through its activation, such as mediating vasoconstriction, activation of platelet aggregation, oxidative stress,

and promotion of inflammation, thereby contributing to the pathogenesis of cardiovascular diseases (Bauer et al. 2014). The expression of *Tbxa2r* decreased transiently in our experiments in the adventitia and then recovered quickly (see Figure 14A). In comparison, the expression of *Tbxa2r* remained consistently low in the media after the injury (see Figure 14B). TXA2 is a potent stimulus for VSMC contraction and platelet deposition after injury, generated by activated platelets at the injured site (Nakahata 2008). TXA2/TBXA2R signaling is commonly thought to promote vascular damage, and TBXA2R antagonists have been proven to inhibit IH development (Ishizuka et al. 2003). TBXA2R is a member of the GPCR family of receptors and couples with $G\alpha_q$, $G\alpha_{12/13}$, and $G\alpha_{i/o}$ proteins known to be involved in cytoskeletal remodeling, cell tension, adhesion, and proliferation (Eckenstaler et al. 2022). TXA/TBXA2R signaling has also been found to mediate the release of S1P in human platelets, which is reduced in the presence of TBXA2R antagonists (Ulrych et al. 2011). No differences in *Tbxa2r* expression between the two genotypes were observed.

***Tf* expression differed in the two genotypes in baseline**

TF serves as a critical initiator of the extrinsic pathway of coagulation. Upon vascular damage, TF is released and binds to coagulation factor VII in the blood to initiate the coagulation cascade and promote thrombin generation (Wilhelm et al. 2023). *Tf* expression in ECs can be induced by thrombin and this process is stimulated by S1P (Takeya et al. 2003). In the murine endotoxin-induced coagulation model, NLRP3/IL-1β signaling has been shown to induce TF generation and release (Shi et al. 2022). In the media of untreated animals, *S1pr3*+/+ mice showed a higher level of *Tf* expression compared to knockout mice (see Figure 15B). Recombinant inhibitors of the TF pathway have been shown to reduce IH lesions through inhibiting PDGF-mediated VSMC proliferation and migration (Roqué et al. 2000). TF activity deficiency was also shown to attenuate IH development in femoral arteries after injury (Pyo et al. 2004). Thus, lower *Tf* expression levels in *S1pr3-/-* mice might contribute to their diminished IH development when compared to wild-type animals. However, the difference in *Tf* expression levels between the two genotypes was lost after the operation. In our study, the expression was significantly down-regulated at

day 4 and remained at a low level thereafter (see Figure 15). A down-regulation of TF after injury has also been observed in a rabbit carotid artery balloon injury model, however, an increase in TF signaling was reported 2 weeks after (Hatakeyama et al. 1998). The differences in species and injury models may explain the nonidentical TF expression alterations in our study. The difference in *Tf* expression dependent on the genotype may disappear after operations due to the compensation of S1PR2. Thus, it remains unclear whether the S1PR3 could regulate *Tf* expression levels, requiring further experiments.

***F2r* expression increased in media after arterial injury**

Activation of *F2r* by thrombin leads to profound shape change in platelets, induction of adhesion proteins, and loss of barrier function in ECs (Flaumenhaft and De Ceunynck 2017). Thrombin acts as a growth factor for VSMCs via F2R signaling (Huang et al. 2009), which could contribute to IH development. Several F2R antagonists were proven to inhibit neointima formation in vascular injury models, indicating the pro-restenosis capacity of F2R (Takada et al. 1998, Andrade-Gordon et al. 2001, Chieng-Yane et al. 2010). In addition, collagen could also induce the conversion of proMMP-1 to MMP-1 during the initiation of coagulation. MMP-1 may activate F2R signaling to promote VSMC dedifferentiation, contributing to arterial stenosis (Austin et al. 2013). Our results showed that in the media, *F2r* was upregulated after injury (see Figure 16B), which was similar to the observations by Fukunaga et al. (Fukunaga et al. 2006). Both elevated expression and activation of *F2r* contribute to thrombin accumulation at the injured site and may promote adhesion and infiltration of inflammatory cells, finally leading to increased endothelial permeability (Lee and Hamilton 2012, Alberelli and De Candi 2014). It has been reported that S1PR3 antagonists can block the S1P-induced upregulation of *F2r* expression in renal tubular epithelial cells (Lin et al. 2022). In our experiments, no differential expression of aortic *F2r* has been found between *S1pr3*+/+ and *S1pr3*-/- mice.

***Pai1* expression decreased after arterial injury**

PAI-1 is known to be expressed in vascular ECs, VSMCs, myocytes, hepatocytes, and adipocytes. After local thrombus formation, the plasminogen activator converts plasminogen into plasmin, which degrades fibrin. As a major

inhibitor of urokinase and tissue-type plasminogen activator (uPA and tPA), PAI-1 appears to play an essential role in determining the response to arterial injury by inhibiting the degradation of fibrin and various extracellular matrix proteins (Fay et al. 2007). In a murine femoral artery injury model, elevated levels of PAI-1 protein were detected 5 days after injury and then decreased (Zou et al. 2007). In a rat carotid artery injury model, a higher level of *Pai1* mRNA was detected in the injured artery 7 days after operations (Simone et al. 2015). In our study we observed no significant elevation of *Pai1* mRNA expression upon injury; only a temporary decrease was measured in *S1pr3-/-* mouse (see Figure 17). Although the *Pai1* expression did not significantly increase after injury, protein levels and activity might be altered, and this may be worth exploring in future experiments. PAI1 has been shown to promote proliferation and inhibit apoptosis in VSMC (Kwaan et al. 2000, Chen et al. 2008). The inhibition of PAI1 in cell-associated plasmin formation and its combination with vitronectin receptors on VSMC may inhibit cell migration (Fay et al. 2007).

Aortic *Cd19* expression did not change after injury

It has been reported that the absence of T cells and B cells, respectively, leads to increased IH lesions after vascular injury. Supplementation of B cells in these experiments attenuated the inflammatory response and reduced the formation of a neointima (Zhu et al. 2002, Dimayuga et al. 2002). The cardiovascular protective effect of B cells is thought to be mediated via the anti-inflammatory factor IL10 (Bodhankar et al. 2014), and interestingly CD19-deficient B cells showed impaired IL10 secretion (Yanaba et al. 2009). An infiltration of CD19(+) B cells has also been detected in human atherosclerotic vulnerable plaques, indicating their participation in atherosclerosis development (Ge et al. 2023). In our study, no change in *Cd19* expression upon vascular injury was observed, and a higher *Cd19* expression level was detected in the adventitia throughout the observation duration (see Figure 18). However, the involvement of B cells during the onset of IH cannot be excluded. It has been reported that B cell chemotaxis towards S1P is dependent on S1PR3 signaling, which is also

essential for B cell development (Donovan et al. 2010), but no S1PR3-dependent change in *Cd19* expression levels was observed in this study.

5.2 Alteration of Sphingosine-1-phosphate concentration in blood and intimal hyperplasia development

The different affinities of S1P to its various receptors and the diversity of G-protein coupling they are involved in lead to multiple effects and even opposing roles of S1P in the vascular system homeostasis.

As a protective factor: (1) S1P/S1PR1 signaling can preserve endothelial barrier function and reduce monocyte adhesion (Camerer et al. 2009, Bolick et al., 2005, Galvani et al. 2015). (2) S1P/S1PR2 signaling can contribute to maintaining the contractile phenotype in VSMCs (Yang et al. 2024). (3) Activation of the S1PR1/S1PR3 promotes endothelium-dependent vasodilation. S1PR3 signaling also regulates the proliferation and migration of ECs and progenitor cells (Walter et al. 2007, Wang et al. 2018). As a detrimental factor: (1) Enhanced S1PR1/S1PR3 signaling promotes VSMC proliferation and migration (Shimizu et al. 2012, Mousseau et al. 2012, Braetz et al. 2018). (2) S1PR2/3 signaling increases endothelial permeability and promotes VSMC-dependent vasoconstriction (Cantalupo et al. 2017). (3) S1PR3 promotes leukocyte rolling on endothelium, enhances macrophage recruitment, and synergizes with S1PR2 signaling, inducing macrophage retention in the vessel wall and enhancing pro-inflammatory factor release (Yang et al. 2018, Heo and Im 2019, Vaidya et al. 2019).

The maintenance of S1P gradients is of significant importance for cardiovascular system, and any modification of S1P levels in blood may impact on the mechanisms of cardiovascular diseases. S1P has been reported to emphasize different downstream signaling dependent on its concentrations (Li et al. 2015). Furthermore, the S1P gradient is a critical initiating factor for lymphocyte circulation, so S1P could also exert pro-inflammation or anti-inflammation function via immune cell migration regulation. Due to the complexity of regulatory networks, the net effect of changes in serum S1P levels on vascular stenosis diseases remains controversial.

5.2.1 The impact of sphingosine-1-phosphate lyase inhibition on sphingosine-1-phosphate concentration and intimal hyperplasia

Firstly, we aimed to increase S1P in the bloodstream by using DOP as an SPL inhibitor. Continuous uptake of DOP via drinking water significantly increased S1P concentrations in serum (see Figure 19A). However, compared to observations by Polzin et al. (Polzin et al. 2023), where the S1P level in plasma increased 4-fold upon the equivalent uptake of DOP, only a slight increase of S1P level in serum was noticeable in our experiments. S1P concentrations are much higher in serum compared to plasma. Platelets have been reported to be responsible for this difference. Due to the lack of S1P lyase activity, platelets store large amounts of S1P and once activated, platelets release S1P which accounts for the elevated S1P levels in a short time (Tolksdorf et al. 2022). Since DOP increases S1P concentration via its function as a SPL inhibitor, the S1P derived from platelets would not be impaired. The increased S1P due to SPL deficiency after DOP application might be partly concealed by S1P derived from platelets during coagulation in serum sample preparation. Determining the S1P level after DOP application in plasma could be a further step in eliminating this factor. In addition, the small S1P increase in this experiment might also be attributed to the influence of vitamin B6 in the diet. As a vitamin B6 antagonist, the same binding site of DOP is competed by vitamin B6 and SPL (Van Veldhoven 2000, Le Stunff et al. 2004). Therefore, Polzin et al. (Polzin et al. 2023) adopted a diet devoid of vitamin B6 to emphasize the SPL inhibitory effect of DOP. However, the lack of vitamin B6 in the diet led to a loss of appetite in mice in our previous trials, resulting in lower body weight. Thus, the adoption of a regular diet was necessary, which could have attenuated the elevation of S1P signaling with the treatment of DOP.

Though the S1P concentration was not elevated dramatically in serum, increased S1P concentrations were observed in the thymus and spleen of DOP treated mice (see Figure 19B, C), demonstrating an effect of the DOP application. Also, the application of DOP led to a significant decrease in peripheral blood CD4(+) and CD8(+) T cells, as well as NK cells (see Figure 19D), which is in accordance with the findings of Schwab et al. (Schwab et al.

2005) and indicates that the S1P gradient between tissue and blood has been affected by the DOP treatment. Studies have demonstrated that mature single-positive thymocytes upregulate S1PR1 and respond to the high S1P environment provided by surrounding vascular cells, thereby departing from the thymus to blood circulation (Schwab and Cyster 2007, Spiegel and Milstien 2011). Although serum S1P level was significantly elevated in this experiment, it probably could not compensate for the imbalance due to the remarkable increase of S1P level in the lymphoid tissues, leading to the failure in lymphocyte egress. A slight decline in NK cells was also observed in this study. Egress and homing of NKs depend on additional chemotactic factors, indicating a relatively lower dependence on S1P/S1PR1 signaling (Ran et al. 2022).

Continuous DOP application significantly reduced lesions in mice compared to the control group after clamping surgeries (see Figure 21A, C, E), indicating a protective effect of DOP in IH development. Hemdan et al. (Hemdan et al. 2016) reported that in a mouse model of sepsis, DOP treatment significantly weakened the destructive effect of VEGF-A on endothelium barrier integrity in treated mice and exerted protective functions via enhanced S1P-S1PR1 signaling. Amplified S1P signaling via direct S1P supplement or oral application of DOP has been validated to be beneficial in narrowing the infarct size under attack of ischemia and reperfusion (Vessey et al. 2008, Brulhart-Meynet et al. 2015, Polzin et al. 2023), indicating the positive role of high S1P level in protecting the cardiovascular system. Clinical reports also demonstrated that patients with higher concentrations of HDL-S1P have a lower risk of coronary in-stent restenosis (Jing et al. 2015).

Li et al. (Li et al. 2015) reported different affinities for S1P of the various S1P receptors in cultured human umbilical vein endothelial cells. These data suggest that physiological levels of S1P primarily activate S1PR1 signaling, leading to $G\alpha_{i/o}$/Rac1 pathway activation and contributing to the protection of the endothelial barrier. However, an about 10-fold increase of S1P then leads to an activation of S1PR2 and the RhoA/ROCK pathway, mediating endothelial barrier damage (Li et al. 2015). In our experiment, the increase in serum S1P levels is not as high as 10-fold of the physiological S1P level so the S1P/S1PR1

signal is considered to take the predominant role in ECs. However, in VSMCs from immunosuppressed rats, amplified S1P/S1PR1 signaling promoted proliferation and migration resulting in neointima formation (Braetz et al. 2018), which is inconsistent with our experimental results. An explanation is that although increased S1P/S1PR1 in VSMC could promote IH progression, the disruption in S1P gradient could inhibit IH by lowering lymphocyte invasion. Transcriptome analyses have revealed that upon balloon injury of the common carotid artery in rats, arteries are rapidly infiltrated with T cells accompanied by an upregulation of interferon-γ (IFN-γ) signaling (Röhl et al. 2020). Accordingly, *Ifn-γ-/-* mice showed significantly reduced neointima formation, indicating its pro-inflammatory function as a cytokine (Tavakoli et al. 2012, Elyasi et al. 2020). Hence, the diminished immune cell participation and IFN-γ derived from the reduced blood lymphocytes might be sufficient to explain DOP inhibiting IH development in our study. More experiments are required to evaluate the S1P concentration-dependent functions in different cell types.

5.2.2 The impact of heparin on sphingosine-1-phosphate concentration and intimal hyperplasia

In our experiments, a single injection of heparin at a dose of 1000 IU/kg reduced serum S1P levels by approximately 50%, whereby the reduction by a single application was only effective over a short period of time (see Figure 20). In addition, we found in previous trials that even a lower dose of heparin (300 IU/kg) decreased S1P level by over 30% within 4 hours. Heparin exhibits anticoagulant properties by inhibiting thrombin and factor Xa. Several speculations about the effect of heparin on S1P have been concluded from existing evidence: (1) By inhibiting factor Xa, heparin can block the induction of SPHK1 transcription, thus reducing S1P biosynthesis in VSMCs (Böhm et al. 2013). (2) Heparin can also suppress the thrombin-induced S1P production in EC (Ye et al. 2021). (3) Factor Xa and thrombin have been demonstrated to regulate platelet activation via F2R signaling; factor Xa inhibitors lead to decreased platelet activation and aggregation, which might potentially attenuate platelet-derived S1P release (Ulrych et al. 2011, Petzold et al. 2020). In this study, it was confirmed, that the application of heparin could lead to a decrease

in serum S1P levels. However, due to its short half-life, the effect of heparin was challenging to sustain.

Early research has demonstrated that the effect of heparin application on IH after arterial injury is dependent on the model of injury, dose of heparin, and protocol of application. Continued postoperative administration can maximize the effect of heparin (Rogers et al. 1993, Edelman and Karnovsky 1994). To avoid the complication of bleeding and maintain the impact of heparin in the long term, osmotic pumps were used to apply heparin in this study. An additional lower dose of heparin was injected intraperitoneally to decrease serum-S1P concentration right after the clamping surgery. Heparin application inhibited IH development in abdominal arteries (see Figure 21B, D, F), consistent with previous studies using other species or artery injury models (Guyton et al. 1980, Wilson et al. 1991). Despite the growing evidence of beneficial effects of heparin on restenosis in various animal models, a single dose of heparin injection into the target artery prior to stent implantation or long-term subcutaneous heparin administration after operations in clinical trials had no beneficial effects (Brack et al. 1995, Wilensky et al. 2000). However, based on its function in anti-coagulation and improving blood compatibility, heparin became the common coating agent for medical devices (Biran and Pond 2017). Interestingly, attenuated IH was commonly observed in research on heparin-coated grafts (Lin et al. 2003, Lin et al. 2004, Cai et al. 2009). Heparin-bonded, self-expanding polytetrafluoroethylene-covered Viabahn stents have been widely used in peripheral arterial diseases, which obtain satisfactory long-term patency (Brendel et al. 2024).

The mechanisms by which heparin affected neointima formation in previous reports included its effects on EC and VSMC proliferation and modulation of growth factors such as bFGF (Aslani et al. 2020). *In vitro* experiments have validated that heparin enhances EC proliferation while inhibiting the expansion of human-derived VSMC lines (Liu et al. 2017b). Moreover, in a rabbit artery injury model, the presence of heparin inhibited IH, probably by reducing macrophage invasion (Cai et al. 2009). Previous studies have not identified serum-S1P as a target for heparin to regulate IH development. We have

mentioned in the introduction (see Part 1.3.4) that intracellular synthesis of S1P induced by FXa promotes VSMC mitogenesis and migration (Böhm et al. 2013), which could be inhibited via heparin application (Rauch et al. 2004). Braetz et al. (Braetz et al. 2018) have suggested in arterial transplantation experiments that VSMC could sense the S1P gradient between vascular tissue (low) and circulation (high) via the expression of S1PR1, thereby migrating from the media to the neointima. The use of heparin significantly reduces the level of S1P in the circulation in this study, which could lead to the disruption of the S1P gradient and prevention of the VSMC inward migration, ultimately inhibiting the development of neointima formation.

In this experiment, it is interesting that although DOP increased serum S1P levels while heparin decreased serum S1P levels, both inhibited IH development after vascular injury. The impact of DOP application on neointima formation might be attributed to amplifying the protective effect of S1P/S1PR1 signaling in the endothelium, preventing immune cell egress into circulation and possibly reducing T cell infiltration in blood vessels. Heparin has been proven to enhance EC proliferation (Liu et al. 2017b), and could inhibit S1P-induced VSMC proliferation and migration into intima during neointima formation. The underlying mechanisms still require further investigation.

5.3 Limitations and outlook

In the first part, we applied the arterial injury model to *S1pr3*+/+ and *S1pr3*-/- mice and uncovered differential mRNA expression of *Adamts15 and Nos2* at several time points after arterial injury in the two genotypes. Nevertheless, the effect of the genotype on protein levels remains unknown. Additional experiments are required to make more precise statements about the *S1pr3*-dependent regulation of these genes. Tissue-specific or cell-type specific knockout of *S1pr3* in mice can be established to investigate the detailed pathways, in which S1PR3 engages in IH development.

In the second part, we investigated the impact of DOP and heparin on serum S1P level and IH. One limitation is that DOP or heparin may affect IH development independently of S1P. DOP application increased S1P levels in serum as well as in lymphoid organs, resulting in the reduction of circulating

lymphocytes, which could in principle influence the evaluation of how high serum S1P levels alone affect neointima formation. The effect of heparin on IH was investigated by applying a heparin pump in this study. However, the dose of heparin was limited due to the intraperitoneal bleeding risk during and after operations. Orally administered FXa inhibitor with a relatively lower risk of bleeding such as apixaban (Agnelli et al. 2020, Dawwas et al. 2022) might be a better choice in future experiments to investigate whether FXa inhibitor could inhibit IH development by affecting S1P signaling. In addition, it was reported that FXa-induced *Sphk1* expression and increased S1P synthesis were mediated by F2R and PAR2 in human aortic VSMC (Böhm et al. 2013). Thus, apixaban can be applied to F2R or PAR2 deficient mice to investigate whether the effect of FXa on S1P concentration and IH progression is F2R/PAR2 dependent.

6. Summary and conclusions

Previous studies showed smaller neointimal lesions in S1PR3-deficient mice. In investigating dynamic gene expression during the inflammatory response to arterial injuries, we found differentially expressed *Adamts15, Nos2*, and *Tf* between *S1pr3*+/+ mice and *S1pr3*-/- mice. In further experiments, the results should be validated at the protein level and the extent to which ADAMTS15, NOS2 and TF contribute to IH should be clarified.

In the second part of this study, SPL inhibition by DOP in mice increased the S1P concentrations in serum and lymphoid organs (thymus and spleen). This compromised the S1P gradient between the blood and lymphoid organs as shown by a notable reduction in circulating lymphocytes. SPL inhibition in mice that underwent aortic clamping surgeries resulted in smaller neointimal lesions compared to the control group. This could be due to enhanced S1P/S1PR1 signaling and/or reduced lymphocyte invasion in arteries. A lymphocyte-specific knockout of S1PR1 could clarify this question. Mice subjected to heparin treatment developed smaller neointimal lesions than controls without heparin, indicating lower serum S1P levels could prevent IH development. However, heparin treatment led to an increased bleeding risk. In further experiments, direct factor Xa inhibitors could help elucidate the mechanism underlying IH inhibition.

Zusammenfassung

In vorausgehenden Untersuchungen zeigten sich kleinere neointimale Läsionen in Sphingosin-1-phosphat (S1P) Rezeptor 3 defizienten (*S1pr3-/-)* Mäusen. In der vorliegenden Arbeit konnte gezeigt werden, daß sich nach einer arteriellen Verletzung die mRNA Expression von ADAMTS15, NOS2 und TF zwischen *S1pr3+/+* und *S1pr3-/-* signifikant unterscheidet. In weiterführenden Experimenten soll gezeigt werden, inwieweit ADAMTS15, NOS2 und TF zur Intimahyperplasie (IH) beitragen.

Im zweiten Teil der Arbeit wurde untersucht, ob eine Veränderung der S1P-Konzentration die Neointimabildung nach Arterienverletzungen beeinflusst. Die Inhibition der S1P-Lyase führte zum Anstieg von S1P im Serum und in Thymus und Milz. Wir konnten zeigen, dass dies zu einer deutlichen Verringerung der Lymphozyten-Zahl im Blut führte. Die Mäuse, bei denen die S1P-Lyase gehemmt wurde, zeigten nach Verletzung der abdominalen Aorta kleinere Neointimaläsionen als die Kontrollgruppe. Dies könnte durch ein verstärktes S1P/S1PR1-Signal und/oder eine verringerte Lymphozyteninvasion in die Arterienwand bedingt sein. Ein lymphozytenspezifischer Knockout des S1PR1 könnte diese Frage klären. Den wichtigen Einfluss von S1P auf die IH konnten wir durch den Einsatz von Heparin im Mausmodell zeigen. Heparin verringerte die S1P-Konzentration im Serum und die Mäuse entwickelten ebenfalls kleinere neointimale Läsionen, allerdings führte dies zu einem erhöhten Blutungsrisiko. In weiterführenden Experimenten könnten direkte Faktor Xa-Inhibitoren den Mechanismus der IH Hemmung aufzuklären helfen.

7. Appendix

Table 8 The list of chemicals

Name	Manufacturer
Buprenovet buprenorphine 0.3 mg/ml	Bayer Vital GmbH
Rimadyl Carporfen 50 g/20ml	Pfizer GmbH
Ringer-Infusion solution	B. Braun Melsungen AG
Baxter Isoflurane 25 0ml	Baxter Deutschland GmbH
Betaisodona solution 0.1 g/ml	ACA Müller/ADAG Pharma AG
Vidisic eye gel carbomer 2 mg/g	Dr. Mann Pharma GmbH
Novaminsuflon-ratiopharm 500mg/ml tropfen	Ratiopharm GmbH
Tramadol hydrochlorid 100mg/L	Grünenthal GmbH
Heparin Natrium 10.000 I.E./ml	B. Braun Melsungen AG
4-Desoxypyridoxin -hydrochlorid 500MG	Sigma-Aldrich Co. LLC.
Narcoren Pentobarbital-sodium 16g/100ml	Boehringer Ingelheim Vetmedica GmbH
Formafix 4% buffered	Grimm med. Logistik GmbH
Enzym Mix	
Hank’s balanced salt solution 500ml	Sigma-Aldrich Co. LLC.
Bovine Serum Albumin	Sigma-Aldrich Co. LLC.
Soybean trypsin inhibitor 100mg	Worthington Biochemical Co.
Elastase type III	Sigma-Aldrich Co. LLC.
Collagenase 10ku	Worthington Biochemical Co.
RNAlaterTM solution	Thermo Fischer Scientific
Tissue-Tek Paraffinwachs TEK III	Sakura Finetek Germany GmbH
Xylol z. A.	Th. Geyer GmbH & Co. KG
Ethanol (70%, 96%, 99%)	Walter CMP
Resorcin fuchsin-Solution nach Weigert 1%	Waldeck GmbH & Co KG
Ferric-Hematoxylin A Weigert	Waldeck GmbH & Co KG
Ferric-Hematoxylin B Weigert	Waldeck GmbH & Co KG

Pikrinsäure-Solution 1,2 %	AppliChem GmbH
Thiazinrot R	Waldeck GmbH & Co KG
Isopropanol (70, 80, 85, 90, 96 & 100 %)	Th. Geyer GmbH & Co. KG
Eukitt Quick-hardening mounting medium	Sigma-Aldrich Co. LLC.
Gibco 2-Mercaptoethanol	Thermo Fischer Scientific

Table 9 The list of surgical instruments

Name	Catalog No.	Manufacturer
Spring scissor (straight)	No.15000-03	Fine Science Tools (F.S.T)
Fine Iris scissor (angled to side, 9 cm)	No.14063-09	Fine Science Tools (F.S.T)
Standard pattern surgical scissor (straight)	No.14001-12	Fine Science Tools (F.S.T)
Dumont #5 forceps (biology tip)	No.11295-10	Fine Science Tools (F.S.T)
Dumont #5/45 forceps	No.11251-35	Fine Science Tools (F.S.T)
Delicate Moria forceps (microserrated)	No.11370-32	Fine Science Tools (F.S.T)
Round handled needle holder (straight with lock)	No.12075-12	Fine Science Tools (F.S.T)
Black micro serrefines (strong pressure)	No.18052-03	Fine Science Tools (F.S.T)
Magnetic fixator retraction system:	No.18200-20	Fine Science Tools (F.S.T)
Small base plate	No.18200-03	Fine Science Tools (F.S.T)
Short fixator	No.18200-01	Fine Science Tools (F.S.T)
Tall fixator	No.18200-02	Fine Science Tools (F.S.T)
Elastomer (2 m roll)	No.18200-07	Fine Science Tools (F.S.T)
Retractors (blunt, 1 mm wide)	No.18200-09	Fine Science Tools (F.S.T)
Retractors (blunt, 2.5 mm wide)	No.18200-10	Fine Science Tools (F.S.T)
Retractors (blunt, 5 mm wide)	No.18200-11	Fine Science Tools (F.S.T)
ETHICON PERMA-HANDTM silk suture (7-0, black)	768G	Johnson & Johnson Medical Ltd
ETHICON ETHILONTM Polyamide 6 suture (10-0, black)	2814G	Johnson & Johnson Medical Ltd
PGA resoquick (6-0, blue)	PRN31502	Healthium Medtech Limited

B.Braun Isis AESCulAP® battery-operated clipper	GT421	Aesculap Suhl GmbH
Leica stereomicroscope M60	10450167	Leica microsystems AG
Harvard apparatus anesthetic vaporizer	34-1040SV	Harvard Apparatus
Alzet pump Model 1007D	10395-18	Durect Corporation

Table 10 The list of research instruments

Name	Catalog No.	Manufacturer
Zeiss Axio Scan Z1	G/017997	Carl Zeiss AG
TissueLyser LT	06949	Qiagen GmbH
Centrifuge 5810	5810YR914582	Eppendorf AG
Thermomixer comfort	5355ZJ047028	Eppendorf AG
Epoch™ Spectrophotometer		BioTek Instruments, Inc.
Bio-Rad T100TM Thermal Cycler	1861096	Bio-Rad laboratories, Inc.
Roter-Gene Q real-time PCR cycler	9001550	Qiagen GmbH
Leica SM2010R slide microtome	00001430	Leica Mikrosysteme Vertrieb GmbH

Table 11 The list of software

Name	Manufacturer	Application
NetScope® Viewer	Net-Base Software GmbH	Histological images
ImageJ program 2.1.0	National Institute of Health, USA	Histological analysis
Gen5™2.0	BioTek®	RNA concentration measurement
Rotor-Gene Q Series, Version 2.3.1	Qiagen GmbH	qPCR measurement
GraphPad Prism® 8	GraphPad Software	Statistics and illustrations
Microsoft Office (Excel, PowerPoint, Word)	Microsoft Corporation	Statistics, illustrations and text processing

Table 12 The list of research kits

Name	Components	Manufacturer
RNeasy Fibrous Tissue Mini Kit (50)	RNeasy Mini Spin Columns Collection tubes (1,5 ml)	Qiagen GmbH

	Collection tubes (2 ml) RLT Puffer Proteinase K RW1 Buffer RPE Buffer RNase-free Water	
Rnase-Free Dnase Set	Rnase-free Dnase I RDD Buffer Rnase-free Water	Qiagen GmbH
High Capacity cDNA Reverse Transcription Kit	10x RT Buffer 10x RT Random Primers 25x dNTP Mix (100mM) MultiScribeTM Reverse Transcripts (50U/µL)	Thermo Fischer Scientific
Rotor-Gene® SYBR® Green PCR Kit (400)	2x Rotor-Gene SYBR Green PCR Master Mix (HotStarTaq®Plus DNA Polymerase, Rotor-Gene SYBR Green PCR Buffer, SYBR Green I dye, dNTP mix (dATP, dCTP, dGTP, dTTP))	Qiagen GmbH
Advanced Protein Assay Reagent	5x Advanced Protein Assay Reagent	Cytoskeleton Inc.

8. References

Aday AW, Matsushita K (2021) Epidemiology of Peripheral Artery Disease and Polyvascular Disease. Circ Res. 128(12):1818-1832.

Agnelli G, Becattini C, Meyer G, Muñoz A, Huisman MV, Connors JM, Cohen A, Bauersachs R, Brenner B, Torbicki A, Sueiro MR, Lambert C, Gussoni G, Campanini M, Fontanella A, Vescovo G, Verso M; Caravaggio Investigators (2020) Apixaban for the Treatment of Venous Thromboembolism Associated with Cancer. N Engl J Med. 23;382(17):1599-1607.

Alberelli MA, De Candia E (2014) Functional role of protease activated receptors in vascular biology. Vascul Pharmacol. 8;62(2):72-81.

Alewijnse AE, Peters SL (2008) Sphingolipid signalling in the cardiovascular system: good, bad or both? Eur J Pharmacol. 585(2-3):292-302.

Allahverdian S, Chaabane C, Boukais K, Francis GA, Bochaton-Piallat ML. Smooth muscle cell fate and plasticity in atherosclerosis (2018) Cardiovasc Res. 15;114(4):540-550.

Allende ML, Yamashita T, Proia RL (2003) G-protein-coupled receptor S1P1 acts within endothelial cells to regulate vascular maturation. Blood 102(10): 3665–7.

Alves NG, Trujillo AN, Breslin JW, Yuan SY (2019) Sphingosine-1-Phosphate Reduces Hemorrhagic Shock and Resuscitation-Induced Microvascular Leakage by Protecting Endothelial Mitochondrial Integrity. Shock. 52(4):423-433.

Andrade-Gordon P ,Derian CK, Maryanoff BE, Zhang HC, Addo MF, Cheung W, Damiano BP, D'Andrea MR, Darrow AL, de Garavilla L, Eckardt AJ, Giardino EC, Haertlein BJ, McComsey DF (2001) Administration of a potent antagonist of PAR-1 attenuates vascular restenosis following balloon angioplasty in rats. J. Pharmacol. Exp. Ther. 298(1):34-42.

Aoki M, Aoki H, Mukhopadhyay P, Tsuge T, Yamamoto H, Matsumoto NM, Toyohara E, Okubo Y, Ogawa R, Takabe K (2019) Sphingosine-1-Phosphate Facilitates Skin Wound Healing by Increasing Angiogenesis

and Inflammatory Cell Recruitment with Less Scar Formation. Int J Mol Sci. 20(14):3381.

Aslani S, Kabiri M, HosseinZadeh S, Hanaee-Ahvaz H, Taherzadeh ES, Soleimani M (2020) The applications of heparin in vascular tissue engineering. Microvasc Res. 2020 (131):104027.

Austin KM, Nguyen N, Javid G, Covic L, Kuliopulos A (2013) Noncanonical matrix metalloprotease-1-protease-activated receptor-1 signaling triggers VSMC dedifferentiation and arterial stenosis. Biol Chem. 9;288(32):23105-15.

Azeloglu EU, Albro MB, Thimmappa VA, Ateshian GA, Costa KD (2008) Heterogeneous transmural proteoglycan distribution provides a mechanism for regulating residual stresses in the aorta. Am. J. Physiol. Heart Circ. Physiol. 294, H1197–H1205.

Baeyens AAL, Schwab SR (2020) Finding a Way Out: S1P Signaling and Immune Cell Migration. Annu Rev Immunol. 38(1):759-784.

Batheja AD, Uhlinger DJ, Carton JM, Ho G, D'Andrea MR (2003) Characterization of serine palmitoyltransferase in normal human tissues. J Histochem Cytochem. 51(5):687-696.

Bauer J, Ripperger A, Frantz S, Ergün S, Schwedhelm E, Benndorf RA (2014) Pathophysiology of isoprostanes in the cardiovascular system: implications of isoprostane-mediated thromboxane A2 receptor activation. Br J Pharmacol. 171(13):3115-3131.

Becker RC, Sexton T, Smyth SS (2018) Translational Implications of Platelets as Vascular First Responders. Circ Res. 122(3):506-522.

Beckman JA, Schneider PA, Conte MS (2021) Advances in Revascularization for Peripheral Artery Disease: Revascularization in PAD. Circ Res. 128(12):1885-1912.

Bian K, Doursout MF, Murad F (2008) Vascular system: role of nitric oxide in cardiovascular diseases. J Clin Hypertens (Greenwich). 10(4):304-10.

Binder MJ, McCoombe S, Williams ED, McCulloch DR, Ward AC (2020) ADAMTS-15 Has a Tumor Suppressor Role in Prostate Cancer. Biomolecules. 28;10(5):682.

Biran R, Pond D (2017) Heparin coatings for improving blood compatibility of medical devices. Adv Drug Deliv Rev. 2017(112):12-23.

Bodhankar S, Chen Y, Vandenbark AA, Murphy SJ, Offner H (2014) Treatment of experimental stroke with IL-10-producing B-cells reduces infarct size and peripheral and CNS inflammation in wild-type B-cell-sufficient mice. Metab Brain Dis. 5;29(1):59-73.

Böhm A, Flößer A, Ermler S, Fender AC, Lüth A, Kleuser B, Schrör K, Rauch BH (2013) Factor-Xa-induced mitogenesis and migration require sphingosine kinase activity and S1P formation in human vascular smooth muscle cells. Cardiovasc Res. 99(3):505-513.

Bolick DT, Srinivasan S, Kim KW, Hatley ME, Clemens JJ, Whetzel A, Ferger N, Macdonald TL, Davis MD, Tsao PS, Lynch KR, Hedrick CC (2005) S1P prevents tumor necrosis factor-{alpha}-mediated monocyte adhesion to aortic endothelium in mice. Arterioscler Thromb Vasc Biol. 25(5):976-981.

Bot M, Van Veldhoven PP, de Jager SC, Johnson J, Nijstad N, Van Santbrink PJ, Westra MM, Van Der Hoeven G, Gijbels MJ, Müller-Tidow C, Varga G, Tietge UJ, Kuiper J, Van Berkel TJ, Nofer JR, Bot I, Biessen EA (2013) Hematopoietic sphingosine 1-phosphate lyase deficiency decreases atherosclerotic lesion development in LDL-receptor deficient mice. PLoS One. 8(5):e63360.

Brack MJ, Ray S, Chauhan A, Fox J, Hubner PJ, Schofield P, Harley A, Gershlick AH (1995) The Subcutaneous Heparin and Angioplasty Restenosis Prevention (SHARP) trial. Results of a multicenter randomized trial investigating the effects of high dose unfractionated heparin on angiographic restenosis and clinical outcome. J Am Coll Cardiol. 26(4):947-54.

Braetz J, Becker A, Geissen M, Larena-Avellaneda A, Schrepfer S, Daum G (2018) Sphingosine-1-phosphate receptor 1 regulates neointimal growth in a humanized model for restenosis. J Vasc Surg. 68(6S):201S-207S.

Brasselet C, Durand E, Addad F, Al Haj Zen A, Smeets MB, Laurent-Maquin D, Bouthors S, Bellon G, de Kleijn D, Godeau G, Garnotel R, Gogly B, Lafont A (2005) Collagen and elastin cross-linking: a mechanism of

constrictive remodeling after arterial injury. Am J Physiol Heart Circ Physiol. 289(5):H2228-33.

Brendel JM, Mangold T, Lescan M, Schmehl J, Ghibes P, Grimm A, Greulich S, Krumm P, Artzner C, Grözinger G, Estler A (2024) Viabahn stent graft for arterial injury management: safety, technical success, and long-term outcome. CVIR Endovasc. 28;7(1):23.

Brouillard P, Dupont L, Helaers R, Coulie R, Tiller GE, Peeden J, Colige A, Vikkula M (2017) Loss of ADAMTS3 activity causes Hennekam lymphangiectasia–lymphedema syndrome3. Hum. Mol. Gen. 26, 4095–4104.

Bruder-Nascimento T, Ferreira NS, Zanotto CZ, Ramalho F, Pequeno IO, Olivon VC, Neves KB, Alves-Lopes R, Campos E, Silva CA, Fazan R, Carlos D, Mestriner FL, Prado D, Pereira FV, Braga T, Luiz JP, Cau SB, Elias PC, Moreira AC, Câmara NO, Zamboni DS, Alves-Filho JC, Tostes RC (2016) NLRP3 Inflammasome Mediates Aldosterone-Induced Vascular Damage. Circulation. 6;134(23):1866-1880.

Brulhart-Meynet MC, Braunersreuther V, Brinck J, Montecucco F, Prost JC, Thomas A, Galan K, Pelli G, Pedretti S, Vuilleumier N, Mach F, Lecour S, James RW, Frias MA (2015) Improving reconstituted HDL composition for efficient post-ischemic reduction of ischemia reperfusion injury. PLoS One. 10(3):e0119664.

Bryan AM, Del Poeta M (2018) Sphingosine-1-phosphate receptors and innate immunity. Cell Microbiol. 20(5):e12836.

Buccheri D, Piraino D, Andolina G, Cortese B (2016) Understanding and managing in-stent restenosis: a review of clinical data, from pathogenesis to treatment. Thorac Dis. 8(10):e1150-e1162.

Cai WW, Gu YJ, Wang XN, Chen CZ (2009) Heparin coating of small-caliber decellularized xenografts reduces macrophage infiltration and intimal hyperplasia. Artif Organs. 33(6):448-55.

Camerer E, Regard JB, Cornelissen I, Srinivasan Y, Duong DN, Palmer D, Pham TH, Wong JS, Pappu R, Coughlin SR (2009) S1P in the plasma

compartment regulates basal and inflammation-induced vascular leak in mice. J Clin Invest. 119(7):1871-1879.

Cantalupo A, Gargiulo A, Dautaj E, Liu C, Zhang Y, Hla T, Di Lorenzo A (2017) S1PR1 Signaling Regulates Blood Flow and Pressure. Hypertension. 70(2):426-434.

Cantalupo A, Zhang Y, Kothiya M, Galvani S, Obinata H, Bucci M, Giordano FJ, Jiang XC, Hla T, Di Lorenzo A (2015) Nogo-B regulates endothelial sphingolipid homeostasis to control vascular function and blood pressure. Nat Med. 21(9):1028-1037.

Chalmers N, Walker PT, Belli AM, Thorpe AP, Sidhu PS, Robinson G, Ransbeeck M, Fearn SA (2013) Randomized trial of the SMART stent versus balloon angioplasty in long superficial femoral artery lesions: the SUPER study. Cardiovasc Intervent Radiol. 36(2):353-361.

Chang S, Song S, Lee J, Yoon J, Park J, Choi S, Park JK, Choi K, Choi C (2014) Phenotypic modulation of primary vascular smooth muscle cells by short-term culture on micropatterned substrate. PLoS One. 9(2):e88089.

Chen D, Abrahams JM, Smith LM, McVey JH, Lechler RI, and Dorling A (2008) Regenerative repair after endoluminal injury in mice with specific antagonism of protease activated receptors on CD34+ vascular progenitors. Blood. 111(8):4155-4164.

Chen X, Fan X, Tan J, Shi P, Wang X, Wang J, Kuang Y, Fei J, Liu J, Dang S, Wang Z (2017) Palladin is involved in platelet activation and arterial thrombosis. Thromb Res. 1(149):1-8.

Chieng-Yane P, Bocquet A, Letienne R, Bourbon T, Sablayrolles S, Perez M, Hatem S, Lompre AM, Le Grand B, David-Dufilho M (2011) Protease-activated receptor-1 antagonist F 16618 reduces arterial restenosis by down-regulation of tumor necrosis factor α and MMP 7 expression, migration, and proliferation of vascular smooth muscle cells. J. Pharmacol. Exp. Ther. 336(3):643-651.

Christoffersen C, Obinata H, Kumaraswamy SB, Galvani S, Ahnström J, Sevvana M, Egerer-Sieber C, Muller YA, Hla T, Nielsen LB, Dahlbäck B

(2011) Endothelium-protective S1P provided by HDL-associated apolipoprotein M. Proc Natl Acad Sci U S A. 108(23):9613-9618.

Chun J, Giovannoni G, Hunter SF (2021) Sphingosine 1-phosphate Receptor Modulator Therapy for Multiple Sclerosis: Differential Downstream Receptor Signalling and Clinical Profile Effects. Drugs. 81(2):207-231.

Cochain C, Channon KM, Silvestre JS (2013) Angiogenesis in the infarcted myocardium. Antioxid Redox Signal. 18(9):1100-1113.

Cornelissen A, Vogt FJ (2019) The effects of stenting on coronary endothelium from a molecular biological view: Time for improvement? Cell Mol Med. 23(1):39-46.

Csányi G, Taylor WR, Pagano PJ (2009) NOX and inflammation in the vascular adventitia. Free Radic Biol Med. 47(9):1254-1266.

Cyster JG, Schwab SR (2012) Sphingosine-1-phosphate and lymphocyte egress from lymphoid organs. Annu Rev Immunol. 30(1):69-94.

Dancevic CM, Fraser FW, Smith AD, Stupka N, Ward AC, McCulloch DR (2013) Biosynthesis and expression of a disintegrin-like and metalloproteinase domain with thrombospondin-1 repeats-15: a novel versican-cleaving proteoglycanase. J. Biol. Chem. 288(52):37267-37276.

Daum G, Winkler M, Moritz E, Müller T, Geffken M, von Lucadou M, Haddad M, Peine S, Böger RH, Larena-Avellaneda A, Debus ES, Gräler M, Schwedhelm E (2020) Determinants of Serum- and Plasma Sphingosine-1-Phosphate Concentrations in a Healthy Study Group. TH Open. 23;4(1):e12-e19.

Dawwas GK, Leonard CE, Lewis JD, Cuker A (2022) Risk for Recurrent Venous Thromboembolism and Bleeding With Apixaban Compared With Rivaroxaban: An Analysis of Real-World Data. Ann Intern Med. 2022 Jan;175(1):20-28. doi: 10.7326/M21-0717. Epub 2021 Dec 7. Erratum in: Ann Intern Med. 175(11):1627-1628.

de Mel A, Jell G, Stevens MM, Seifalian AM (2008) Biofunctionalization of biomaterials for accelerated in situ endothelialization: a review. Biomacromolecules. 9(11):2969-2979.

de Nardo D, Latz E (2011) NLRP3 inflammasomes link inflammation and metabolic disease. Trends Immunol. 32(8):373-379.

Déglise S, Bechelli C, Allagnat F (2023) Vascular smooth muscle cells in intimal hyperplasia, an update. Front Physiol. 13(1):1081881.

Didangelos A, Mayr U, Monaco C, Mayr M (2012) Novel role of ADAMTS-5 protein in proteoglycan turnover and lipoprotein retention in atherosclerosis. J Biol Chem. 1;287(23):19341-5.

Diebel ME, Diebel LN, Liberati DM (2019) Protective effects of plasma products on the endothelial-glycocalyx barrier following trauma-hemorrhagic shock: Is sphingosine-1 phosphate responsible? J Trauma Acute Care Surg. 87(5):1061-1069.

Dimayuga P, Cercek B, Oguchi S, Fredrikson GN, Yano J, Shah PK, Jovinge S, Nilsson J (2002) Inhibitory effect on arterial injury-induced neointimal formation by adoptive B-cell transfer in Rag-1 knockout mice. Arterioscler Thromb Vasc Biol. 22(4):644-649.

Ding J, Wang K, Liu W, She Y, Sun Q, Shi J, Sun H, Wang DC, Shao F (2016) Pore-forming activity and structural autoinhibition of the gasdermin family. Nature. 535(7610):111-116.

Donovan EE, Pelanda R, Torres RM (2010) S1P3 confers differential S1P-induced migration by autoreactive and non-autoreactive immature B cells and is required for normal B-cell development. Eur J Immunol. 40(3):688-98.

Duncan SE, Gao S, Sarhene M, Coffie JW, Linhua D, Bao X, Jing Z, Li S, Guo R, Su J, Fan G (2020) Macrophage activities in myocardial infarction and heart failure. Cardiol Res Pract. 2020(4375127):1-16.

Dupuis LE, Nelson EL, Hozik B, Porto SC, Rogers-DeCotes A, Fosang A, Kern CB (2019) Adamts5-/- Mice Exhibit Altered Aggrecan Proteolytic Profiles That Correlate With Ascending Aortic Anomalies. Arterioscler Thromb Vasc Biol. 39(10):2067-2081.

Eckenstaler R, Ripperger A, Hauke M, Petermann M, Hemkemeyer SA, Schwedhelm E, Ergün S, Frye M, Werz O, Koeberle A, Braun H, Benndorf RA (2022) A ThromboxaneA2 Receptor-Driven COX2-

Dependent Feedback Loop That Affects Endothelial Homeostasis and Angiogenesis. Arterioscler Thromb Vasc Biol. 42(4):444-461.

Edelman ER, Karnovsky MJ (1994) Contrasting effects of the intermittent and continuous administration of heparin in experimental restenosis. Circulation. 89(2):770-6.

Egom EE, Mamas MA, Chacko S, Stringer SE, Charlton-Menys V, El-Omar M, Chirico D, Clarke B, Neyses L, Cruickshank JK, Lei M, Fath-Ordoubadi F (2013) Serum sphingolipids level as a novel potential marker for early detection of human myocardial ischaemic injury. Front Physiol. 4(130):1-10.

Elyasi A, Voloshyna I, Ahmed S, Kasselman LJ, Behbodikhah J, De Leon J, Reiss AB (2020) The role of interferon-γ in cardiovascular disease: an update. Inflamm Res. 69(10):975-988.

English D, Welch Z, Kovala AT, Harvey K, Volpert OV, Brindley DN, Garcia JG (2000) Sphingosine 1-phosphate released from platelets during clotting accounts for the potent endothelial cell chemotactic activity of blood serum and provides a novel link between hemostasis and angiogenesis. Faseb J. 14(14):2255-2265.

Fay WP, Garg N, Sunkar M (2007) Vascular functions of the plasminogen activation system. Arterioscler Thromb Vasc Biol. 27(6):1231-1237.

Feuerborn R, Becker S, Potì F, Nagel P, Brodde M, Schmidt H, Christoffersen C, Ceglarek U, Burkhardt R, Nofer JR (2017) High density lipoprotein (HDL)-associated sphingosine 1-phosphate (S1P) inhibits macrophage apoptosis by stimulating STAT3 activity and survivin expression. Atherosclerosis. 257(1):29-37.

Flaumenhaft R, De Ceunynck K (2017) Targeting PAR1: Now What? Trends Pharmacol Sci. 38(8):701-716.

Fu Y, Gao C, Liang Y, Wang M, Huang Y, Ma W, Li T, Jia Y, Yu F, Zhu W, Cui Q, Li Y, Xu Q, Wang X and Kong W (2016) Shift of Macrophage Phenotype Due to Cartilage Oligomeric Matrix Protein Deficiency Drives Atherosclerotic Calcification. Circ. Res. 119(2):261-276.

Fu Y, Huang Y, Yang Z, Chen Y, Zheng J, Mao C, Li Z, Liu Z, Yu B, Li T, Wang M, Xu C, Zhou Y, Zhao G, Jia Y, Guo W, Jia X, Zhang T, Li L, Liu Z, Guo S, Ma M, Zhang H, Liu B, Du J, Wang W, Tang C, Gao P, Xu Q, Wang X, Liu J, Sun J, Kong W (2021) Cartilage oligomeric matrix protein is an endogenous beta-arrestin-2-selective allosteric modulator of AT1 receptor counteracting vascular injury. Cell Res. 31(7):773-790.

Fu Y, Kong W (2017) Cartilage Oligomeric Matrix Protein: Matricellular and Matricrine Signaling in Cardiovascular Homeostasis and Disease. Curr. Vasc. Pharmacol. 15(3):186–196.

Fukunaga R, Hirano K, Hirano M, Niiro N, Nishimura J, Maehara Y, Kanaide H (2006) Upregulation of proteinase-activated receptors and hypercontractile responses precede development of arterial lesions after balloon injury. Physiol Heart Circ Physiol. 11;291(5):H2388-95.

Fyrst H, Saba JD (2010) An update on sphingosine-1-phosphate and other sphingolipid mediators. Nat Chem Biol. 6(7):489-497.

Gaengel K, Niaudet C, Hagikura K, Laviña B, Muhl L, Hofmann JJ, Ebarasi L, Nyström S, Rymo S, Chen LL, Pang MF, Jin Y, Raschperger E, Roswall P, Schulte D, Benedito R, Larsson J, Hellström M, Fuxe J, Uhlén P, Adams R, Jakobsson L, Majumdar A, Vestweber D, Uv A, Betsholtz C (2012) The sphingosine-1-phosphate receptor S1PR1 restricts sprouting angiogenesis by regulating the interplay between VE-cadherin and VEGFR2. Dev Cell. 23(3):587-599.

Galkina E, Ley K (2007) Vascular adhesion molecules in atherosclerosis. Arterioscler Thromb Vasc Biol. 27(11):2292-2301.

Galvani S, Sanson M, Blaho VA, Swendeman SL, Obinata H, Conger H, Dahlbäck B, Kono M, Proia RL, Smith JD, Hla T (2015) HDL-bound sphingosine 1-phosphate acts as a biased agonist for the endothelial cell receptor S1P1 to limit vascular inflammation. Sci Signal. 8(389):ra79.

Ganbaatar B, Fukuda D, Shinohara M, Yagi S, Kusunose K, Yamada H, Soeki T, Hirata KI, Sata M (2021) Inhibition of S1P Receptor 2 Attenuates Endothelial Dysfunction and Inhibits Atherogenesis in Apolipoprotein E-Deficient Mice. J Atheroscler Thromb. 28(6):630-642.

Ge P, Li H, Ya X, Xu Y, Ma L, He Q, Wang R, Liu Z, Zhang Q, Zhang Y, Wang W, Zhang D, Zhao J (2023) Single-cell atlas reveals different immune environments between stable and vulnerable atherosclerotic plaques. Front Immunol. 13(1):1085468.

Goetzl EJ, Graler MH (2004) Sphingosine 1-phosphate and its type 1 G protein-coupled receptor: trophic support and functional regulation of T lymphocytes. J Leukoc Biol, 76(1):30-35.

Grabski AD, Shimizu T, Deou J, Mahoney WM Jr, Reidy MA, Daum G (2009) Sphingosine-1-phosphate receptor-2 regulates expression of smooth muscle alpha-actin after arterial injury. Arterioscler Thromb Vasc Biol. 29(10):1644-50.

Greiwe G, Moritz E, Amschler K, Poppe A, Sarwari H, Nierhaus A, Kluge S, Reichenspurner H, Zoellner C, Schwedhelm E, Daum G, Tampe B, Winkler MS (2021) Dynamics of Vascular Protective and Immune Supportive Sphingosine-1-Phosphate During Cardiac Surgery. Front Immunol. 12(1):761475.

Guyton JR, Rosenberg RD, Clowes AW, Karnovsky MJ (1980) Inhibition of rat arterial smooth muscle cell proliferation by heparin. In vivo studies with anticoagulant and nonanticoagulant heparin. Circ Res. 46(5):625-34.

Hänel P, Andréani P, Gräler MH (2007) Erythrocytes store and release sphingosine 1-phosphate in blood. FASEB J. 21(4):1202-1209.

Harris AK, Shen J, Radford J, Bao S, Hambly BD (2009) GM-CSF deficiency delays neointima formation in a normolipidemic mouse model of endoluminal endothelial damage. Immunol Cell Biol. 87(2):122-130.

Hatakeyama K, Asada Y, Marutsuka K, Kataoka H, Sato Y, Sumiyoshi A (1998) Expression of tissue factor in the rabbit aorta after balloon injury. Atherosclerosis. 8;139(2):265-71.

Haynes V., Elfering S.L., Squires R.J., Traaseth N., Solien J., Ettl A., Giulivi C (2003) Mitochondrial Nitric-Oxide Synthase: Role in Pathophysiology. IUBMB Life. 55:599–603.

He W, Wan H, Hu L, Chen P, Wang X, Huang Z, Yang ZH, Zhong CQ, Han J (2015) Gasdermin D is an executor of pyroptosis and required for interleukin-1β secretion. Cell Res. 25(1):1285-1298.

Hemdan NY, Weigel C, Reimann CM, Gräler MH (2016) Modulating S1P signaling with DOP or FTY720 alleviates vascular and immune defects in mouse sepsis. Eur J Immunol. 46(12):2767-2777.

Heo JY, Im DS (2019) Pro-Inflammatory Role of S1P3 in Macrophages. Biomol Ther (Seoul). 27(4):373-380.

Huang YL, Shi GY, Lee H, Jiang MJ, Huang BM, Wu HL, Yang HY (2009) Thrombin induces nestin expression via the transactivation of EGFR signalings in rat vascular smooth muscle cells. Cell Signal. 21(6):954-968.

Hui DY (2008) Intimal hyperplasia in murine models. Curr Drug Targets. 9(3):251-60.

Humphrey JD, Milewicz DM, Tellides G, Schwartz MA (2014) Cell biology. Dysfunctional mechanosensing in aneurysms. Science. 2014(344): 477–479.

Iessi E, Marconi M, Manganelli V, Sorice M, Malorni W, Garofalo T, Matarrese P (2020) On the role of sphingolipids in cell survival and death. Int Rev Cell Mol Biol. 351(1):149-195.

Igarashi J, Michel T (2009) Sphingosine-1-phosphate and modulation of vascular tone. Cardiovasc Res. 82(2):212-220.

Inoue S, Nakazawa T, Cho A, Davastan F, Shilling D, Daum G, Reidy M (2007) Regulation of arterial lesions in mice depends on differential smooth muscle cell migration: A role for sphingosine-1-phosphate receptors. J Vasc Surg. 46(4):756-763.

Inoue T, Croce K, Morooka T, Sakuma M, Node K, Simon DI (2011) Vascular Inflammation and Repair: Implications for Re-Endothelialization, Restenosis, and Stent Thrombosis. Cardiovasc. Interv. 4(10):1057-1066.

Ishii I, Ye X, Friedman B, Kawamura S, Contos JJ, Kingsbury MA, Yang AH, Zhang G, Brown JH, Chun J (2002) Marked perinatal lethality and cellular signaling deficits in mice null for the two sphingosine 1-

phosphate (S1P) receptors, S1P2/LPB2/EDG-5 and S1P3/LPB3/EDG-3. Biol Chem. 277(28):25152–25159.

Ishizuka T, Matsumura K, Matsui T, Takase B, Kurita A (2003) Ramatroban, a thromboxane A2 receptor antagonist, prevents macrophage accumulation and neointimal formation after balloon arterial injury in cholesterol-fed rabbits. J Cardiovasc Pharmacol. 4;41(4):571-8.

Ji J, Xu F, Li L, Chen R, Wang J, Hu WC (2010) Activation of adventitial fibroblasts in the early stage of the aortic transplant vasculopathy in rat. Transplantation. 89(8):945-953.

Jiang Y (2021) Clamping of the infrarenal aorta results in intimal hyperplasia and distinct changes of S1P receptor expression in the intima-media and adventitia. Med. diss.thesis. Hamburg University.

Jin F, Hagemann N, Sun L, Wu J, Doeppner TR, Dai Y, Hermann DM (2018) HDL promotes angiogenesis via S1P3-dependent VEGFR2 activation. Angiogenesis. 21(2):381-394.

Jin L (2011) The actin associated protein palladin in smooth muscle and in the development of diseases of the cardiovasculature and in cancer. J Muscle Res Cell Motil. 8;32(1):7-17.

Jin L, Gan Q, Zieba BJ, Goicoechea SM, Owens GK, Otey CA, Somlyo AV (2010) The actin associated protein palladin is important for the early smooth muscle cell differentiation. PLoS One. 5(9):e12823.

Jin L, Kern MJ, Otey CA, Wamhoff BR, Somlyo AV (2007) Angiotensin II, focal adhesion kinase, and PRX1 enhance smooth muscle expression of lipoma preferred partner and its newly identified binding partner palladin to promote cell migration. Circ Res. 100(6):817-825.

Jing XD, Wei XM, Deng SB, Du JL, Liu YJ, She Q (2015) The relationship between the high-density lipoprotein (HDL)-associated sphingosine-1-phosphate (S1P) and coronary in-stent restenosis. Clin Chim Acta. 15;446:248-52.Jonnalagadda D, Sunkara M, Morris AJ, Whiteheart SW (2014) Granule-mediated release of S1P by activated platelets. Biochim Biophys Acta. 1841(11):1581-1589.

Jozefczuk E, Guzik TJ, Siedlinski M (2020) Significance of S1P in cardiovascular physiology and pathology. Pharmacol Res. 156(1):104793.

Jukema JW, Verschuren JJW, Ahmed TAN, Quax PHA (2012) Restenosis after PCI. Part 1:Pathophysiology and risk factors. Nat Rev Cardiol. 9(1):53-62.

Katunaric B, SenthilKumar G, Schulz ME, De Oliveira N, Freed JK (2022) S1P (Sphingosine-1-Phosphate)-Induced Vasodilation in Human Resistance Arterioles During Health and Disease. Hypertension. 79(10):2250-2261.

Keul P, Lucke S, von Wnuck Lipinski K, Bode C, Graler M, Heusch G, Levkau B (2011) Sphingosine-1-phosphate receptor 3 promotes recruitment of monocyte/macrophages in inflammation and atherosclerosis. Circ Res, 108(3):314-323.

Keul P, Peters S, von Wnuck Lipinski K, Schröder NH, Nowak MK, Duse DA, Polzin A, Weske S, Gräler MH, Levkau B (2022) S1P Lyase Inhibition Aggravates Atherosclerosis and Induces Plaque Rupture in ApoE-/-Mice. Int J Mol Sci. 23(17):9606.

Kibbe M, Billiar T, Tzeng E. Inducible nitric oxide synthase and vascular injury (1999) Cardiovasc Res.15;43(3):650-7.

Kibbe MR, Tzeng E, Gleixner SL, Watkins SC, Kovesdi I, Lizonova A, Makaroun MS, Billiar TR, Rhee RY (2001) Adenovirus-mediated gene transfer of human inducible nitric oxide synthase in porcine vein grafts inhibits intimal hyperplasia. J Vasc Surg.7;34(1):156-65.

Kim D, Tian W, Wu TT, Xiang M, Vinh R, Chang JL, Gu S, Lee S, Zhu Y, Guan T, Schneider EC, Bao E, Dixon JB, Kao P, Pan J, Rockson SG, Jiang X, Nicolls MR (2023) Abnormal Lymphatic Sphingosine-1-Phosphate Signaling Aggravates Lymphatic Dysfunction and Tissue Inflammation. Circulation. 148(16):1231-1249.

Kitano T, Usui S, Takashima SI, Inoue O, Goten C, Nomura A, Yoshioka K, Okajima M, Kaneko S, Takuwa Y, Takamura M (2019) Sphigosine-1-phosphate receptor 1 promotes neointimal hyperplasia in a mouse model of carotid artery injury. Biochem Biophys Res Commun. 26;511(1):179-184.

Kitatani K, Idkowiak-Baldys J, Hannun YA (2008) The sphingolipid salvage pathway in ceramide metabolism and signaling. Cell Signal. 20(6):1010-1018.

Koch CD, Lee CM, Apte SS (2020) Aggrecan in Cardiovascular Development and Disease. J Histochem Cytochem. 68(11):777-795.

Koelling S, Clauditz TS, Kaste M, Miosge N (2006) Cartilage oligomeric matrix protein is involved in human limb development and in the pathogenesis of osteoarthritis. Arthritis Res Ther. 2006;8(3):R56.

Kono M, Mi Y, Liu Y, Sasaki T, Allende ML, Wu YP, Yamashita T, Proia RL (2004) The sphingosine-1-phosphate receptors S1P1, S1P2, and S1P3 function coordinately during embryonic angiogenesis. J Biol Chem. 279(28):29367-29373.

Krock BL, Skuli N, Simon MC (2011) Hypoxia-induced angiogenesis: good and evil. Genes Cancer. 2(12):1117-1133.

Książek M, Chacińska M, Chabowski A, Baranowski M (2015) Sources, metabolism, and regulation of circulating sphingosine-1-phosphate. J Lipid Res. 56(7):1271-1281.

Kurano M, Yatomi Y (2018) Sphingosine 1-Phosphate and Atherosclerosis. J Atheroscler Thromb Jan 1;25(1):16-26.

Kwaan HC, Wang J, Svoboda K, Declerck PJ (2000) Plasminogen activator inhibitor 1 may promote tumour growth through inhibition of apoptosis. Br J Cancer. 82(10):1702-1708.

Laird JR, Jain A, Zeller T, Feldman R, Scheinert D, Popma JJ (2014) Nitinol stent implantation in the superficial femoral artery and proximal popliteal artery: twelve-month results from the complete SE multicenter trial. Endovasc Ther. 21(2):202-212.

Landeen LK, Dederko DA, Kondo CS, Hu BS, Aroonsakool N, Haga JH, Giles WR (2008) Mechanisms of the negative inotropic effects of sphingosine-1-phosphate on adult mouse ventricular myocytes. Am J Physiol Heart Circ Physiol. 294(2):H736-H749.

Lee H, Hamilton JR (2012) Physiology, pharmacology, and therapeutic potential of protease-activated receptors in vascular disease. Pharmacol Ther. 5;134(2):246-59.

Lewis ND, Haxhinasto SA, Anderson SM, Stefanopoulos DE, Fogal SE, Adusumalli P, Desai SN, Patnaude LA, Lukas SM, Ryan KR, Slavin AJ, Brown ML, Modis LK (2013) Circulating monocytes are reduced by sphingosine-1-phosphate receptor modulators independently of S1P3. J Immunol, 190(7):3533-3540.

Li J, Huang Y, Zhang Y, Liu P, Liu M, Zhang M, Wu R (2023) S1P/S1PR signaling pathway advancements in autoimmune diseases. Biomol Biomed. 23(6):922-935.

Li Q, Chen B, Zeng C, Fan A, Yuan Y, Guo X, Huang X, Huang Q (2015) Differential activation of receptors and signal pathways upon stimulation by different doses of sphingosine-1-phosphate in endothelial cells. Exp Physiol. 100(1):95-107.

Li XD, Hong MN, Chen J, Lu YY, Ye MQ, Ma Y, Zhu DL, Gao PJ (2020) Adventitial fibroblast-derived vascular endothelial growth factor promotes vasa vasorum-associated neointima formation and macrophage recruitment. Cardiovasc Res. 116(3):708-720.

Libby P (2017) Interleukin-1 Beta as a Target for Atherosclerosis Therapy. J. Am. Coll. Cardiol. 1(70):2278–2289.

Liman TG, Endres M (2012) New vessels after stroke: postischemic neovascularization and regeneration. Cerebrovasc Dis. 33(5):492-499.

Lin PH, Chen C, Bush RL, Yao Q, Lumsden AB, Hanson SR (2004) Small-caliber heparin-coated ePTFE grafts reduce platelet deposition and neointimal hyperplasia in a baboon model. J Vasc Surg. 39(6):1322-8.

Lin PH, Chronos NA, Marijianowski MM, Chen C, Bush RL, Conklin B, Lumsden AB, Hanson SR (2003) Heparin-coated balloon-expandable stent reduces intimal hyperplasia in the iliac artery in baboons. J Vasc Interv Radiol. 14(5):603-11.

Lin Q, Long C, Wang Z, Wang R, Shi W, Qiu J, Mo J, Xie Y (2022) Hirudin, a thrombin inhibitor, attenuates TGF-β-induced fibrosis in renal proximal

tubular epithelial cells by inhibition of protease-activated receptor 1 expression via S1P/S1PR2/S1PR3 signaling. Exp Ther Med. 1;23(1):3.

Lind M., Hayes A., Caprnda M., Petrovic D., Rodrigo L., Kruzliak P., Zulli A (2017) Inducible Nitric Oxide Synthase: Good or Bad? Biomed. Pharmacother.93:370–375.

Liu J, Sugimoto K, Cao Y, Mori M, Guo L, Tan G (2020) Serum Sphingosine 1-Phosphate (S1P): A Novel Diagnostic Biomarker in Early Acute Ischemic Stroke. Front Neurol. 11(985):1-10.

Liu JR, Wu J, Yu XC, Qian X, Xiong R, Wang HF, Yu DF, Liu FF, He SY (2017) Heparin-derived oligosaccharide inhibits vascular intimal hyperplasia in balloon-injured carotid artery. Chin J Nat Med. 15(6):442-450.

Liu T, Zhang L, Joo D, Sun SC (2017a) NF-κB signaling in inflammation. Signal Transduct. Target. Ther. 2(1):e17023.

Liu Y, Wada R, Yamashita T, Mi Y, Deng CX, Hobson JP, Rosenfeldt HM, Nava VE, Chae SS, Lee MJ, Liu CH, Hla T, Spiegel S, Proia RL (2000) Edg-1, the G protein-coupled receptor for sphingosine-1-phosphate, is essential for vascular maturation. J Clin Invest. 106(8):951–61.

Lv H, Wang H, Quan M, Zhang C, Fu Y, Zhang L, Lin C, Liu X, Yi X, Chen J, Wang X, Chen T, Ai D Kong W, Zhu Y (2021) Cartilage oligomeric matrix protein fine-tunes disturbed flow-induced endothelial activation and atherogenesis. Matrix Biol. 95(1):32-51.

Majesky MW, Lindner V, Twardzik DR, Schwartz SM, Reidy MA (1991) Production of transforming growth factor beta 1 during repair of arterial injury. J Clin. Investig. 88(1):904-910.

Majesky MW, Weiser-Evans MCM (2022) The adventitia in arterial development, remodeling, and hypertension. Biochem Pharmacol. 205:115259.

Marx SO, Totary-Jain H, Marks AR (2011) Vascular smooth muscle cell proliferation in restenosis. Circ Cardiovasc Interv. 4(1):104-111.

Mascall KS, Small GR, Gibson G, Nixon GF (2012) S1P-induced release of TIMP-2 from vascular smooth muscle cells inhibits angiogenesis. J Cell Sci. 125(Pt 9):2267-2275.

Mead TJ, Apte SS (2018) ADAMTS proteins in human disorders. Matrix Biol. 71-72:225-239.

Medlin MD, Staus DP, Dubash AD, Taylor JM, Mack CP (2010) Sphingosine 1-phosphate receptor 2 signals through leukemia-associated RhoGEF (LARG), to promote smooth muscle cell differentiation. Arterioscler Thromb Vasc Biol. 9;30(9):1779-86.

Mei M, Liu M, Mei Y, Zhao J, Li Y (2023) Sphingolipid metabolism in brain insulin resistance and neurological diseases. Front Endocrinol (Lausanne). 6(14):1243132.

Meissner A, Miro F, Jiménez-Altayó F, Jurado A, Vila E, Planas AM (2017) Sphingosine-1-phosphate signalling-a key player in the pathogenesis of Angiotensin II-induced hypertension. Cardiovasc Res. 113(2):123-133.

Melnik T, Jordan O, Corpataux JM, Delie F, Saucy F (2022) Pharmacological prevention of intimal hyperplasia: A state-of-the-art review. Pharmacol Ther. 235(1):108157.

Mensah SA, Cheng MJ, Homayoni H, Plouffe BD, Coury AJ, Ebong EE (2017) Regeneration of glycocalyx by heparan sulfate and S1P restores inter-endothelial communication. PLoS One. 12(10):e0186116.

Merrill AH Jr (2011) Sphingolipid and glycosphingolipid metabolic pathways in the era of sphingolipidomics. Chem Rev. 111(10):6387-6422.

Milutinović A, Šuput D, Zorc-Pleskovič R (2020) Pathogenesis of atherosclerosis in the tunica intima, media, and adventitia of coronary arteries: An updated review. Bosn J Basic Med Sci. 5;20(1):21-30.

Mizugishi K, Yamashita T, Olivera A, Miller GF, Spiegel S, Proia RL (2005) Essential role for SPHKs in neural and vascular development. Mol Cell Biol. 25(24):11113-11121.

Moos MP, John N, Gräbner R, Nossmann S, Günther B, Vollandt R, Funk CD, Kaiser B, Habenicht AJ (2005) The lamina adventitia is the major site of immune cell accumulation in standard chow-fed apolipoprotein E-deficient mice. Arterioscler Thromb Vasc Biol. 25(11):2386-2391.

Mousseau Y, Mollard S, Richard L, Nizou A, Faucher-Durand K, Cook-Moreau J, Qiu H, Baaj Y, Funalot B, Fourcade L, Sturtz FG (2012) Fingolimod

inhibits PDGF-B-induced migration of VSMC by down-regulating the S1PR1/S1PR3 pathway. Biochimie. 94(12):2523-2531.

Mussbacher M, Salzmann M, Brostjan C, Hoesel B, Schoergenhofer C, Datler H, Hohensinner P, Basílio J, Petzelbauer P, Assinger A, Schmid JA (2019) Cell Type-Specific Roles of NF-κB Linking Inflammation and Thrombosis. Front Immunol. 10(1):85.

Myit S, Delafontaine P, Bochaton-Piallat ML, Giraud S, Gabbiani G, Brink M (2003) Different growth properties of neointimal and medial smooth muscle cells in response to growth factors. J Vasc Res. 40(2):97-104.

Nagahashi M, Yamada A, Aoyagi T, Allegood J, Wakai T, Spiegel S, Takabe K (2016) Sphingosine-1-phosphate in the lymphatic fluid determined by novel methods. Heliyon. 2(12):e00219.

Nakahata N (2008) Thromboxane A2: physiology/pathophysiology, cellular signal transduction and pharmacology. Pharmacol Ther. 4;118(1):18-35.

Nussbaum C, Bannenberg S, Keul P, Gräler MH, Gonçalves-de-Albuquerque CF, Korhonen H, von Wnuck Lipinski K, Heusch G, de Castro Faria Neto HC, Rohwedder I, Göthert JR, Prasad VP, Haufe G, Lange-Sperandio B, Offermanns S, Sperandio M, Levkau B (2015) Sphingosine-1-phosphate receptor 3 promotes leukocyte rolling by mobilizing endothelial P-selectin. Nat Commun. 6(6416):1-12.

Obinata H, Hla T (2019) S1P and inflammation. Int Immunol. 31(9):617-625.

Ogretmen B (2018) Sphingolipid metabolism in cancer signalling and therapy. Nat Rev Cancer. 18(1):33-50.

Okamoto E, Couse T, De Leon H, Vinten-Johansen J, Goodman RB, Scott NA, Wilcox JN (2001) Perivascular inflammation after balloon angioplasty of porcine coronary arteries. Circulation. 104(18):2228-2235.

Omeh DJ, Shlofmitz E (2023) Restenosis of Stented Coronary Arteries. In: StatPearls [online at Internet]. Treasure Island (FL): StatPearls Publishing.
URL:https://www.ncbi.nlm.nih.gov/books/NBK545139/[Accessed:08.08.2023,10:57]

Onishi A, St Ange K, Dordick JS, Linhardt RJ (2016) Heparin and anticoagulation. Front Biosci (Landmark Ed). 21(7):1372-1392.

Ono Y, Kurano M, Ohkawa R, Yokota H, Igarashi K, Aoki J, Tozuka M, Yatomi Y (2013) Sphingosine 1-phosphate release from platelets during clot formation: close correlation between platelet count and serum S1P concentration. Lipids Health Dis. 12(20):1-7.

Ostermann G, Weber KSC, Zernecke A, Schröder A, Weber C (2002) JAM-1 is a ligand of the β2 integrin LFA-1 involved in transendothelial migration of leukocytes. Nat. Immunol. 3(1):151-158.

Panetti TS (2002) Differential effects of sphingosine 1-phosphate and lysophosphatidic acid on endothelial cells. Biochim Biophys Acta. 1582(1-3):190-196.

Pappu R, Schwab SR, Cornelissen I, Pereira JP, Regard JB, Xu Y, Camerer E, Zheng YW, Huang Y, Cyster JG, Coughlin SR (2007) Promotion of lymphocyte egress into blood and lymph by distinct sources of sphingosine-1-phosphate. Science. 316(5822):295-298.

Pasterkamp G, de Kleijn DP, Borst C (2000) Arterial remodeling in atherosclerosis, restenosis and after alteration of blood flow: potential mechanisms and clinical implications. Cardiovasc Res. 45(4):843-852.

Peet C, Ivetic A, Bromage DI, Shah AM (2020) Cardiac monocytes and macrophages after myocardial infarction. Cardiovasc Res. 116(6):1101-1112.

Peng Z, Shu B, Zhang Y, Wang M (2019) Endothelial Response to Pathophysiological Stress. Arterioscler. Thromb. Vasc. 39(1):e233-e243.

Peters SL, Alewijnse AE (2007) Sphingosine-1-phosphate signaling in the cardiovascular system. Curr Opin Pharmacol. 7(2):186-192.

Petzold T, Thienel M, Dannenberg L, Mourikis P, Helten C, Ayhan A, M'Pembele R, Achilles A, Trojovky K, Konsek D, Zhang Z, Regenauer R, Pircher J, Ehrlich A, Lüsebrink E, Nicolai L, Stocker TJ, Brandl R, Röschenthaler F, Strecker J, Saleh I, Spannagl M, Mayr CH, Schiller HB, Jung C, Gerdes N, Hoffmann T, Levkau B, Hohlfeld T, Zeus T, Schulz C, Kelm M, Polzin A (2020) Rivaroxaban Reduces Arterial Thrombosis by

Inhibition of FXa-Driven Platelet Activation via Protease Activated Receptor-1. Circ Res. 14;126(4):486-500.

Polzin A, Dannenberg L, Benkhoff M, Barcik M, Keul P, Ayhan A, Weske S, Ahlbrecht S, Trojovsky K, Helten C, Haberkorn S, Flögel U, Zeus T, Müller T, Gräler MH, Kelm M, Levkau B (2023) Sphingosine-1-phosphate improves outcome of no-reflow acute myocardial infarction via sphingosine-1-phosphate receptor 1. ESC Heart Fail. 10(1):334-341.

Potì F, Ceglarek U, Burkhardt R, Simoni M, Nofer JR (2015) SKI-II--a sphingosine kinase 1 inhibitor--exacerbates atherosclerosis in low-density lipoprotein receptor-deficient (LDLR-/-) mice on high cholesterol diet. Atherosclerosis. 240(1):212-215.

Potì F, Gualtieri F, Sacchi S, Weißen-Plenz G, Varga G, Brodde M, Weber C, Simoni M, Nofer JR (2013) KRP-203, sphingosine 1-phosphate receptor type 1 agonist, ameliorates atherosclerosis in LDL-R-/- mice. Arterioscler Thromb Vasc Biol. 33(7):1505-1512.

Prager B, Spampinato SF, Ransohoff RM (2015) Sphingosine 1-phosphate signaling at the blood-brain barrier. Trends Mol Med. 21(6):354-363.

Pyne NJ, Pyne S (2017) Sphingosine 1-Phosphate Receptor 1 Signaling in Mammalian Cells. Molecules. 22(3):344.

Pyo RT, Sato Y, Mackman N, Taubman MB (2004) Mice deficient in tissue factor demonstrate attenuated intimal hyperplasia in response to vascular injury and decreased smooth muscle cell migration. Thromb Haemost. 92(3):451-458.

Ran GH, Lin YQ, Tian L, Zhang T, Yan DM, Yu JH, Deng YC (2022) Natural killer cell homing and trafficking in tissues and tumors: from biology to application. Signal Transduct Target Ther. 29;7(1):205.

Rauch BH (2014) Sphingosine 1-phosphate as a link between blood coagulation and inflammation. Cell Physiol Biochem. 34(1):185-196.

Rauch BH, Millette E, Kenagy RD, Daum G, Clowes AW (2004) Thrombin- and factor Xa-induced DNA synthesis is mediated by transactivation of fibroblast growth factor receptor-1 in human vascular smooth muscle cells. Circ Res. 94(3):340-345.

Rogers C, Karnovsky MJ, Edelman ER (1993) Inhibition of experimental neointimal hyperplasia and thrombosis depends on the type of vascular injury and the site of drug administration. Circulation. 88(3):1215-21.

Röhl S, Rykaczewska U, Seime T, Suur BE, Diez MG, Gådin JR, Gainullina A, Sergushichev AA, Wirka R, Lengquist M, Kronqvist M, Bergman O, Odeberg J, Lindeman JHN, Quertermous T, Hamsten A, Eriksson P, Hedin U, Razuvaev A, Matic LP (2020) JVS Vasc Sci. 7(1):13-27.

Roqué M, Reis ED, Fuster V, Padurean A, Fallon JT, Taubman MB, Chesebro JH, Badimon JJ (2000) Inhibition of tissue factor reduces thrombus formation and intimal hyperplasia after porcine coronary angioplasty. J Am Coll Cardiol. 36(7):2303-2310.

Rotmans JI, Velema E, Verhagen HJ, Blankensteijn JD, de Kleijn DP, Stroes ES, Pasterkamp G (2004) Matrix metalloproteinase inhibition reduces intimal hyperplasia in a porcine arteriovenous-graft model. J Vasc Surg. 39(2):432-439.

Roy R, Wilcox J, Webb AJ, O'Gallagher K (2023) Dysfunctional and Dysregulated Nitric Oxide Synthases in Cardiovascular Disease: Mechanisms and Therapeutic Potential. Int J Mol Sci. 15;24(20):15200.

Sammani S, Moreno-Vinasco L, Mirzapoiazova T, Singleton PA, Chiang ET, Evenoski CL, Wang T, Mathew B, Husain A, Moitra J, Sun X, Nunez L, Jacobson JR, Dudek SM, Natarajan V, Garcia JGN (2010) Differential effects of sphingosine 1-phosphate receptors on airway and vascular barrier function in the murine lung. Am J Respir Cell Mol Biol. 43(4):394-402.

Santamaria S (2020) ADAMTS-5: a difficult teenager turning 20. Int. J. Exp. Pathol. 101(1-2):4–20.

Santamaria S, Yamamoto K, Teraz-Orosz A, Koch C, Apte SS, de Groot R, Lane DA, Ahnström J (2019) Exosites in Hypervariable Loops of ADAMTS Spacer Domains control Substrate Recognition and Proteolysis. Sci Rep. 29;9(1):10914.

Sattler K, Gräler M, Keul P, Weske S, Reimann CM, Jindrová H, Kleinbongard P, Sabbadini R, Bröcker-Preuss M, Erbel R, Heusch G, Levkau B (2015)

Defects of High-Density Lipoproteins in Coronary Artery Disease Caused by Low S1P Content: Correction by Sphingosine-1-Phosphate-Loading. J Am Coll Cardiol. 66(13):1470-1485.

Sattler KJ, Elbasan S, Keul P, Elter-Schulz M, Bode C, Gräler MH, Bröcker-Preuss M, Budde T, Erbel R, Heusch G, Levkau B (2010) Sphingosine 1-phosphate levels in plasma and HDL are altered in coronary artery disease. Basic Res Cardiol. 105(6):821-832.

Schwab SR, Cyster JG (2007) Finding a way out: lymphocyte egress from lymphoid organs. Nat Immunol. 8(12):1295-301.

Schwab SR, Pereira JP, Matloubian M, Xu Y, Huang Y, Cyster JG (2005) Lymphocyte sequestration through S1P lyase inhibition and disruption of S1P gradients. Science. 309(5741):1735-1739.

Schwedhelm E, Schwieren L, Tiedt S, von Lucadou M, Gloyer NO, Böger R, Magnus T, Daum G, Thomalla G, Gerloff C, Choe CU (2021) Serum Sphingosine-1-Phosphate Levels Are Associated With Severity and Outcome in Patients With Cerebral Ischemia. Stroke. 52(12):3901-3907.

Shao X, Liu K, Fan Y, Ding Z, Chen M, Zhu M, Weinstein LS, Li H, Li H (2015) Gαs Relays Sphingosine-1-Phosphate Receptor 1 Signaling to Stabilize Vascular Endothelial-Cadherin at Endothelial Junctions to Control Mouse Embryonic Vascular Integrity. J Genet Genomics. 42(11):613-624.

Shen SC, Xu J, Cheng C, Xiang XJ, Hong BY, Zhang M, Gong C, Ma LK (2024) Macrophages promote the transition from myocardial ischemia reperfusion injury to cardiac fibrosis in mice through GMCSF/CCL2/CCR2 and phenotype switching. Acta Pharmacol Sin. 5;45(5):959-974.

Shi J, Tang Y, Liang F, Liu L, Liang N, Yang X, Zhang N, Yi Z, Zhong Y, Wang W, Zhao K (2022) NLRP3 inflammasome contributes to endotoxin-induced coagulation. Thromb Res. 6(214):8-15.

Shi Y, O'Brien JE, Fard A, Mannion JD, Wang D, Zalewski A (1996b) Adventitial Myofibroblasts Contribute to Neointimal Formation in Injured Porcine Coronary Arteries. Circulation. 94(7):1655-1664.

Shi Y, O'Brien JE, Fard A, Zalewski A (1996a) Transforming Growth Factor-β1 Expression and Myofibroblast Formation During Arterial Repair. Arterioscler. Thromb. Vasc. Biol. 16(10):1298-1305.

Shimizu T, De Wispelaere A, Winkler M, D'Souza T, Caylor J, Chen L, Dastvan F, Deou J, Cho A, Larena-Avellaneda A, Reidy M, Daum G (2012) Sphingosine-1-phosphate receptor 3 promotes neointimal hyperplasia in mouse iliac-femoral arteries. Arterioscler Thromb Vasc Biol. 32(4):955-961.

Shimizu T, Nakazawa T, Cho A, Dastvan F, Shilling D, Daum G, Reidy MA (2007) Sphingosine 1-phosphate receptor 2 negatively regulates neointimal formation in mouse arteries. Circ Res. 101(10):995-1000.

Shirali AS, McDonald AI, Mack JJ, Iruela-Arispe ML (2016) Reproducible Arterial Denudation Injury by Infrarenal Abdominal Aortic Clamping in a Murine Model. J Vis Exp. 24;(117):54755.

Siedlinski M, Nosalski R, Szczepaniak P, Ludwig-Gałęzowska AH, Mikołajczyk T, Filip M, Osmenda G, Wilk G, Nowak M, Wołkow P, Guzik TJ (2017) Vascular transcriptome profiling identifies Sphingosine kinase 1 as a modulator of angiotensin II-induced vascular dysfunction. Sci Rep. 7(44131):1-13.

Sigwart U, Puel J, Mirkovitch V, Joffre F, Kappenberger L (1987) Intravascular stents to prevent occlusion and restenosis after transluminal angioplasty. N Engl J Med. 19;316(12):701-6.

Simone TM, Higgins SP, Archambeault J, Higgins CE, Ginnan RG, Singer H, Higgins PJ (2015) A small molecule PAI-1 functional inhibitor attenuates neointimal hyperplasia and vascular smooth muscle cell survival by promoting PAI-1 cleavage. Cell Signal. 27(5):923-33.

Singh M, Gersh BJ, McClelland RL, Ho KK, Willerson JT, Penny WF, Holmes DR Jr (2004) Clinical and angiographic predictors of restenosis after percutaneous coronary intervention: insights from the Prevention of Restenosis With Tranilast and Its Outcomes (PRESTO) trial. Circulation. 109(22):2727-2731.

Skoura A, Michaud J, Im DS, Thangada S, Xiong Y, Smith JD, Hla T (2011) S1P receptor-2 function in myeloid cells regulates vascular inflammation and atherosclerosis. Arterioscler Thromb Vasc Biol. 31(1):81-85.

Snider AJ, Orr Gandy KA, Obeid LM (2010) Sphingosine kinase: Role in regulation of bioactive sphingolipid mediators in inflammation. Biochimie. 92(6):707-715.

Soltau I, Mudersbach E, Geissen M, Schwedhelm E, Winkler MS, Geffken M, Peine S, Schoen G, Debus ES, Larena-Avellaneda A, Daum G (2016) Serum-Sphingosine-1-Phosphate Concentrations Are Inversely Associated with Atherosclerotic Diseases in Humans. PLoS One. 11(12):e0168302.

Song P, Rudan D, Zhu Y, Fowkes FJI, Rahimi K, Fowkes FGR, Rudan I (2019) Global, regional, and national prevalence and risk factors for peripheral artery disease in 2015: an updated systematic review and analysis. Lancet Glob Health. 7(8):e1020-e1030.

Spiegel S, Milstien S (2011) The outs and the ins of sphingosine-1-phosphate in immunity. Nat Rev Immunol. 11(6):403-415.

Stenmark KR, Yeager ME, El Kasmi KC, Nozik-Grayck E, Gerasimovskaya EV, Li M, Riddle SR, Frid MG (2013) The adventitia: essential regulator of vascular wall structure and function. Annu Rev Physiol. 75(1):23-47.

Stone PH, Coskun AU, Kinlay S, Clark ME, Sonka M, Wahle A, Ilegbusi OJ, Yeghiazarians Y, Popma JJ, Orav J, Kuntz RE, Feldman CL (2003) Effect of endothelial shear stress on the progression of coronary artery disease, vascular remodeling, and in-stent restenosis in humans: in vivo 6-month follow-up study. Circulation. 108(4):438-444.

Suna G, Wojakowski W, Lynch M, Barallobre-Barreiro J, Yin X, Mayr U, Baig F, Lu R, Fava M, Hayward R, Molenaar C, White SJ, Roleder T, Milewski KP, Gasior P, Buszman PP, Buszman P, Jahangiri M, Shanahan CM, Hill J, Mayr M (2018) Extracellular Matrix Proteomics Reveals Interplay of Aggrecan and Aggrecanases in Vascular Remodeling of Stented Coronary Arteries. Circulation. 9;137(2):166-183.

Swan DJ, Kirby JA, Ali S (2010) Vascular biology: the role of sphingosine 1-phosphate in both the resting state and inflammation. J Cell Mol Med. 14(1):2211-2222.

Takada M,Tanaka H,Yamada T, Ito O, Kogushi M, Yanagimachi M, Kawamura T, Musha T, Yoshida F, Ito M, Kobayashi H, Yoshitake S, Saito I (1998) Antibody to thrombin receptor inhibits neointimal smooth muscle cell accumulation without causing inhibition of platelet aggregation or altering hemostatic parameters after angioplasty in rat. Circ. Res. 82(9), 980-987.

Takahashi M (2022) NLRP3 inflammasome as a key driver of vascular disease. Cardiovasc Res. 29;118(2):372-385.

Takeya H, Gabazza EC, Aoki S, Ueno H, Suzuki K (2003) Synergistic effect of sphingosine 1-phosphate on thrombin-induced tissue factor expression in endothelial cells. Blood. 102(1):1693-1700.

Tang RH, Zheng XL, Callis TE, Stansfield WE, He J, Baldwin AS, Wang DZ, Selzman CH (2008) Myocardin inhibits cellular proliferation by inhibiting NF-kappaB(p65)-dependent cell cycle progression. Proc Natl Acad Sci U S A. 105(9):3362-3367.

Tani M, Ito M, Igarashi Y (2007) Ceramide/sphingosine/sphingosine 1-phosphate metabolism on the cell surface and in the extracellular space. Cell Signal. 19(2):229-237.

Tavakoli NN, Harris AK, Sullivan DR, Hambly BD, Bao S (2012) Interferon-γ deficiency reduces neointimal formation in a model of endoluminal endothelial injury combined with atherogenic diet. Int J Mol Med. 30(3):545-52.

Tieu BC, Lee C, Sun H, Lejeune W, Recinos A 3rd, Ju X, Spratt H, Guo DC, Milewicz D, Tilton RG, Brasier AR (2009) An adventitial IL-6/MCP1 amplification loop accelerates macrophage-mediated vascular inflammation leading to aortic dissection in mice. Clin Invest. 119(12):3637-3651.

Tigges U, Komatsu M, Stallcup WB (2013) Adventitial pericyte progenitor/mesenchymal stem cells participate in the restenotic response to arterial injury. J Vasc Res. 50(2):134-144.

Tolksdorf C, Moritz E, Wolf R, Meyer U, Marx S, Bien-Möller S, Garscha U, Jedlitschky G, H. Rauch B (2022) Platelet-derived S1P and its relevance for the communication with immune cells in multiple human diseases. Int J Mol Sci. 23(18):10278.

Tsai HC, Han MH (2016) Sphingosine-1-Phosphate (S1P) and S1P Signaling Pathway: Therapeutic Targets in Autoimmunity and Inflammation. Drugs. 76(11):1067-79.

Ulrych T, Böhm A, Polzin A, Daum G, Nusing RM, Geisslinger G, Hohlfeld T, Schrör K, Rauch BH (2011) Release of sphingosine-1-phosphate from human platelets is dependent on thromboxane formation. J Thromb Haemost. 9(4):790-798.

Vaidya M, Jentsch JA, Peters S, Keul P, Weske S, Gräler MH, Mladenov E, Iliakis G, Heusch G, Levkau B (2019) Regulation of ABCA1-mediated cholesterol efflux by sphingosine-1-phosphate signaling in macrophages. J Lipid Res. 60(3):506-515.

Van Veldhoven P.P (2000) Sphingosine-1-phosphate lyase. Methods Enzymol. 2000 (311):244–254.

Venkataraman K, Lee YM, Michaud J, Thangada S, Ai Y, Bonkovsky HL, Parikh NS, Habrukowich C, Hla T (2008) Vascular endothelium as a contributor of plasma sphingosine 1-phosphate. Circ Res. 102(6):669-676.

Vessey DA, Li L, Kelley M, Karliner JS (2008) Combined sphingosine, S1P and ischemic postconditioning rescue the heart after protracted ischemia. Biochem Biophys Res Commun. 375(3):425-429.

von Lucadou, Mirjam (2021) Die Rolle von Sphingosin-1-phosphat und Sphingosin-1-phosphat Rezeptor 3 bei der Restenose. Med. diss. thesis. Hamburg University.

Walter DH, Rochwalsky U, Reinhold J, Seeger F, Aicher A, Urbich C, Spyridopoulos I, Chun J, Brinkmann V, Keul P, Levkau B, Zeiher AM, Dimmeler S, Haendeler J (2007) Sphingosine-1-phosphate stimulates the functional capacity of progenitor cells by activation of the CXCR4-dependent signaling pathway via the S1P3 receptor. Arterioscler Thromb Vasc Biol. 27(2):275-282.

Wamhoff BR, Lynch KR, Macdonald TL, Owens GK (2008) S1P receptor subtypes differentially regulate smooth muscle cell phenotype. Arterioscler Thromb Vasc Biol. 28(8):1454-61.

Wang H, Huang H, Ding SF (2018) Sphingosine-1-phosphate promotes the proliferation and attenuates apoptosis of Endothelial progenitor cells via S1PR1/S1PR3/PI3K/Akt pathway. Cell Biol Int. 42(11):1492-1502.

Wang K, Kessler PD, Zhou Z, Penn MS, Forudi F, Zhou X, Tarakji K, Kibbe M, Kovesdi I, Brough DE, Topol EJ, Lincoff AM (2003) Local adenoviral-mediated inducible nitric oxide synthase gene transfer inhibits neointimal formation in the porcine coronary stented model. Mol Ther. ;57(5 Pt 1):597-603.

Wang N, Li JY, Zeng B, Chen GL (2023a) Sphingosine-1-Phosphate Signaling in Cardiovascular Diseases. Biomolecules. 13(5):818.

Wang X, Qiu Z, Dong W, Yang Z, Wang J, Xu H, Sun T, Huang Z, Jin J (2022) S1PR1 induces metabolic reprogramming of ceramide in vascular endothelial cells, affecting hepatocellular carcinoma angiogenesis and progression. Cell Death Dis. 13(9):768.

Wang Y, Wang C, He Q, Chen G, Yu J, Cang J, Zhong M (2023b) Inhibition of sphingosine-1-phosphate receptor 3 suppresses ATP-induced NLRP3 inflammasome activation in macrophages via TWIK2-mediated potassium efflux. Front Immunol. 31;14:1090202.

Warboys CM, Weinberg PD (2021) S1P in the development of atherosclerosis: roles of hemodynamic wall shear stress and endothelial permeability. Tissue Barriers. 9(4):1959243.

Wen JK, Han M (2000) Comparative study of induction of iNOS mRNA expression in vascular cells of different species. Biochemistry (Mosc). 65(12):1376-1379.

Wilensky RL, Tanguay JF, Ito S, Bartorelli AL, Moses J, Williams DO, Bailey SR, Martin J, Bucher TA, Gallant P, Greenberg A, Popma JJ, Weissman NJ, Mintz GS, Kaplan AV, Leon MB (2000) Heparin infusion prior to stenting (HIPS) trial: final results of a prospective, randomized, controlled trial

evaluating the effects of local vascular delivery on intimal hyperplasia. Am Heart J. 139(6):1061-70.

Wilhelm G, Mertowska P, Mertowski S, Przysucha A, Strużyna J, Grywalska E, Torres K (2023) The Crossroads of the Coagulation System and the Immune System: Interactions and Connections. Int J Mol Sci. 24(16):12563.

Wilson NV, Salisbury JR, Kakkar VV (1991) Effect of low molecular weight heparin on intimal hyperplasia. Br J Surg. 78(11):1381-3.

Wilson PC, Fitzgibbon WR, Garrett SM, Jaffa AA, Luttrell LM, Brands MW, El-Shewy HM (2015) Inhibition of Sphingosine Kinase 1 Ameliorates Angiotensin II-Induced Hypertension and Inhibits Transmembrane Calcium Entry via Store-Operated Calcium Channel. Mol Endocrinol. 29(6):896-908.

Wolf D, Ley K (2019) Immunity and Inflammation in Atherosclerosis. Circ Res. 124(2):315-327.

Xiong Y, Hla T (2014) S1P control of endothelial integrity. Curr Top Microbiol Immunol. 378(1):85-105.

Xiong Y, Yang P, Proia RL, Hla T (2014) Erythrocyte-derived S1P is essential for vascular development. J Clin Invest. 124(11):4823-4828.

Yanaba K, Bouaziz JD, Matsushita T, Tsubata T, Tedder TF (2009) The development and function of regulatory B cells expressing IL-10 (B10 cells) requires antigen receptor diversity and TLR signals. J Immunol. 15;182(12):7459-72.

Yang J, Yang L, Tian L, Ji X, Yang L, Li L (2018) Sphingosine 1-Phosphate (S1P)/S1P Receptor2/3 Axis Promotes Inflammatory M1 Polarization of Bone Marrow-Derived Monocyte/Macrophage via G(α)i/o/PI3K/JNK Pathway. Cell Physiol Biochem. 49(5):1677-1693.

Yang S, Li HW, Tian JY, Wang ZK, Chen Y, Zhan TT, Ma CY, Feng M, Cao SF, Zhao Y, Li X, Ren J, Liu Q, Jin LY, Wang ZQ, Jiang WY, Zhao YX, Zhang Y, Liu X (2024) Myeloid-derived growth factor suppresses VSMC dedifferentiation and attenuates postinjury neointimal formation in rats by

activating S1PR2 and its downstream signaling. Acta Pharmacol Sin. 45(1):98-111.

Yang X, Yang Y, Guo J, Meng Y, Li M, Yang P, Liu X, Aung LHH, Yu T, Li Y (2021) Targeting the epigenome in in-stent restenosis: from mechanisms to therapy. Mol Ther Nucleic Acids. 23(1):1136-1160.

Yatomi Y, Ohmori T, Rile G, Kazama F, Okamoto H, Sano T, Satoh K, Kume S, Tigyi G, Igarashi Y, Ozaki Y (2000) Sphingosine 1-phosphate as a major bioactive lysophospholipid that is released from platelets and interacts with endothelial cells. Blood. 96(10):3431-3438.

Yatomi Y, Yamamura S, Hisano N, Nakahara K, Igarashi Y, Ozaki Y (2004) S1P breakdown in platelets. J Biochem. 136(4):495-502.

Ye H, Zhang Y, Huang Y, Li B, Cao R, Dai L, Huang B, Tian P, Li L, Han Y (2021) Bivalirudin Attenuates Thrombin-Induced Endothelial Hyperpermeability via S1P/S1PR2 Category: Original Articles. Front Pharmacol. 3(12):721200.

Yerasi C, Case BC, Forrestal BJ, Torguson R, Weintraub WS, Garcia-Garcia HM, Waksman R (2020) Drug-Coated Balloon for De Novo Coronary Artery Disease: JACC State-of-the-Art Review. J Am Coll Cardiol. 75(9):1061-1073.

Zeng T, Gan J, Liu Y, Shi L, Lu Z, Xue Y, Xiong R, Liu L, Yang Z, Lin Y, Yuan J (2020) ADAMTS-5 Decreases in Aortas and Plasma From Aortic Dissection Patients and Alleviates Angiotensin II-Induced Smooth Muscle-Cell Apoptosis. Front Cardiovasc Med. 14(7):136.

Zeng Y, Adamson RH, Curry FR, Tarbell JM (2014) S1P protects endothelial glycocalyx by inhibiting syndecan-1 shedding. Am J Physiol Heart Circ Physiol. 306(3):H363-H372.

Zeng Y, Liu XH, Tarbell J, Fu B (2015) S1P induced synthesis of glycocalyx on endothelial cells. Exp Cell Res. 339(1):90-95.

Zhang F, Xia Y, Yan W, Zhang H, Zhou F, Zhao S, Wang W, Zhu D, Xin C, Lee Y, Zhang L, He Y, Gao E, Tao L (2016) Sphingosine 1-phosphate signaling contributes to cardiac inflammation, dysfunction, and

remodeling following myocardial infarction. Physiol Heart Circ Physiol. 310(2):H250-H261.

Zhang J, Honbo N, Goetzl EJ, Chatterjee K, Karliner JS, Gray MO (2007) Signals from type 1 sphingosine 1-phosphate receptors enhance adult mouse cardiac myocyte survival during hypoxia. Am J Physiol Heart Circ Physiol. 293(5):H3150-H3158.

Zhang L, Zeng M, Fan J, Tarbell JM, Curry FR, Fu BM (2016) Sphingosine-1-phosphate Maintains Normal Vascular Permeability by Preserving Endothelial Surface Glycocalyx in Intact Microvessels. Microcirculation. 23(4):301-310.

Zhou C, Kuang Y, Li Q, Duan Y, Liu X, Yue J, Chen X, Liu J, Zhang Y, Zhang L (2022) Endothelial S1pr2 regulates post-ischemic angiogenesis via AKT/eNOS signaling pathway. Theranostics. 12(11):5172-5188.

Zhu B, Reardon CA, Getz GS, Hui DY (2002) Both apolipoprotein E and immune deficiency exacerbate neointimal hyperplasia after vascular injury in mice. Arterioscler Thromb Vasc Biol. 22(3):450-455.

Zhu Q, Xia M, Wang Z, Li PL, Li N (2011) A novel lipid natriuretic factor in the renal medulla: sphingosine-1-phosphate. Am J Physiol Renal Physiol. 301(1):F35-41.

Zou Y, Qi Y, Roztocil E, Nicholl SM, Davies MG (2007) Patterns of kinase activation induced by injury in the murine femoral artery. J Surg Res. 142(2):332-40.

9. Abbreviations

AC	Adenylyl cyclase
ADAMTS	A disintegrin and metalloproteinase with thrombospondin motifs
AngII	Angiotensin II
Apo	Apolipoprotein
ATP	Adenosine triphosphate
bFGF	Basic fibroblast growth factor
C1P	Ceramide-1-phosphate
cAMP	Cyclic adenosine monophosphate
CD	Cluster of differentiation
cDNA	Complementary deoxyribonucleic acid
COMP	Cartilage oligomeric matrix protein
COX2	Cytochrome C oxidase subunit II
CSF2	Colony stimulating factor 2/ Granulocyte-macrophage colony-stimulating factor
CT	Cycle threshold
DAG	Diacylglycerol
DNA	Deoxyribonucleic acid
DOP	Deoxypyridoxine
EC	Endothelial cells
ECM	Extracellular matrix
EEL	External elastic lamina
EG	Endothelial glycocalyx
EPC	Endothelial progenitor cell
ER	Elastic recoil
ERK	Extracellular signal-regulated kinase
EvG	Elastic van Gieson
FACS	Fluorescence-activated cell sorting
GAPDH	Glyceraldehyde-3-phosphate dehydrogenase
GPCR	G-protein-coupled receptor
GTPase	Guanosine triphosphatases
HDL	High-density lipoprotein

IEL	Inner elastic lamina
I/M	Area of Neointima/Area of Media
IFN-γ	Interferon-γ
IGF-1	Insulin-like growth factor 1
IH	Intimal hyperplasia
IL-1β	Interleukin-1 beta
IL-6	Interleukin-6
IP3	Inositol-1,4,5-triphosphate
LC-MS/MS	Liquid chromatography-tandem mass spectrometry
LDL	Low-density lipoproteins
LPS	Lipopolysaccharides
MMP	Matrix metalloproteinase
mRNA	Messenger ribonucleic acid
NK cell	Natural killer cell
NLRP3	Nucleotide-binding oligomerization domain, leucine-rich repeat, and pyrin domain containing 3
NO	Nitric oxide
NOS2	Nitric oxide synthase 2/ inducible nitric oxide synthase
NOS3	Nitric oxide synthase 3/ endothelial nitric oxide synthase
PALLD	Palladin
PAI-1	Plasminogen activator inhibitor-1
Palmitoyl CoA	Palmitoyl coenzyme A
PAR-1	Protease-activated receptor 1/ Coagulation factor II thrombin receptor
PDGF	Platelet-derived growth factor
PGI2	Prostaglandin I2
PG	Proteoglycan
PI3K	Phosphoinositide 3-kinases
PIP3	Phosphatidylinositol 3,4,5-trisphosphate
PKB	Protein kinase B
PKC	Protein kinase C
PLC	Phospholipase C
RNA	Ribonucleic acid

ROCK	Rho-associated protein kinase
RT-qPCR	Real-time quantitative polymerase chain reaction
S1P	Sphingosine-1-phosphate
S1PR	Sphingosine-1-phosphate receptor
SEM	standard error of the mean
SMA	α-smooth muscle actin
SPHK	Sphingosine kinase
SPL	Sphingosine-1-phosphate lyases
Spns2	Spinster homolog 2
SPT	Serine palmitoyltransferase
TXA2	Thromboxane A2
TBXA2R	Thromboxane A2 Receptor
TF	Tissue factor
TGF-β	Transdermal growth factor-β
TNFα	Tumor necrosis factor-alpha
tPA	Tissue-type plasminogen activator
uPA	Urokinase plasminogen activator
VEGF	Vascular endothelial growth factor
VLDL	Very low-density lipoprotein
VSMC	Vascular smooth muscle cells
WT	Wild-type

10. Figure list

11. Table list

12. Declaration of personal contribution

This study was conducted at the University Hospital Hamburg-Eppendor (UKE) under the supervision of Prof. Dr. rer. nat. Edzard Schwedhelm. The project was designed and processed with the guidance of Prof. Dr. med. Elke Oetjen, Dr. Günter Daum and Dr. Markus Geißen.

The animal experiments and gene expression level determination were performed by me independently. The histology analysis was completed with the support from Sophia Deden. The fluorescence-activated cell sorting in blood samples was completed in collaboration with Dr. rer. nat. Björn Rissiek. The S1P concentration measurements were carried out with the help of Prof. Dr. rer. nat. Edzard Schwedhelm and Dr. Mirjam von Lucadou. The statistical analysis was carried out by me.

I wrote this manuscript myself. The sources used were explicitly cited in the thesis.

13. Eidesstattliche Versicherung

Ich versichere ausdrücklich, dass ich die Arbeit selbständig und ohne fremde Hilfe, insbesondere ohne entgeltliche Hilfe von Vermittlungs- und Beratungsdiensten, verfasst, andere als die von mir angegebenen Quellen und Hilfsmittel nicht benutzt und die aus den benutzten Werken wörtlich oder inhaltlich entnommenen Stellen einzeln nach Ausgabe (Auflage und Jahr des Erscheinens), Band und Seite des benutzten Werkes kenntlich gemacht habe. Das gilt insbesondere auch für alle Informationen aus Internetquellen.

Soweit beim Verfassen der Dissertation KI-basierte Tools („Chatbots“) verwendet wurden, versichere ich ausdrücklich, den daraus generierten Anteil deutlich kenntlich gemacht zu haben. Die „Stellungnahme des Präsidiums der Deutschen Forschungsgemeinschaft (DFG) zum Einfluss generativer Modelle für die Text- und Bilderstellung auf die Wissenschaften und das Förderhandeln der DFG“ aus September 2023 wurde dabei beachtet.

Ferner versichere ich, dass ich die Dissertation bisher nicht einem Fachvertreter an einer anderen Hochschule zur Überprüfung vorgelegt oder mich anderweitig um Zulassung zur Promotion beworben habe.

Ich erkläre mich damit einverstanden, dass meine Dissertation vom Dekanat der Medizinischen Fakultät mit einer gängigen Software zur Erkennung von Plagiaten überprüft werden kann.

Datum 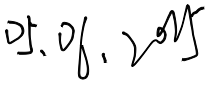 Unterschrift 

14. Acknowledgement

First of all, I would like to thank Professor Dr. Edzard Schwedhelm, my supervisor, for offering me the opportunity to study in his laboratory, being open to all my questions, and supporting me in my science work. I greatly benefit from his helpful advice in my application to study at Hamburg Universit and my project. Many thanks to him for his help in the lab work training and financial support.

I would like to express my appreciation to Dr. Markus Geißen, Dr. Mirjam von Lucadou, and Sophia Deden for their encouragement throughout my research. I would like to thank Markus Geißen for always being available for my technical questions and being patient with all my concerns in daily life. Thanks to Mirjam von Lucadou for completing the S1P concentration determination in this study and to Sophia Deden for helping me with histology slice preparation and analysis. I could not have adapted to life here so well without their sincere help.

I also would like to thank Dr. rer. nat. Björn Rissiek for his work on fluorescence-activated cell sorting in mice peripheral blood samples.

Sincere gratitude should also go to Dr. Günter Daum who helped me select target genes for expression analyses. With his explanation of scientific questions and advice on result analysis, I completed my project and this thesis.

Many thanks to Prof. Dr. Elke Oetjen for scientific suggestions on my research. She and Sabine Schröder always warmly welcomed me to their laboratory, and were always helpful with my questions.

I appreciate the support from the China Scholarship Council (CSC), which offered scholarships covering my daily costs. I also appreciate Deutsches Zentrum für Herz-Kreislauf-Forschung (DZHK) for financial support on the research.

Finally, my cordial thanks go to my family and friends for always loving me unconditionally. They offered understanding and accompaniment throughout my life, being my strongest support.